Department of Civil Engineering DTU

Tim Gudmand-Høyer
Lars Zenke Hansen

Stability of Concrete Columns

Volume 1

PHD THESIS

BYG • DTU

Stability of Concrete Columns

Tim Gudmand-Høyer
Lars Zenke Hansen

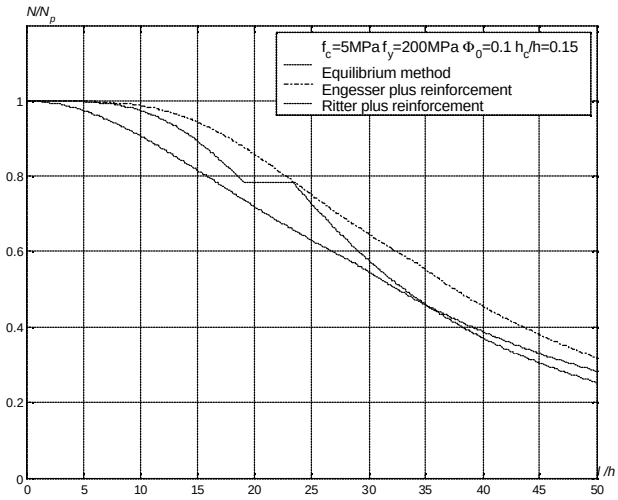

Department of Civil Engineering
DTU-building 118
2800 Kgs. Lyngby
http://www.byg.dtu.dk

2002

1 Preface

This report is prepared as a partial fulfilment of the requirements for obtaining the Ph.D. degree at the Technical University of Denmark. The two authors have contributed equally. The content of this investigation is relevant for the Ph.D. projects of both authors and thus the investigations have been coordinated by writing this paper jointly[1].

The work has been carried out at the Department of Structural Engineering and Materials, Technical University of Denmark (BYG•DTU), under the supervision of Professor, dr. techn. M. P. Nielsen.

We would like to thank our supervisor for the valuable advise, for the inspiration and the many and rewarding discussions and criticism to this work.

Thanks are also due to our co-supervisor M. Sc. Ph.D. Bent Steen Andreasen, RAMBØLL, M. Sc. Ph.D.-student Karsten Findsen, BYG•DTU, M. Sc. Ph.D.-student Jakob Laugesen, BYG•DTU, M. Sc. Ph.D. Bent Feddersen RAMBØLL and Architect MAA Søren Bøgh MURO for their engagement and criticism to the present work and our Ph.D.-projects in general.

The Ph.D project of Lars Z. Hansen if financed by MURO and RAMBØLL. This support is herby gratefully acknowledged.

Lyngby, November 2002.

Tim Gudmand-Høyer Lars Zenke Hansen

[1] Further details may be found in section 11.1.

2 Summary

In this paper an investigation of reinforced concrete columns and beam-columns are carried out. The theory is general but this investigation is limited to statically determined beam-columns and certain other special columns. The columns considered correspond to the tests reported in the literature.

A linear elastic – perfectly plastic material behaviour of the reinforcement and a parabolic material behaviour of the concrete with no tensile strength are assumed. The maximum strain of the concrete in compression is limited in the traditional way.

The behaviour of columns and beam-columns are analysed numerically and compared with experimental data from the literature. A good agreement has been found.

Further the results of calculations according to the Danish Code of Practice (DS411) have been compared with experiments. A good, but a bit conservative, agreement has been found.

The comparison between the two calculation procedures and experiments covers 311 tests of which 200 are eccentrically loaded beam-columns, 73 are concentrically loaded columns and 38 are laterally loaded beam-columns.

A short investigation of the shape of the deflection curve is included in order to justify a simplified calculation formula for the deflection in the mid point of the beam. This simplification is also used in the Danish Code of Practice.

3 Resume

I nærværende rapport undersøges opførslen af armerede betonsøjler og bjælkesøjler. Teorien er generel, men indskrænkes her til at behandle statisk bestemte bjælkesøjler og en række specielle søjler. De behandlede søjler svarer til søjler med hvilke der er rapporteret forsøg i litteraturen.

Armeringen antages at opføre sig lineærelastisk-ideal plastisk med flydespændingen f_y i både træk og tryk. Betonen antages at have en parabolsk arbejdskurve i tryk og trækstyrken sættes til nul. Den maksimale tøjning for beton i tryk er begrænset på traditionel måde.

På denne baggrund er søjlers opførelse analyseret numerisk og der er foretaget sammenligninger med forsøg indsamlet fra litteraturen. Der er fundet god overensstemmelse.

Ydermere er der foretaget beregninger, som baserer sig på metoder i den danske norm for betonkonstruktioner, DS411 1999. Sammenligninger med forsøg har vist, at der er god overensstemmelse. Beregningsmetoden er lidt på den sikre side.

Fra litteraturen er samlet 311 forsøg, som fordeler sig med 200 forsøg med excentrisk normalkraft, 73 med en centralt angribende normalkraft og 38 forsøg hvor der udover en central normalkraft er påført en tværbelastning.

Der er i forbindelse med rapporten også foretaget en undersøgelse af udbøjningskurvens form. Dette er gjort for at verificere brugen af et simpelt udtryk for udbøjningen i bjælkemidten. Denne simplificering bliver også brugt i den danske norm for betonkonstruktioner.

4 Table of contents

5 Notation

The most commonly used symbols are listed below. Exceptions from the list may appear. They will be commented upon in the text.

Geometry

h	Height of a cross-section
b	Width of a cross-section
k	Core radius
k	$0{,}8 - 400\frac{f_c}{E_{0cr}}$
A, A_c	Area of a cross-section
A_s	Area of reinforcement at the bottom face
A_s'	Area of reinforcement at the top face
A_{sc}	Area of reinforcement in compression
I	Moment of inertia
i	Radius of inertia
h_c	Distance from the bottom face to the centre of the bottom reinforcement
h_c'	Distance from the top face to the centre of the top reinforcement
y_0	Distance from the top face to the neutral axis
l	Length of a beam or column
e	Eccentricity
$e_{i,t}$	Initial eccentricity at top
$e_{i,b}$	Initial eccentricity at bottom
u	Deflection
u_m	Deflection in the mid section
k	Curvature
k_Y	Curvature when bottom reinforcement yields
a	Parameter of shape
x, y, z	Cartesian coordinates

Physic

k	$\sqrt{\frac{N}{EI}}$
k	$\frac{a}{e_{cy}\left(\frac{l}{h}\right)^2}$
e	Strain
e_c	Strain in concrete
e_{cy}	Strain in concrete at the stress f_c
e_{cu}	Maximum strain in concrete
e_s	Strain in reinforcement
e_{sy}	Yield strain of reinforcement
s	Stress
s_c	Stress in concrete
s_s	Stress in reinforcement
s_{cr}	Critical stress (stress in the concrete at failure due to instability)
s_E	Critical Euler stress
f_c	Compressive strength of concrete
f_y	Yield strength of reinforcement
E_s	Modulus of elasticity of the reinforcement
E_{c0}	Initial modulus of elasticity of the concrete
E_s	Tangent modulus of concrete
n	Ratio between the stiffness of the reinforcement and the concrete
r	Reinforcement ratio
Φ_0	Degree of Reinforcement
$\Phi_{e_{cy}}$	$\frac{A_s E_s e_{cy}}{bhf_c}$
C_c	Resulting compressive force in concrete
C_s	Resulting compressive force in reinforcement
T	Resulting tensile force in reinforcement
N	Axial load
N_p	Maximum compressive load
N_c	Maximum compressive load, concrete only

N_{cr}	Critical load (load at failure due to instability)
M	Bending moment
M_Y	Bending moment when bottom reinforcement yields
M_0	Applied bending moment
M_p	Maximum bending moment
P	Point load
p	Line load

6 Introduction

A column is defined as a structural element loaded by a concentric axial load only. A beam-column is defined as a beam loaded with axial load and an applied moment, either from an eccentrically applied axial load or a transverse load. These structural members may collapse due to instability. This type of failure is sudden and therefore very dangerous.

This investigation sets out to analyse columns and beam-columns. It aims to justify present design procedures, mainly the procedures used in the Danish Code of Practice, by theoretical calculations and by comparing the methods with experiments. These experiments are taken from the literature where numerous investigations have been reported.

The paper will be subdivided into two sections. The first one deals with theoretical calculations based on the so-called equilibrium method, which to some extent will be compared with existing methods. Furthermore some simplified procedures are suggested, which may be used instead of the traditional method suggested in the Danish Code of Practice.
In the second section, a comparison with experiments and the equilibrium method and the Danish Code of Practice will be presented. This comparison will be subdivided into 3 parts, one for concentrically loaded columns, one for eccentrically loaded columns and one for laterally loaded columns.

At the end, concluding remarks on the investigation will be presented.

7 Theory

7.1 Introduction

In this chapter a theoretical investigation is made on columns and beam-columns. A column is defined as an element loaded by a concentric axial load. Eccentrically loaded elements, laterally loaded elements and elements loaded with a combination of these actions are defined as beam-columns.

The chapter is subdivided into 3 sections. These sections concern the material behaviour and assumptions made in the theoretical analysis, analysis of columns and beam-columns respectively.
Short descriptions of the most common of the existing methods are made in both the second and the third section. This is followed by an analysis based on the equilibrium method. This method is compared with existing methods for columns and used to analyse the behaviour of beam-columns. Furthermore simplified solutions to calculate the moment-curvature relationship and the interaction diagram are proposed.

7.2 Material behaviour, assumptions and definitions

7.2.1 Material behaviour

In order to analyse the behaviour of a reinforced concrete column and a beam-column some basic assumptions regarding the material behaviour for concrete and reinforcement have to be introduced. In this paper effects from unloading and possible subsequent reloading are neglected. In some parts of the paper concrete is modelled as a linear elastic material and in some parts a more accurate modelling of the actual behaviour is considered.
Numerous investigations have been made concerning the stress-strain relationship for both concrete and reinforcement. In this paper the stress-strain relationship of concrete in

compression is assumed parabolic until the maximum strain e_{cu} is reached. The tensile strength of concrete is set to zero. The reinforcement is assumed to behave linear elastic-perfectly plastic in both compression and tension. This is illustrated in Figure 7.1, where only the stress-strain relationship for reinforcement in tension is shown.

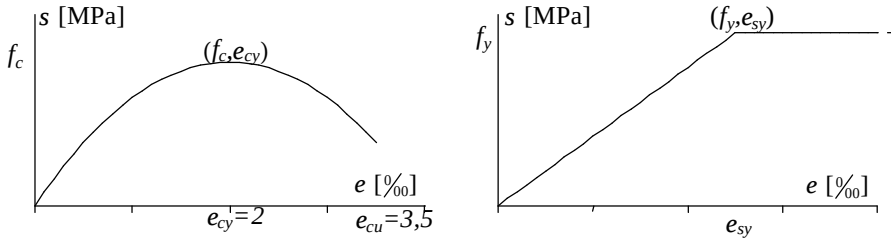

Figure 7.1 The assumed material behaviour for concrete and reinforcement

The variation of the compressive stresses in the concrete is determent by (7.1).

$$s_c = f_c \frac{e}{e_{cy}}\left(2 - \frac{e}{e_{cy}}\right) \tag{7.1}$$

7.2.2 Assumptions

In the forthcoming analyses of columns and of beam-columns the following assumptions are made regarding the behaviour:

- Plane cross-sections remain plane and normal to the curve of deflection. Thus shear strains are neglected (Bernoulli-beam)
- The strain in the concrete and in the reinforcement is the same. This means that the bond between concrete and reinforcement is considered perfect.
- Transverse bars (stirrups) have no influence on the axial stresses and strains. They are supplied to prevent longitudinal reinforcement from buckling and as shear reinforcement in beam-columns.

Definitions

The reinforcement ratio r is defined as:

$$r = \frac{A_s + A_s'}{A_c} = \frac{A_s + A_s'}{bh} \tag{7.2}$$

The degree of reinforcement Φ_0 is defined as:

$$\Phi_0 = \frac{A_s f_y}{b h_e f_c} \tag{7.3}$$

Maximum compressive load is defined as:

$$N_p = bhf_c + (A_s + A_s')f_y \tag{7.4}$$

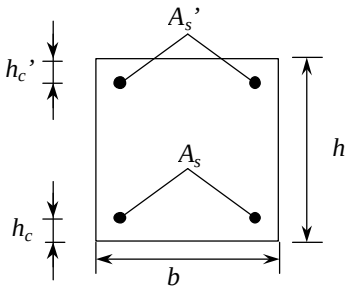

Figure 7.2. Cross-section

The sectional forces are defined as illustrated in Figure 7.3. Thus a positive moment gives tensile stresses in the bottom of a beam-column and the axial load is positive in compression. Statical equivalence is used to express the sectional forces by the stresses in the section in a cross-section.

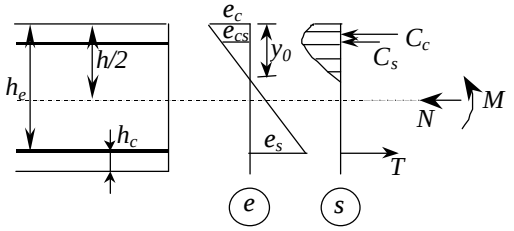

Figure 7.3. Stress and strain distribution in cross-section analysis

7.3 Columns

7.3.1 Existing methods

In this section some of the existing methods used in stability analysis of concrete columns are presented. The methods of interest here are the linear elastic solution and the solutions presented by Engesser and Ritter.

7.3.1.1 Instability of linear elastic columns

Instability of linear elastic columns are analysed either by solving the column differential equation or by the energy method.

In Figure 7.4 a simply supported column is shown.

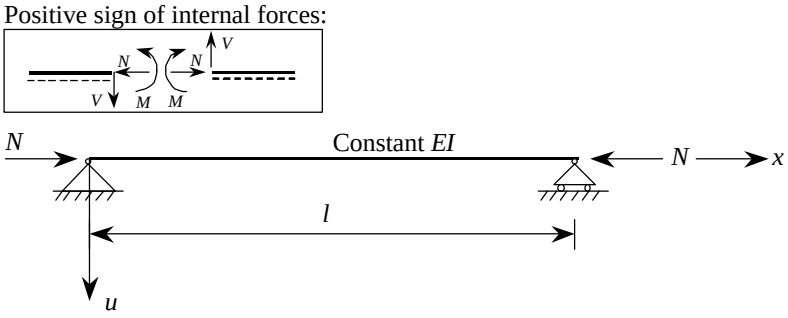

Figure 7.4 Simply supported column concentrically loaded

Moment equilibrium immediately gives:

$$M - N \cdot u = 0 \tag{7.5}$$

The bending moment is determined by $M = -EI \frac{d^2u}{dx^2}$, which inserted in (7.5) gives the differential equation:

$$EI \frac{d^2u}{dx^2} + N \cdot u = 0 \tag{7.6}$$

This is an ordinary homogeneous second order differential equation, which must be solved using the boundary conditions.

$$\begin{aligned} u(x=0) &= 0 \\ u(x=l) &= 0 \end{aligned} \tag{7.7}$$

It is convenient to introduce a factor *k*, given by.

$$k^2 = \frac{N}{EI} \tag{7.8}$$

Equation (7.6) may then be rewritten as:

$$\frac{d^2u}{dx^2} + k^2 \cdot u = 0 \tag{7.9}$$

The complete solution to (7.9) is:

$$u = A \cdot \cos kx + B \cdot \sin kx \tag{7.10}$$

The constants A and B are determined from the boundary conditions and besides the trivial solution $A = B = 0$ the solution to the differential equation requires:

$$\sin kl = 0 \Leftrightarrow kl = p + n \cdot p \quad n = 0,1,2\ldots \tag{7.11}$$

The axial load solutions to this problem are the so-called eigenvalues and the corresponding solution $u(x)$ is an eigenfunction. The magnitude of the eigenfunctions can not be determined from the differential equation, the only information is the shape.

The lowest value of N is found for $kl = p$ which gives the well-known Euler equation:

$$N_{cr} = \frac{p^2 EI}{l^2} \tag{7.12}$$

As seen from equation (7.12) the load-carrying capacity calculated from the Euler equation goes to infinity when $l \to 0$.

Euler's equation can only be used if the material has constant modulus of elasticity in the entire interval from zero stress to the compressive strength of the material. If the moment of inertia varies with x this has to be taken into consideration when solving the differential equation (7.9).

Since all materials have a limited strength, the Euler equation has to be cut off at this strength, see Figure 7.5.

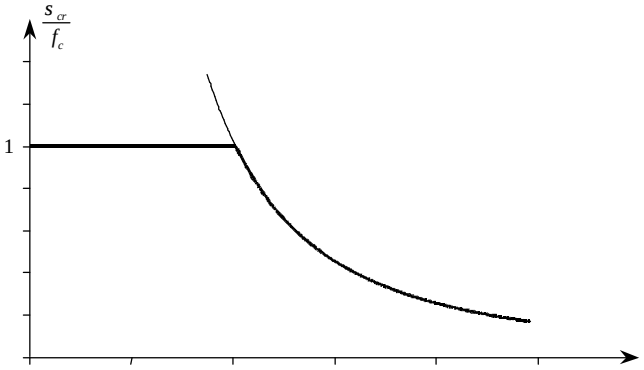

Figure 7.5 The Euler curve with a cut off at the compressive strength f_c

The energy method for a column provides a criterion, which determines whether the column is stable or not. The criterion for a stable column is:

$$\int_0^L EI \frac{d^2u}{dx^2} dx - \int_0^L N \left(\frac{du}{dx} \right)^2 dx > 0 \quad (N \text{ positive in compression}) \tag{7.13}$$

Equation (7.13) states that for a stable column, the bending energy for an arbitrary state of deflections is larger than the work done by the axial load for the same state of deflections. The energy method is equivalent to the equilibrium method.

7.3.1.2 Inelastic prediction of the critical load

7.3.1.2.1 Engesser´s first column formula

A column with non-linear material behaviour belongs to an area in which numerous investigations have been made. Engesser stated his first theory in 1890 (see [5]). This theory was based on the Euler equation [2], with a modification of the modulus of elasticity. His idea was to introduce the tangent modulus of the stress-strain relationship at the current stress level, i.e. to use the inclination of the tangent (E_s) as the elastic modulus of the material, see Figure 7.6. Then the critical stress may be calculated by the formula:

$$s_{cr} = \frac{N_{cr}}{A_c} = \frac{p^2 E_s}{\left(\frac{l}{i}\right)^2} \tag{7.14}$$

Since this theory does not consider whether a layer in the concrete is reloaded or unloaded, Engesser stated a second theory in 1895 taken this into account. He assumed that loaded concrete has the stiffness equal to the tangent modulus and unloaded concrete has the initial stiffness (the stiffness for $s = 0$). Engesser's second theory thus leads to more complicated calculations. In 1946 Shanley [1] proved, by calculations and experimental investigations that the critical load is only a little higher than that given by Engesser's first theory, which was shown to furnish the load for which deflections of a perfect column become possible. In return, he proved that Engesser's second theory provided an upper limit for the critical load. This suggests that for practical purposes the first theory of Engesser may be used.

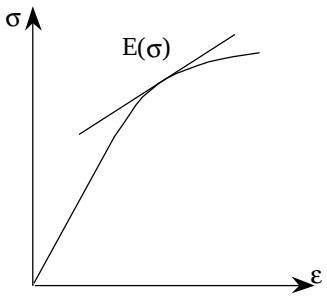

Figure 7.6. Stress-strain curve for a soft material in general.

For a parabolic stress-strain relation (illustrated in Figure 7.1) the stiffness is determined by:

$$E_s = E_0\sqrt{1-\frac{s}{f_c}} \tag{7.15}$$

If equation (7.15) is inserted into equation (7.14) and the equation is solved for the critical stress, equation (7.16) is obtained.

$$\frac{s_{cr}}{f_c} = \frac{1}{2}\frac{s_E}{f_c}\left(\sqrt{\left(\frac{s_E}{f_c}\right)^2+4}-\frac{s_E}{f_c}\right) \tag{7.16}$$

where $s_E = \dfrac{p^2 E_0}{\left(\dfrac{l}{i}\right)^2}$

A simple way of including the influence of the reinforcement is to assume that the concrete determines the critical stress and the contribution from the reinforcement are calculated on the basis of this critical stress. This means that the critical load for the column in general should be calculated as:

$$N_{cr} = s_{cr}bh + s_s A_s \tag{7.17}$$

This simplification leads to an underestimation of the critical stress since the stiffness of the reinforced column is higher than the stiffness of the unreinforced column.
If the yielding of the reinforcement is included, formula (7.17) may be written as:

$$N_{cr} = \min\begin{cases} s_{cr}bh(1+nr) \\ s_{cr}bh + A_s f_y \end{cases} \tag{7.18}$$

where A_s is the entire area of reinforcement and n is the ratio $E_s/500f_c$. The ratio n could also have been calculated as s_s/s_{cr}. This is not done since an equal way of introducing the reinforcement is preferred.

7.3.1.2.2 Ritter's column formula

Equation (7.16) is, in terms of history, considered complicated because it contains a square root. This led to the simplification made by Ritter.
The Ritter equation is also derived from the Euler equation by assuming a stiffness-stress relation for concrete as:

$$E_s = E_{c0}\left(1-\frac{s}{f_c}\right) \tag{7.19}$$

The difference between the Ritter stiffness and the stiffness corresponding to a parabolic stress-strain curve is illustrated in Figure 7.7. It is seen that the simplification used by Ritter is conservative.

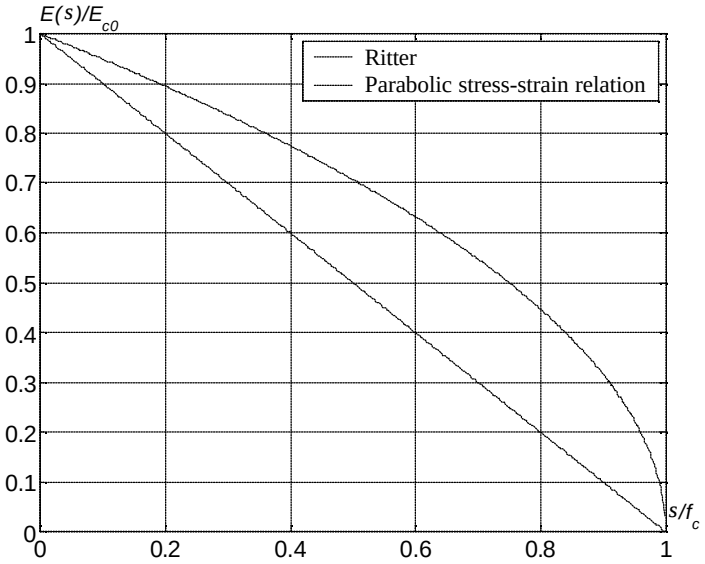

Figure 7.7. Stifness-stress relations as described by (7.19) and (7.15).

Inserting the Ritter stiffness into Eulers column formula leads to the Ritter column formula:

$$s_{cr,Ritter} = \frac{f_c}{1 + \frac{f_c}{p^2 E_{c0}} \left(\frac{l}{i} \right)^2} \tag{7.20}$$

Results of calculations from Ritter's as well as Engesser's column formula are shown in Figure 7.8 for two different initial module of elasticity.

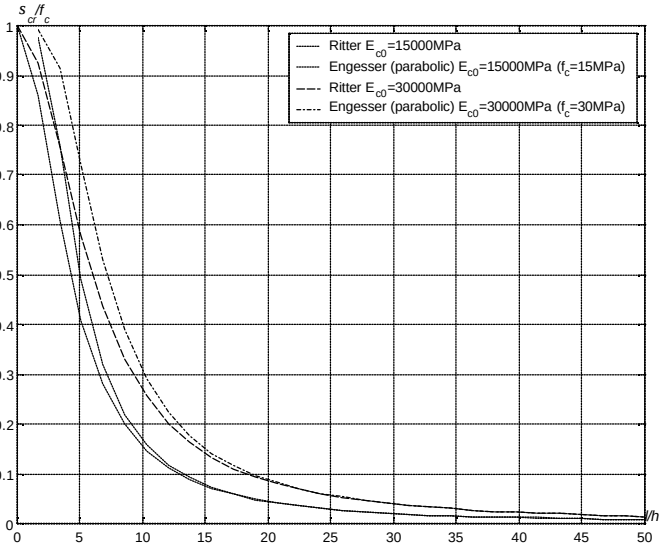

Figure 7.8. Critical stress for e_{cy}=0,2%.

The reinforcement is included in the same way as for Engesser's formula, i.e.:

$$N_{cr} = \min \begin{cases} s_{cr} bh(1+nr) \\ s_{cr} bh + A_s f_y \end{cases} \tag{7.21}$$

where A_s also denotes the entire area of reinforcement.

According to [27] the modular ratio may approximated by:

$$n = \frac{E_s}{500\, f_c} \tag{7.22}$$

Under the assumption of a parabolic stress-strain relation the secant modulus of elasticity corresponds to an arbitrary strain e is:

$$E_{s,sek} = \frac{\left(2e_{cy} - e\right) f_c}{e_{cy}^{\,2}} \tag{7.23}$$

The modular ratio then becomes:

$$n = \frac{E_s e_{cy}^{\,2}}{\left(2e_{cy} - e\right) f_c} \tag{7.24}$$

It appears that the modular ratio depends on the strain at the critical load. It also appears that if failure occurs at a strain close to the strain corresponding to maximum concrete stress (e = e_{cy} = 0,2%) the two formulas ((7.22) and (7.24)) are identical.

For a critical load leading to a strain lower than the strain at maximum concrete stress, the simple formula (7.22) overestimates the modular ratio. This means that the contribution from the reinforcement is overestimated. However, in [27] this overestimation of the stress in the reinforcement is considered compensated by the underestimation of the stiffness when determining the critical stress. This is confirmed by the numerical calculations carried out later on.

7.3.2 Danish Code of Practice, DS411

In the Danish Code of Practice, DS411, the procedure for calculating the load-carrying capacity of columns is based on the critical stress calculated by Ritter's equation.

$$s_{cr,Ritter} = \frac{f_c}{1 + \frac{f_c}{p^2 E_{0cr}} \left(\frac{l}{i} \right)^2} \tag{7.25}$$

where

$$E_{0cr} = \min \begin{cases} 1000\, f_c \\ 0{,}75 \cdot 51000 \dfrac{f_c}{f_c + 13} \end{cases} \tag{7.26}$$

The reinforcement is included as described previously,

$$N_{cr} = \min \begin{cases} s_{cr} A_c (1 + n r) \\ s_{cr} A_c + f_y A_{sc} \end{cases} \tag{7.27}$$

where A_{sc} is the area of the longitudinal reinforcement and $n = \dfrac{E_s}{500\, f_c}$.

7.3.3 The equilibrium method

For columns made of materials with softening the load-carrying capacity may be reached long before failure in the critical section. Thus the load-carrying capacity must be determined by a maximum condition. This method normally used for beam-columns may also be used for concentrically loaded columns. In this paper this method is named the equilibrium method. For a column simply supported at both ends the maximum deflection in the mid point may be determined as:

$$u_{\max} = \frac{1}{a} k l^2 \tag{7.28}$$

where k is the curvature in the mid point and a is a form parameter dependent on the curvature function along the column.

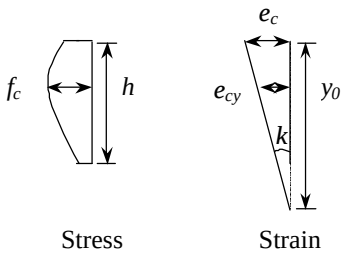

Figure 7.9. Stresses and strains in a cross-section.

Cross-section analysis is carried out expressing statical equivalence between sectional forces (stress resultants) and stresses.

The equations of statical equivalence for an unreinforced column with a rectangular cross-section and with a maximum deflection determined by (7.28) (see Figure 7.9) are:

Projection equation:

$$N = b\int_{y_0-h}^{y_0} f_c e_c \frac{y}{y_0} e_{cy}\left(2 - e_c \frac{y}{y_0} e_{cy}\right)$$
$$N = b\left(f_c \frac{e_c}{y_0 e_{cy}}\left(y_0{}^2 - (y_0-h)^2\right) - \frac{1}{3} f_c \frac{e_c{}^2}{y_0{}^2 e_{cy}{}^2}\left(y_0{}^3 - (y_0-h)^3\right)\right) \quad (7.29)$$

Moment equation:

$$M = b\int_{y_0-h}^{y_0} f_c e_c \frac{y}{y_0} e_{cy}\left(2 - e_c \frac{y}{y_0} e_{cy}\right) y$$
$$M = b\left(\frac{2}{3} f_c \frac{e_c}{y_0 e_{cy}}\left(y_0{}^3 - (y_0-h)^3\right) - \frac{1}{4} f_c \frac{e_c{}^2}{y_0{}^2 e_{cy}{}^2}\left(y_0{}^4 - (y_0-h)^4\right)\right) \quad (7.30)$$

The moment in the mid point is:

$$M = Nu = N\frac{1}{a} k l^2 \quad (7.31)$$

Combining(7.29), (7.30) and (7.31) leads to a determination of e_c:

$$\frac{e_c}{e_{cy}} = \frac{\frac{y_0}{h}\left(\frac{1}{8}k + 2\frac{y_0}{h}(12+k) - 12 - \sqrt{k^2\left(1+4\left(\frac{y_0}{h}\right)^2\right) - 4k\left(\frac{y_0}{h}+2\right) + 576\frac{y_0}{h}\left(\frac{y_0}{h}-1\right) + 144}\right)}{8\left(3\left(\frac{y_0}{h}\right)^2 - 3\frac{y_0}{h} + 1\right)} \quad (7.32)$$

where $k = \dfrac{a}{e_{cy}\left(\dfrac{l}{h}\right)^2}$

Inserting (7.32) into (7.29) leads to a determination of the axial load as a function of y_0. By letting y_0 go towards infinity the maximum axial load may be found. This is equivalent to letting the deflection go towards zero and furnishes a limiting criterion of stability since the column is no longer deflected, and the maximum load is therefore the same as the critical load for which deflection becomes possible. The critical load is found to be:

$$\frac{N_{cr}}{bhf_c} = \frac{k}{6}\left(\sqrt{1-\frac{1}{12^2}k^2} - k\right) \tag{7.33}$$

and the critical stress is:

$$\frac{s_{cr}}{f_c} = \frac{k}{6}\left(\sqrt{1-\frac{1}{12^2}k^2} - k\right) \tag{7.34}$$

By comparing (7.34) with (7.16) it is seen that the critical stress found by Engesser´s column formula and the critical stress found by the statical equivalence method are identical if $a = p^2$. Normally a is set to 10, as suggested in [27].

If the curvature is constant a = 8, and if the curvature is parabolic a= 9,6. The influence of a is illustrated in Figure 7.10.

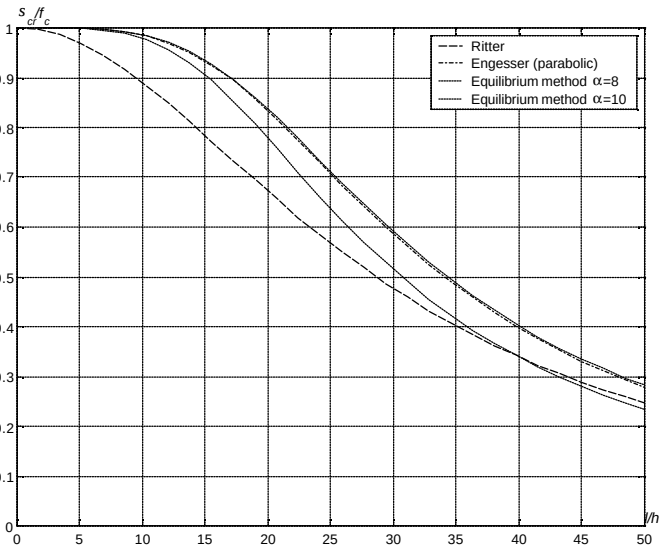

Figure 7.10. Results from calculations e_{cy}*=0,2%.*

Reinforcement may be taken into account as described previously. The equilibrium condition depends on whether yielding occurs in the reinforcement or not. This leads to three different cases.

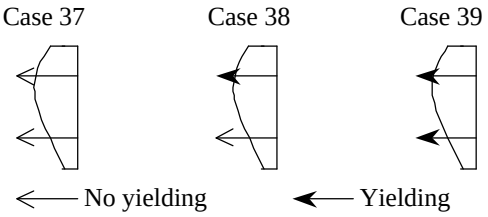

Figure 7.11. Illustration of three different cases with and without yielding in the reinforcement. Regarding the nubering af cases, see Figure 7.27

The three formulas, and their limitations, are determined for the column with a rectangular cross-section shown in Figure 7.12. The calculations may be done analytically as in the case of an unreinforced cross-section.

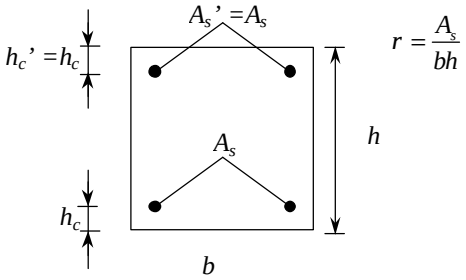

Figure 7.12.Cross-section of the column used in the calculations.

If it is assumed that $h_c' = h_c$ and $A_s' = A_s$ the following results are found:

$$\frac{e_{c37}}{e_{cy}} = \frac{1}{12}k + \Phi_{e_{cy}} + 1 - \sqrt{\left(\Phi_{e_{cy}} + 1\right)^2 - \Phi_{e_{cy}} k\left(2\left(\frac{h_c}{h}\right)^2 - 2\frac{h_c}{h} + \frac{1}{3}\right) + \frac{1}{12^2}k^2} \tag{7.35}$$

$$\frac{e_{c38}}{e_{cy}} = \frac{f_y}{e_{cy}E_s} \tag{7.36}$$

$$\frac{e_{c39}}{e_{cy}} = \frac{1}{12}k + 1 - \sqrt{\frac{1}{12^2}k^2 + 2\Phi_{e_{cy}} + 1} \tag{7.37}$$

$$\frac{N_{37}}{bhf_c} = -\left(\frac{e_{c37}}{e_{cy}}\right)^2 + 2\frac{e_{c37}}{e_{cy}}\left(1 + \Phi_0\right) \tag{7.38}$$

$$\frac{N_{38}}{bhf_c} = -\left(\frac{e_{c38}}{e_{cy}}\right)^2 + 2\frac{e_{c37}}{e_{cy}} - 2\Phi_0 \tag{7.39}$$

$$\frac{N_{39}}{bhf_c} = -\left(\frac{e_{c39}}{e_{cy}}\right)^2 + 2\frac{e_{c39}}{e_{cy}} + 2\Phi_0 \tag{7.40}$$

where $\Phi_{e_{cy}} = \frac{A_s E_s e_{cy}}{bhf_c}$ and $k = \frac{a}{e_{cy}\left(\frac{l}{h}\right)^2}$

In Figure 7.13 the results of the calculations are shown for f_y=200 MPa. N_p is defined in section 7.2.

From Figure 7.13 it appears that a horizontal line governs the load-carrying capacity in a small *l*/*h*-interval. Above this line the column formula valid for yielding of all reinforcement bars (formula (7.40)) is used and below the column formula valid for no yielding in all reinforcement bars (formula (7.38)) is used. The column formula found for yielding only in the top reinforcement bars (formula (7.39)) results in the horizontal part.

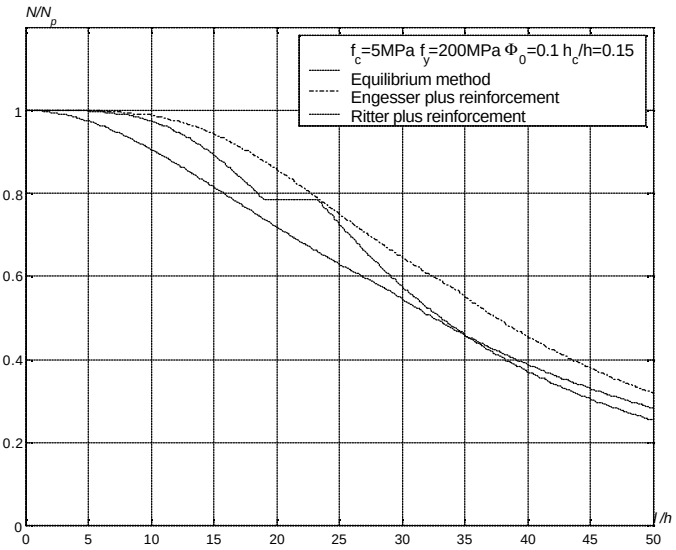

Figure 7.13. Results from calculations for a=8, b=250mm, h=250, E_s=2·10^{5}MPa, e_{cy}=0,2%, f_c=5MPa, f_y=200MPa,F_0=0,10, h_c/h=0,15.

As illustrated in Figure 7.14, formula (7.38) is the only formula used if f_y>400 MPa. With a modulus of elasticity of 2·10^5 MPa for the reinforcement, this means that the yield strain for the reinforcement is the same as, or higher than, the strain a maximum concrete stress

(e_{cy}=0,2%). In general the presence of a horizontal part only depends on whether the yield strain for the reinforcement is higher than the strain at maximum concrete stress or not.

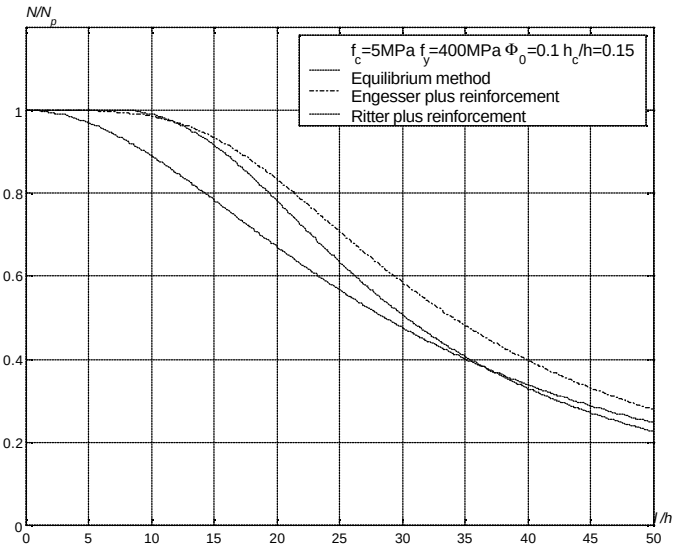

Figure 7.14 Results for a=8, b=250mm, h=250, $E_s=2\cdot10^5$MPa, e_{cy}=0,2%, f_c=5MPa, f_y=400MPa, F_0=0,10, h_c/h=0,15.

The “width” of the horizontal part depends mainly on the degree of reinforcement as may be seen by comparing Figure 7.15 with Figure 7.13 where only the degree of reinforcement is varied. This is as expected since the horizontal part originates from yielding or no yielding of the reinforcement.

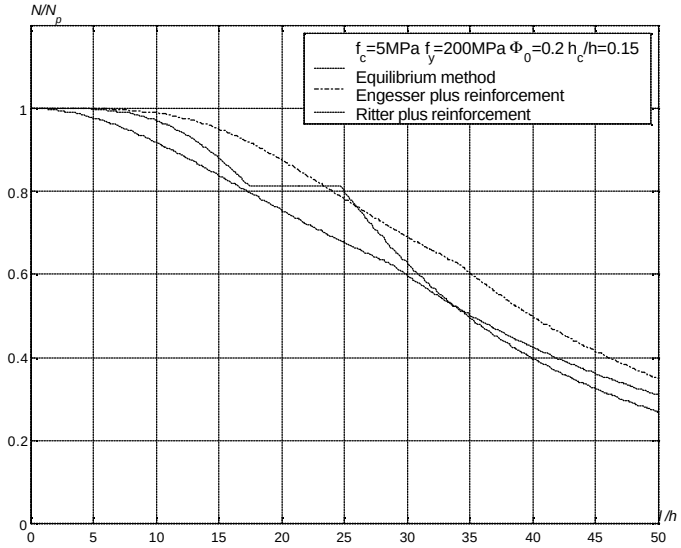

Figure 7.15 Results for a=8, b=250mm, h=250, $E_s=2*10^5$MPa, e_{cy}=0,2%, f_c=5MPa, f_y=200MPa,F_0=0,20, h_c/h=0,15.

As seen in Figure 7.13, Figure 7.14 and Figure 7.15 there are regions where Ritter´s modified column formula overestimates the critical load. This is the case for columns with a *l*/*h*-ratio higher than 40. However, these plots are for a concrete strength of 5 MPa. From Figure 7.16 it appears that there is no overestimation for higher strengths of concrete (in this case 35MPa).

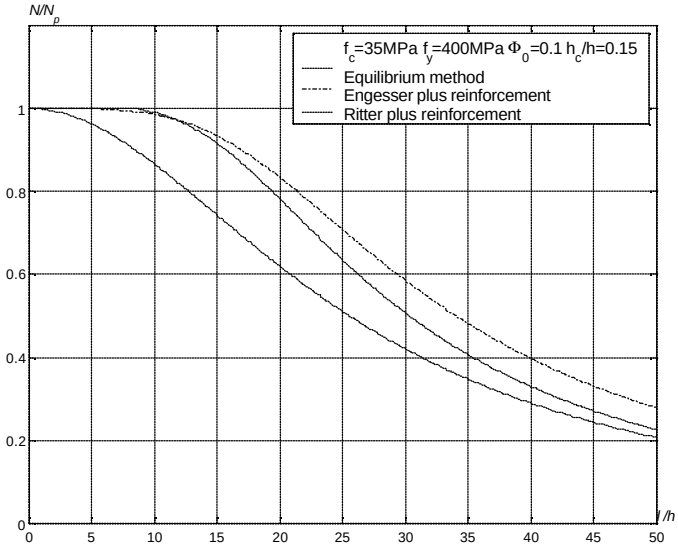

Figure 7.16 Results for a=8, b=250mm, h=250, $E_s=2\cdot10^5$MPa, e_{cy}=0,2%, f_c=35MPa, f_y=400MPa,F_0=0,10, h_c/h=0,15.

The calculations are made under the assumption that the strain at maximum concrete stress remains constant at 0,2%, independently of the compressive strength. This means that the modulus of elasticity changes as a function of the compressive strength. As the strength increases the error in the formula used to express the modulus of elasticity in the Ritter column formula (see section 7.3.1.2.2) gets more pronounced.

In Figure 7.13 to Figure 7.16 a is set to 8. As described in section 7.4.4 a = 8 is a conservative value and normally a is set at 10. If a is set at 10 the critical load found by the equilibrium formulas is almost the same at the critical load found by the modified Engesser formula. This may be seen in Figure 7.17.

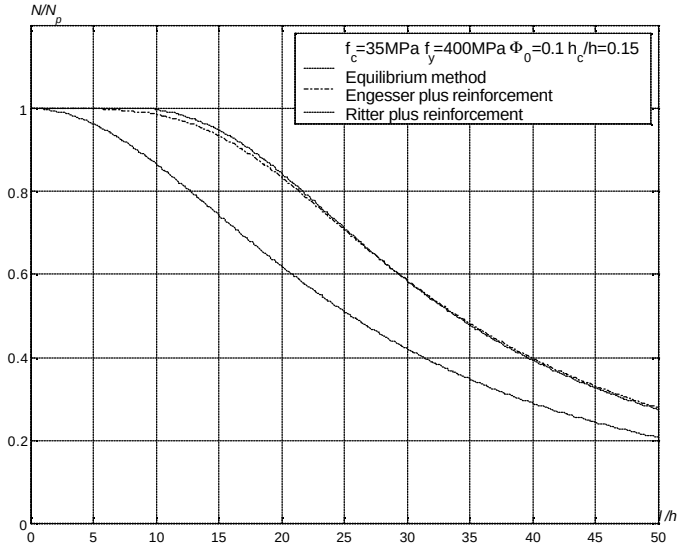

Figure 7.17. Results for a=10, b=250mm, h=250, $E_s=2\cdot10^5$MPa, e_{cy}=0,2%, f_c=35MPa, f_y=400MPa,F_0=0,10, h_c/h=0,15

An interesting result of the equilibrium formulas is found where the yield strain of the reinforcement is high and when the case 37 of Figure 7.11 is used for all slenderness ratios. In this situation the highest critical load is found for a column with a slenderness ratio different from zero. This is illustrated in Figure 7.18. It appears that the maximum critical load in the case considered is found for $l/h \approx 6$. The explanation is the following: The strain is decreasing as the slenderness ratio increases at all times as shown in Figure 7.19. However, since the strain is larger than the yield strain for the concrete for small slenderness ratios the contribution from the concrete to the load-carrying capacity does not decrease with an increasing slenderness ratio. Maximum concrete contribution is of course found where the critical strain equals the strain at maximum concrete and when combined with the contribution from the reinforcement it is evident that maximum is found for a slenderness ratio different from zero.

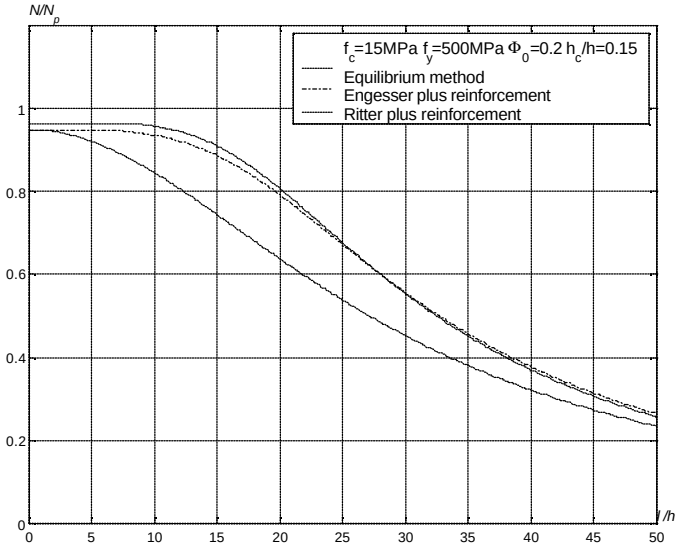

Figure 7.18 Results for a=10, b=250mm, h=250, $E_s=2\times10^5$MPa, e_{cy}=0,2%, f_c=15MPa, f_y=500MPa,F_0=0,20, h_c/h=0,15.

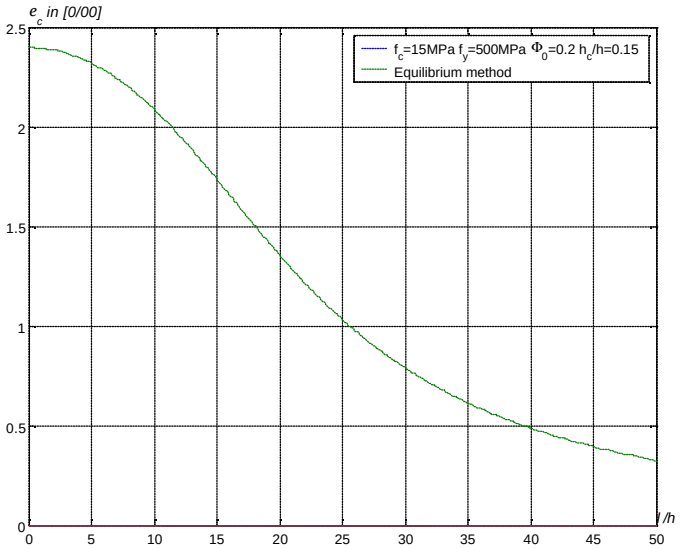

Figure 7.19 Results for a=10, b=250mm, h=250, $E_s=2\times10^5$MPa, e_{cy}=0,2%, f_c=15MPa, f_y=500MPa,F_0=0,20, h_c/h=0,15.

7.4 Beam-columns

7.4.1 Existing methods

7.4.1.1 Stability of linear elastic beam-columns

In this section, the solution of the linear elastic problem for beam-columns is briefly introduced. The load carrying capacity for beam-columns loaded with an eccentric axial load and concentrically axial load along with lateral loading will be derived. These two cases are treated by the equilibrium method.

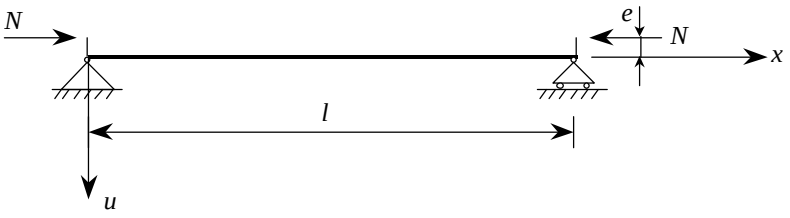

Figure 7.20 Statical system of an eccentrically loaded beam-column

The equilibrium equation for the deflected beam-column loaded with an eccentric axial load becomes:

$$M - M_0 - N \cdot u = 0 \tag{7.41}$$

where $M_0 = Ne$. With $M = -EI \frac{d^2u}{dx^2}$ we get

$$EI \frac{d^2u}{dx^2} + N \cdot (u + e) = 0 \tag{7.42}$$

This is an inhomogeneous second order differential equation, which must be solved with the boundary conditions,

$$\begin{aligned} u(x = 0) &= 0 \\ u(x = l) &= 0 \end{aligned} \tag{7.43}$$

The complete solution is a sum of the homogeneous and one inhomogeneous solution. Equation (7.42) may be rewritten as:

$$\frac{d^2u}{dx^2} + k^2 \cdot (u + e) = 0 \tag{7.44}$$

The solution of (7.44) is:

$$u = A \cdot \sin kx + B \cdot \cos kx + e \tag{7.45}$$

The constants *A* and *B* are determined from the boundary conditions. This gives the following values for A and B.

$$B = 0 \text{ and } A = \frac{e}{\sin kl} \tag{7.46}$$

When (7.46) is inserted into (7.45) equation (7.45), the latter equation with some geometric substitutions are made, becomes:

$$u(x) = \frac{e}{\cos\frac{kl}{2}}\left(\cos\left(\frac{kl}{2} - kx\right) - \cos\frac{kl}{2}\right) \tag{7.47}$$

The maximum deflection is obtained for $x = l/2$

$$u_{\left(x=\frac{l}{2}\right)} = \frac{e}{\cos\frac{kl}{2}}\left(1 - \cos\frac{kl}{2}\right) \tag{7.48}$$

When this solution is inserted into the equilibrium equation the combinations of *N* and *M*, which the beam can carry, may be determined.

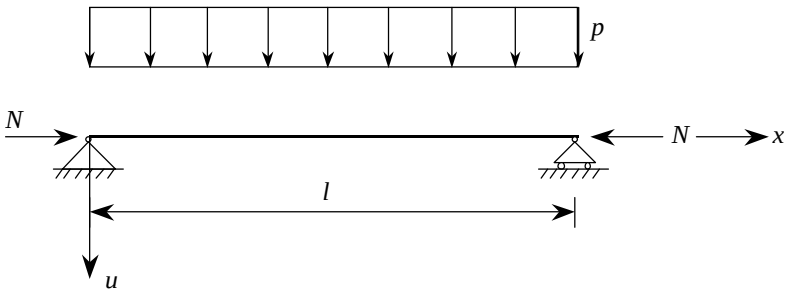

Figure 7.21.Beam-column with lateral load.

For beam-columns with lateral load and a concentrically axial load, the procedure is the same as above. The differential equation is found to be:

$$EI\frac{d^4u}{dx^4} + N\frac{d^2u}{dx^2} = p \tag{7.49}$$

The complete solution is:

$$u = A\cdot\sin kx + B\cdot\cos kx + Cx + D + \frac{px^2}{2N} \tag{7.50}$$

The constants A, B, C and D are found from the boundary conditions

$$u=0,\ x=0:\ B=-D=\frac{p}{k^2N}$$
$$u=0,\ x=l:\ A=\frac{p}{k^2N}\left(\frac{1-\cos kl}{\sin kl}\right)\ \text{and}\ \ C=\frac{pl}{2N} \tag{7.51}$$

The deflection is at maximum in the mid point due to symmetry. The magnitude is determined by:

$$u_{\left(x=\frac{l}{2}\right)}=\frac{5}{384}\frac{pl^4}{EI}\frac{12\left(\sec\frac{kl}{2}-2-\frac{1}{4}(kl)^2\right)}{5\left(\frac{kl}{2}\right)^4} \tag{7.52}$$

It is seen from equation (7.52) that the deflection is equal to the deflection for the laterally loaded beam multiplied by a factor. For further details see [3] and [5].

7.4.2 Danish Code of Practice, DS411

In DS411 "Method I" is valid for calculation of the load-carrying capacity of beam-columns. This method is based on a linear elastic material behaviour for concrete in compression with a modulus of elasticity for section analysis equal to $500f_c$. The maximum compressive stress is given by equation (7.53)

$$f_c^*=\begin{cases}1{,}25\,f_c\\ 1{,}25\,f_c\left(1-0{,}2\frac{s_{c,\min}}{f_c}\right)\end{cases} \tag{7.53}$$

The maximum stress in the concrete in the case of cracked cross-section is determined by the upper equation in (7.53). When the entire cross-section is in compression the maximum stress is determined by the lower equation in (7.53).

Based on the assumptions stated above a cross-section analysis is performed and based on the stress state the deflection is calculated as:

$$u=\frac{1}{10}\frac{s_{c,\max}-s_{c,\min}}{E_{cr}\Delta h}l^2 \tag{7.54}$$

where $s_{c,\min}$ is set equal to zero when the cross-section is cracked and Δh is the distance between the levels of the section with the stresses $s_{c,max}$ and $s_{c,min}$, respectively. To include the non-linear behaviour of the concrete a modulus of elasticity (E_{cr}), which vary with the stress state, is introduced. This is calculated as:

$$E_{cr}=\left(1-k\frac{s_{c,\max}}{f_c}-(1-k)\frac{s_{c,\min}}{f_c}\right)E_{0cr} \tag{7.55}$$

where

$$k = 0{,}8 - 400\frac{f_c}{E_{0cr}} \tag{7.56}$$

and

$$E_{0cr} = \min\begin{cases}1000\, f_c \\ 0{,}75 E_0\end{cases} \tag{7.57}$$

This modulus of elasticity is only used for the calculation of deflections.

The calculations using this method are compared with the equilibrium method in Figure 7.22. The equilibrium method is described in the next section.

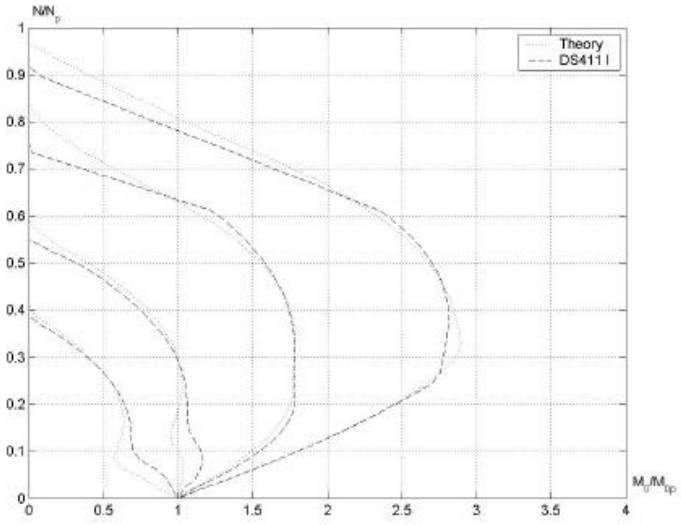

Figure 7.22 The Danish Code of Practice method compared with the equilibrium method

The agreement is seen to be good.

In the Danish Code of Practice, another method is suggested. This method is referred to as "Method II". The procedure is to calculate the maximum moment and axial load from a cross-section analysis, where the stress block of the concrete is a square with the maximum stress equal to f_c and the extent of 4/5 y_0. From this, the load-carrying capacity is calculated from the equilibrium equation with the deflection set as

$$u = \frac{1}{a}\frac{e_{cu} + e_{sy}}{h_e} l^2 \tag{7.58}$$

The deflection calculation assumes that the reinforcement yields. The deflection obtained from equation (7.58) is often conservative, however in the case of columns where material failure determines the load carrying capacity it is a good approximation.

In Figure 7.23, Method I and Method II are compared with the statical equivalence method. The calculations are made for a rectangular cross-section where $h = b = 250$ mm, $h_c' = h_c = 20$ mm, $A_s = A_s' = 2\frac{p}{4}16^2$, $f_y = 500$ MPa, $f_c = 20$ MPa and l/h=10.

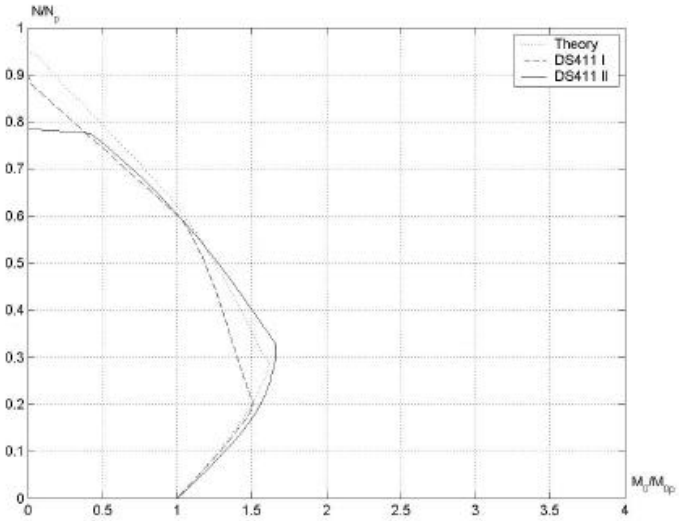

Figure 7.23 Calculation made by the theory using parabolic stress block, Method I and Method II

It is seen that if $M_0/M_{0p} = 1{,}5$ the maximum axial load obtained by using Method I is 0,2 N_p and 0,4 N_p by using Method II. This means using Method II leads to an increase of 50 % in load-carrying capacity.

However, as the slenderness is increased Method II becomes conservative as illustrated in Figure 7.24.

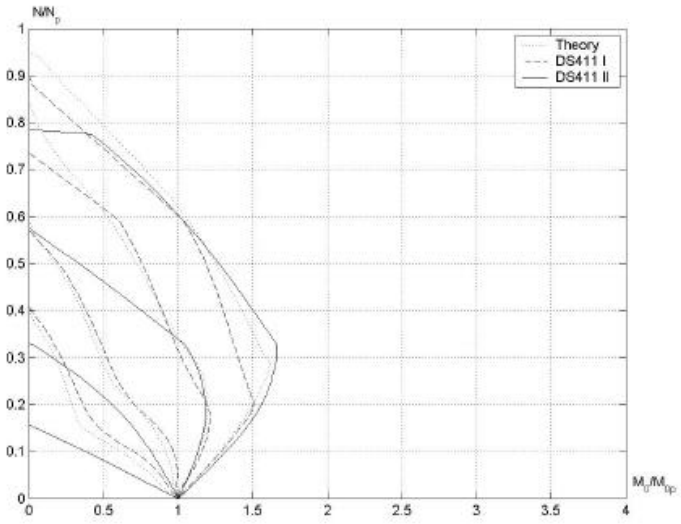

Figure 7.24 Calculations for l/h=10, 20, 30 and 40

7.4.3 Moment-curvature relation

To describe the behaviour of a beam-column one needs the moment curvature relationship. The load-carrying capacity for a given axial load may either be determined from the moment – curvature diagram or from an applied moment – curvature diagram.

For a columns with a given length, loaded with a given axial load, the right-hand side of the equilibrium equation, (7.59),

$$M = M_0 + Nu \tag{7.59}$$

for a deflected beam element may be plotted as a straight line in the moment curvature diagram. The inclination of the line is proportional to the axial load. The intersection points of the straight line and the moment-curvature relationship determine the deflections possible for a given load. Thus the whole curve showing the applied moment, M_0, as a function of the curvature may be constructed as shown in Figure 7.25. It is seen that the maximum applied moment corresponds to the point where the straight line is a tangent to the moment-curvature diagram. In the case shown in Figure 7.25 the maximum load corresponds to the point where yielding in the bottom reinforcement begins. Another case is illustrated in Figure 7.26 where maximum load is found before yielding in the bottom reinforcement begins. The transition point between the two cases corresponds to a change from case 31 to 32. The case numbers are shown in Figure 7.27.

The situation shown in Figure 7.26 only occurs for slender beam-columns. Figure 7.26 has been drawn for a length-height ratio of 35.

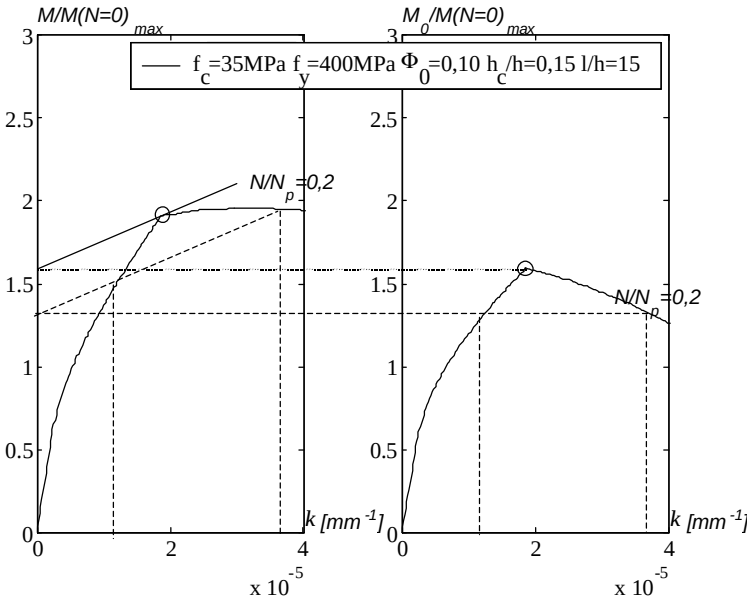

Figure 7.25. Moment versus curvature and applied moment, M_0, versus curvature.

Figure 7.25 also shows that the straight line may intersect the moment curvature diagram in two points, which enables the applied moment variation with the curvature to have a downward section as shown in Figure 7.25 (right hand side of the figure). Furthermore, this means that the beam-column is stable for curvatures smaller than or equal to the curvature corresponding to the point where the straight line is a tangent to the moment curvature diagram. For other applied loads, the beam-column is unstable.

The combinations of M_0 and N, corresponding to critical loads of the beam, are most easily found from the applied moment curvature relationship. For one level of the axial load, a unique M_0 –k-relationship exists and the maximum of this curve is the critical combination of N and M_0.

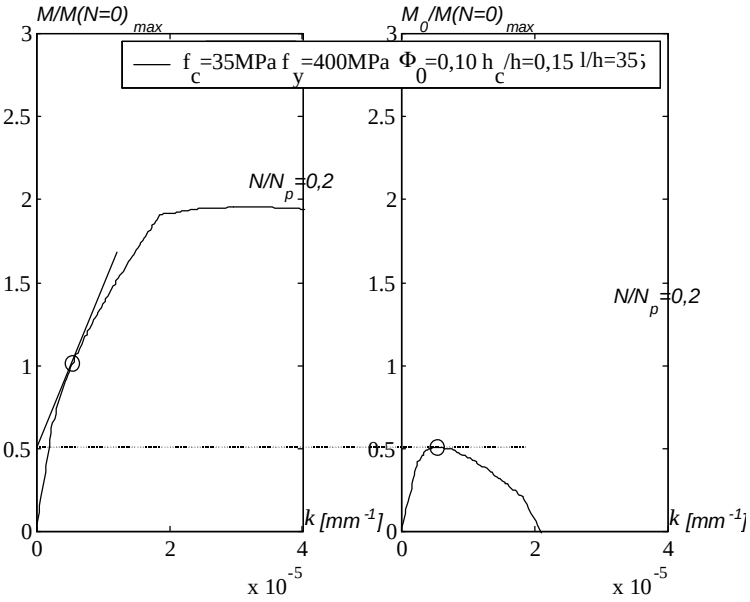

Figure 7.26 Moment versus curvature and applied moment versus curvature.

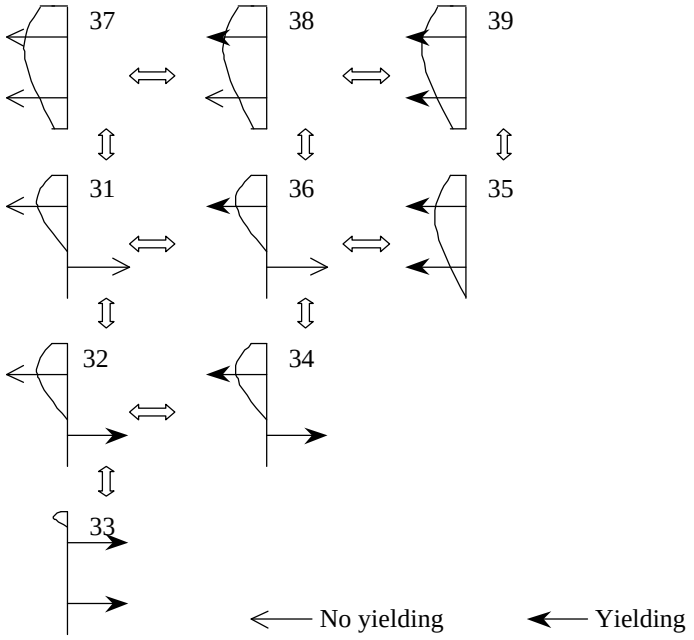

Figure 7.27 The moment curvature relationship is based on nine cross-section analyses.

Cross-section analysis is carried out expressing statical equivalence between the sectional forces (stress resultants) and the stresses.

The different situations are shown in Figure 7.27, where the cases are numbered from 31 to 39.

The procedure in each case is for a certain axial load and concrete strain to find the distance from the top face of the cross-section to the neutral axis (y_0) by solving the projection equation and then calculate the moment and the curvature.

The case 31 is shown in Figure 7.28, with the notation used.

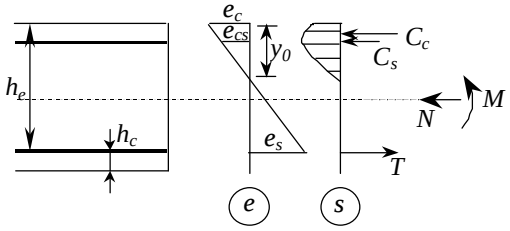

Figure 7.28 Stress and the strain distribution in cross-section analysis

The variation of the stresses and the strains is described in section 7.2.

The projection equation is

$$N = C_c + C_s - T$$

where

$$C_c = b\int_0^{y_0} s_c dy$$

$$C_c = b\int_0^{y_0} f_c \frac{e_c \frac{y}{y_0}}{e_{cy}}\left(2 - \frac{e_c \frac{y}{y_0}}{e_{cy}}\right)dy = \frac{f_c b}{e_{cy}} e_c \left(1 - \frac{e_c}{3e_{cy}}\right) y_0$$

$$C_s = s_{cs} A_{sc} = e_{sc} E_s A_s = \frac{y_0 - h_c}{y_0} e_c E_s A_{sc}$$

$$T = s_s A_s = e_s E_s A_s = \frac{h_e - y_0}{y_0} e_c E_s A_{sc}$$

The moment equation is

$$M = M_c + C_s(y_0 - h_c) + T(h_e - y_0) + N\left(\frac{h}{2} - y_0\right)$$

where

$$M_c = b\int_0^{y_0} s_c y dy$$

$$M_c = b\int_0^{y_0} f_c \frac{e_c \frac{y}{y_0}}{e_{cy}}\left(2 - \frac{e_c \frac{y}{y_0}}{e_{cy}}\right) y dy = \frac{f_c b}{e_{cy}} e_c \left(\frac{2}{3} - \frac{e_c}{4e_{cy}}\right) y_0^2$$

By solving these equations for the nine cases the M-k relationship and the M_0-k relationship may be obtained for a specific beam-column.

In the following the data listed in Table 7.1 are used if nothing else is noted.

In Figure 7.29 the M-k -relationship is shown. The dependency of the degree of reinforcement ratio, the compressive strength and the yield strength can be seen in Figure 7.29.

b [mm]	h [mm]	h_c [mm]	l [mm]	f_c [MPa]	e_{cy} [‰]	f_y [MPa]	Φ_0 []
250	250	20	3000	15	2	300	0.05

Table 7.1. The data used in present calculations if other values are not listed.

The value of the axial load used in Figure 7.29 is 2/9 N_p.

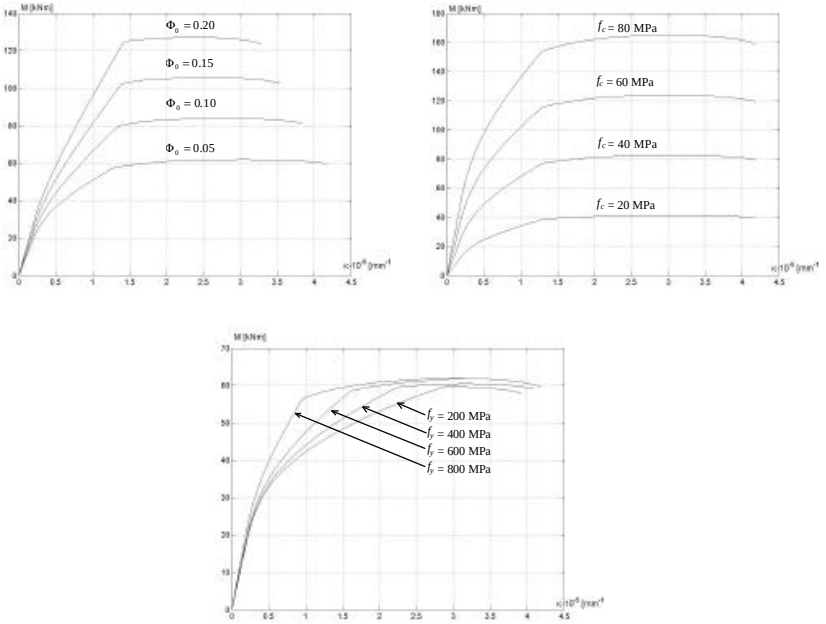

Figure 7.29 Moment curvature relationship when the degree of reinforcement, the compressive strength and the yield strength are varied. Normal force 2/9 N_p

In Figure 7.30 and Figure 7.31, the data as listed in Table 7.1 are used to illustrate the variation of the M-k relationship and M_0-k relationship for different axial loads:

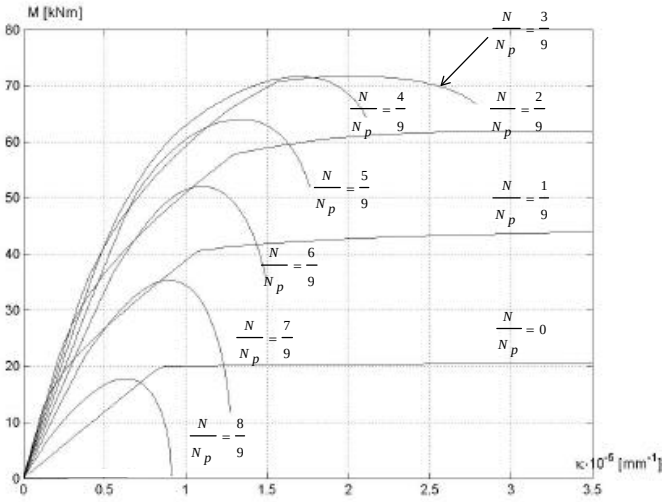

Figure 7.30 Moment-curvature relationship for different axial loads

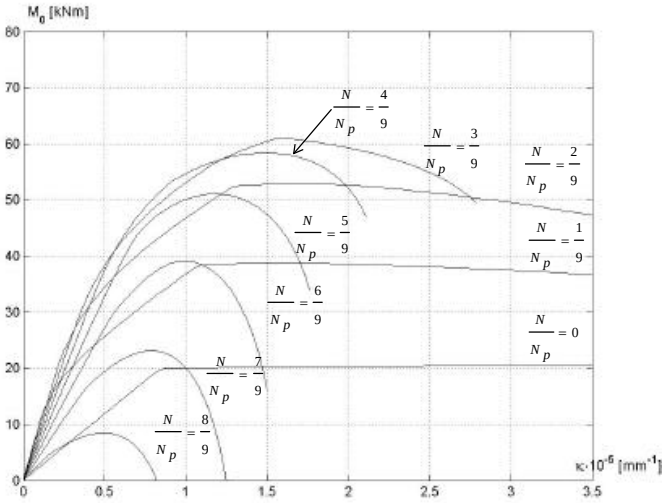

Figure 7.31 Applied moment-curvature relationship for the same axial loads as in Figure 7.30

$\frac{N}{N_p}$	M-interval in kNm	Case
0	$0 \le M \le 20$	31
	$M \ge 20$	32
$\frac{1}{9}$	$0 \le M \le 10$	37
	$10 \le M \le 40$	31
	$M \ge 40$	32 and 34
$\frac{2}{9}$	$0 \le M \le 20$	37
	$20 \le M \le 58$	31
	$58 \le M \le 60$	32
	$M \ge 60$	32 and 34
$\frac{3}{9}$	$0 \le M \le 29$	37
	$29 \le M \le 65$	31
	$M \ge 65$	34 and 36
$\frac{4}{9}$	$0 \le M \le 38$	37
	$38 \le M \le 60$	31
	$M \ge 60$	36
$\frac{5}{9}$	$0 \le M \le 45$	37
	$45 \le M \le 51$	31
	$M \ge 51$	36
$\frac{6}{9}$	$0 \le M \le 35$	37
	$M \ge 35$	36 and 38
$\frac{7}{9}$	$0 \le M \le 12$	37
	$M \ge 12$	37 and 38
$\frac{8}{9}$	$0 \le M \le 7$	37 and 38
	$M \ge 7$	38

Table 7.2 The situations for which the moment curvature relationship is calculated

Table 7.2 shows that a great variety of N levels may be described by the same cases. All curves in Figure 7.30 except for $N = 0$ starts in situation 37, where the entire cross section is in compression, then the case changes to one of the cases where the compression zone is smaller than the depth of the cross section. For $\frac{N}{N_p} \le \frac{5}{9}$ the case after 37 is 31 (dependent on the degree of reinforcement). For N larger than this level the case will be 36 since the axial

load is large and therefore the top face reinforcement yields (also dependent on the reinforcement ratio). The moment-curvature relationship changes its shape for an N level above 3/9. At this level the compressive reinforcement begins to yield before the tension reinforcement yields indicating that the depth of the cracked part of the cross section is reduced. After this level there is no slope discontinuity in the moment-curvature relation.

7.4.4 Deflection shape and comparison with simplified method

Up to now the mid point deflection has been calculated as

$$u_m = \frac{1}{a} k l^2 \tag{7.60}$$

In this section, an analysis of the deflection of the entire beam-column is carried out. This analysis is made for an eccentrically loaded beam-column simply supported at both ends. The analysis is done iteratively by subdividing the beam into smaller sections. In Figure 7.32 the procedure is illustrated by a flow diagram.

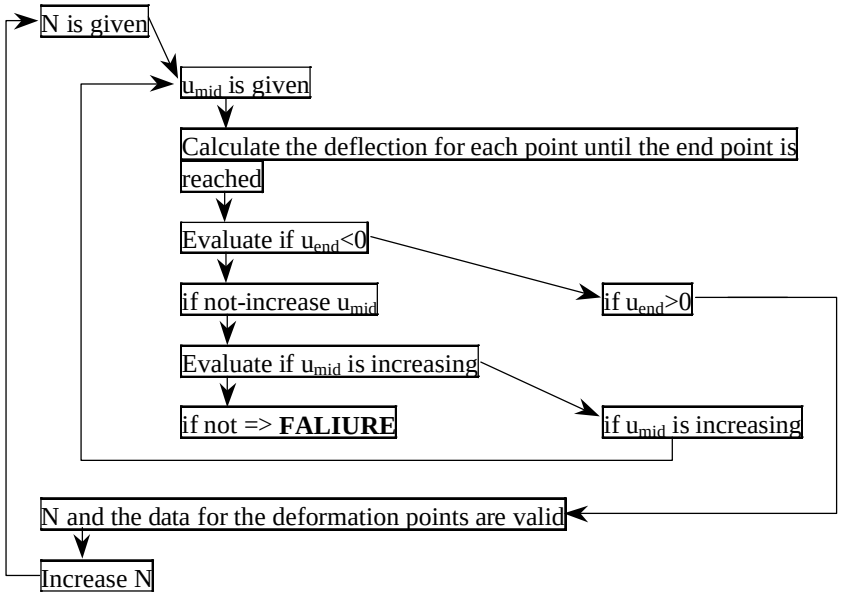

Figure 7.32. Flow diagram for deflection calculations.

As seen, the deflection is found by varying the axial load until failure occurs. The deflections are calculated from the midpoint towards the end. The deflection in the midpoint is increased gradually until the deflection at the end points are zero, unless an increase in the midpoint deflection does not lead to an increase of the end point deflections. If an increase in the

midpoint deflection does not lead to an increase in the end point deflections the beam-column will fail at the corresponding value of the axial load[2].

The deflection has been calculated assuming each beam section to have constant curvature.

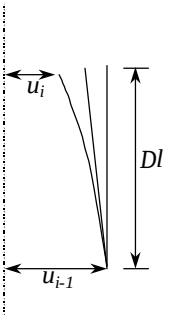

$$u_i = u_{i-1} - \frac{1}{2} k_{i-1} \Delta l^2 - u'_{i-1} \Delta l$$

$$u'_i = k_{i-1} \Delta l + u'_{i-1}$$

Figure 7.33. Calculation of deflections.

In Figure 7.34 plots of the calculations are shown for two beam-columns with different lengths. These plots show the variation of the curvature (the plots on the left) and the deflection along the beam-column (to the right). For the two plots showing the variation of the curvature, lines of constant curvature and lines of a triangular curvature are shown. If the curvature is constant a in (7.60) is 8 and for triangular one a is12.

[2] This corresponds to accelerations perpendicular to the beam axis

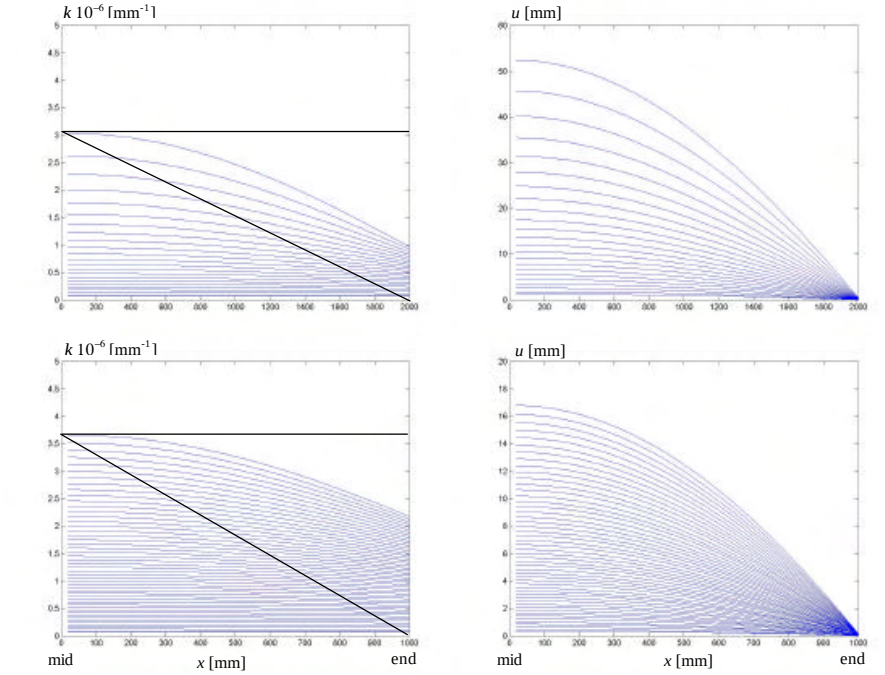

Figure 7.34. Left: Curvature as a function of the length (measured from the midpoint of the beam-column).Right: Deflection as a function of the length for two beam-columns. The plots in the top are for a beam-column with a total length of 4000mm and the plots in the bottom are for a beam-column with a total length of 2000mm .They both have a cross-section of 100x100mm^2, $A_s=A'_s=50mm^2$, $h_c=h'_c=10mm$, $e=50mm$,$f_c=30MPa$,$f_y=400MPa$ and $e_{cy}=0,2\%$.

As seen the curvature found from a more thorough analysis, is somewhere between constant and triangular. The beam-column with a length of 2000mm (the bottom) is seen to be closer to a constant curvature (a=8) than the beam-column with the length of 4000mm. This is as expected since a short beam-column will have almost a constant curvature and a long beam-column will have an almost triangular variation of the curvature. A long eccentrically loaded column actually has a curvature variation, which may be described as a combination of a constant and a sine-function as for linear elastic beam-columns, since the concrete will behave almost linear elastic in this case.

Although the plots are only valid for two beam-columns the behaviour is the same for any beam-column.

No quantitative evaluation of the error made by using (7.60) and $a = 10$ is made in this paper. Such an evaluation would depend on many geometrical and physical parameters and the form of loading. It is believed that the error is of minor importance.

The procedure described above may also be used to determine the behaviour of a beam-column when proportionally loaded. In Figure 7.35 the calculations are compared with measured load deflection curves. The main data are given in Table 7.3. In these plots both the model taking into account the actual variation of the curvature (solid) and the simplified model (dashed) with $a = 10$ are plotted.
Results are also shown from some of the test described in section 12.5. In some of these tests load cycles with loading and unloading have been applied. The main data of the tests are also given in Table 7.3.

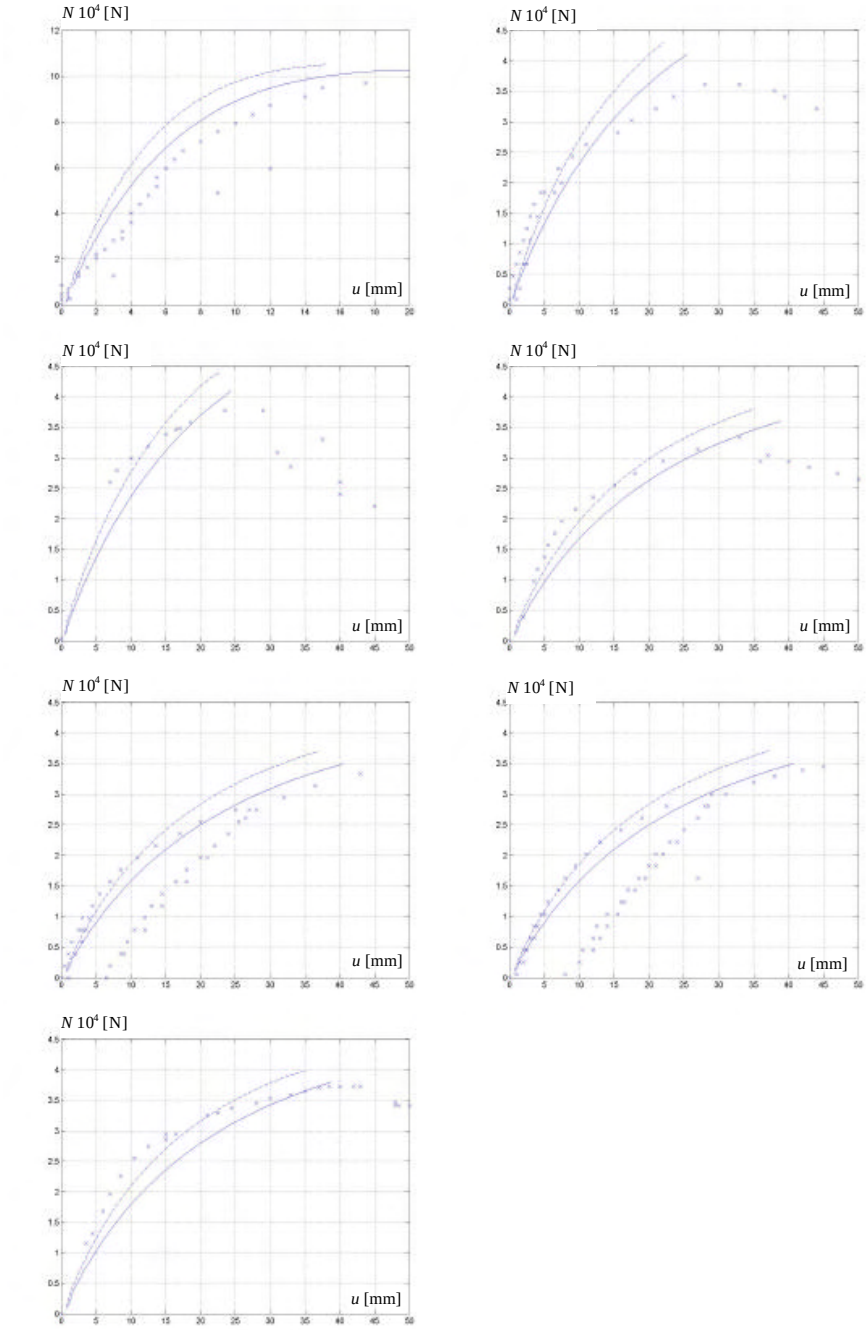

Figure 7.35.Results of calculations plotted along with measurements for beam-column I_5, II_4, II_5, III_1, III_2, III_3, III_4 (in that order) taken from [17]. The x-axis shows the deflection in the midpoint in mm and the y-axis is the axial load in N.

		I_5	*II_4*	*II_5*	*III_1*	*III_2*	*III_3*	*III_4*
Age	[days]	22	11	3	25	25	25	15
L	[mm]	2940	2940	2940	3540	3540	3540	3540
b	[mm]	154	154	154	154	154	154	154
h	[mm]	100	100	100	100	100	100	100
e	[mm]	20	50	50	50	50	50	50
h_c=h_c'=	[mm]	12,5	12,5	12,5	12,5	12,5	12,5	12,5
W_n*	[kg/cm^2]	327,0	307,0	322,0	335,0	292,0	290,0	396,0
*Conversion factor***	[]	0,80	0,80	0,80	0,80	0,80	0,80	0,80
f_c	[MPa]	25,7	24,1	25,3	26,3	22,9	22,8	31,1
e_{cy}	[$^0/_{00}$]	2,0	2,0	2,0	2,0	2,0	2,0	2,0
fy	[kg/cm^2]	2942,3	2787,5	2776,3	3332,5	3320,0	3325,0	3333,0
fy	[MPa]	288,6	273,5	272,4	326,9	325,7	326,2	327,0
A_s= A_s'=	[mm^2]	77,0	77,0	77,0	77,0	77,0	77,0	77,0
A_s/A_c	[%]	1,0	1,0	1,0	1,0	1,0	1,0	1,0

* W_n is the compressive strength of a cube 200x200x200mm^3.

** The conversion factor is the relation between the cube strength and the cylinder strength.

Table 7.3. Main data for the beam-column tests in [17]

The predictions of the behaviour of the beam-columns show good agreement with the measurements. It is seen that the model accurately taking into account the variation of the curvature along the beam column overestimates the deflection for low axial load. This is as expected since the model neglects the tensile strength of concrete, which has a significant influence for low axial load.

The calculations and the comparisons with test demonstrates that the simplified model is sufficiently accurate for the analysis in this paper and for practical purposes.

7.4.5 Simplification of the moment-curvature relationship

Since the detailed calculation of the moment-curvature relation for a beam-column is not suitable for practical design a simplification is desired. The simplification suggested here

consist of choosing a few characteristic points on the curve and then simplifying the curve with straight lines through the characteristic points.
In Figure 7.36, the moment-curvature relation is plotted along with some important point related to the cases in Figure 7.27.

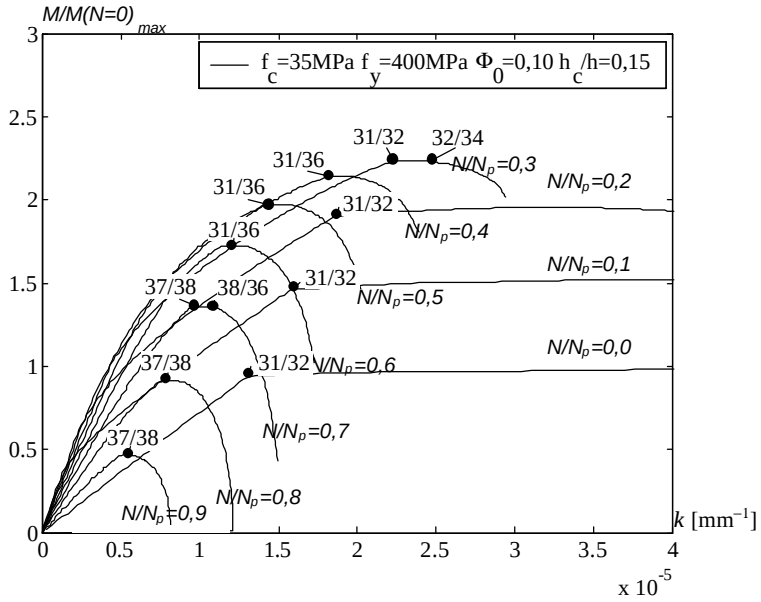

Figure 7.36. Moment-curvature relation and transition points for the different cases (see Figure 7.27).

From Figure 7.36 it is seen that the points of interest are the transition points between the following cases.

31/32	yielding in the bottom
31/32 → 32/34	yielding in the bottom → yielding in both top and bottom
31/36	yielding in the top
37/38 → 38/36	yielding in the top → $y_0<h$
37/38	yielding in the top

Figure 7.36 shows that the peak of the moment-curvature diagram is reached where yielding occurs in the bottom for low axial loads and in the top for high axial loads. A distinction between a low and a high axial load may be found by considering the situation where yielding in both top and bottom occurs simultaneously. It is seen, that the plot for N/N_p=0,3 has a small flat part. If the axial load is increased, this flat part will narrow into a point. This is the point where yielding occurs in the top and the bottom simultaneously.

For high axial loads, a straight line from the origin to the peak is a good approximation to of the curve. The curve after the peak is of no importance since the intersection with the straight load line always takes place before or at the peak. In Figure 7.36, the criterion for high axial load would be that N is larger than approximately $0{,}7N_p$. In general terms this is the axial load for which the moment calculated by assuming yielding in the top in the uncracked state ($y_0>h$) is larger than the moment calculated by assuming yielding in the top in the cracked state ($y_0<h$).

For axial loads lower than this level, a calculation of a second point is needed in order to have a good approximation. It is obvious that an important situation is the transition from the uncracked to the cracked cross-section. In addition, the situation where the bottom reinforcement changes from tension to compression is of interest. The points marking these situations are shown in Figure 7.37.

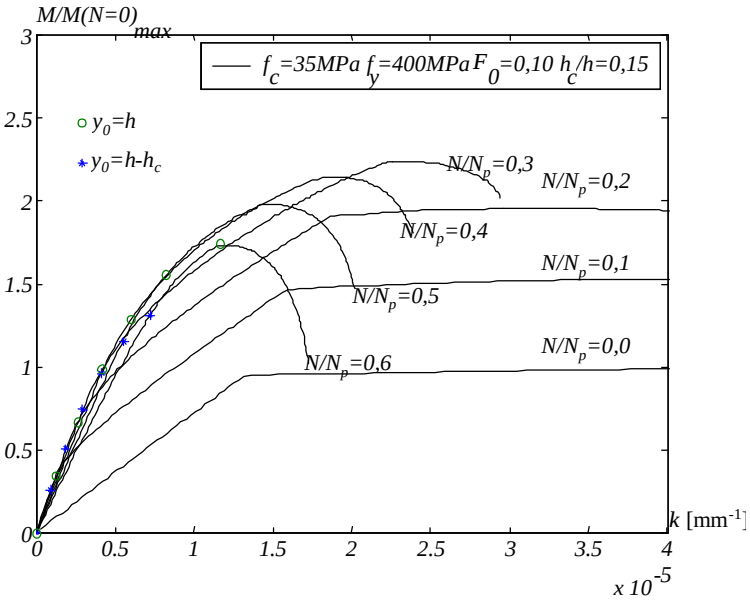

Figure 7.37. Moment- curvature relation and transition points.

The point corresponding to zero stress in the bottom reinforcement seems to be the best point to choose. Of course, the approximation is improved if several points are used, but it is believed that two points are sufficient.

In Figure 7.38 and Figure 7.39, the simplified moment-curvature relations are shown for different axial loads.

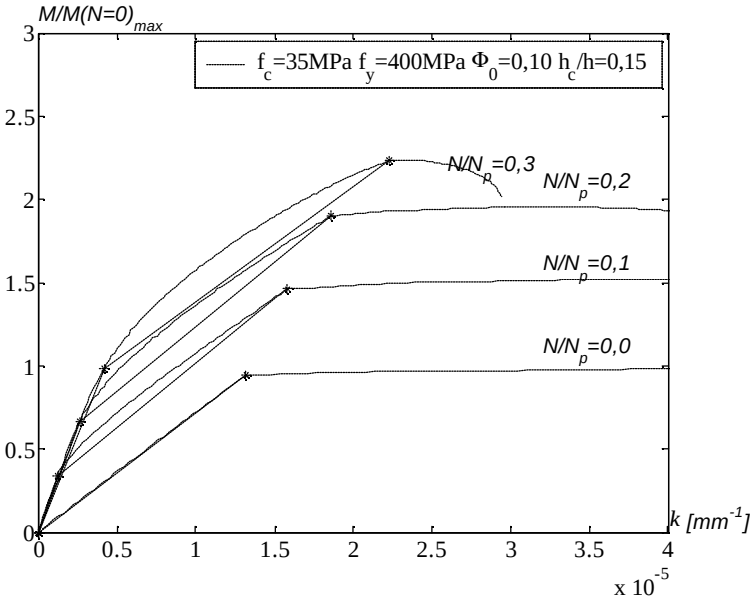

Figure 7.38. Moment-curvature relations and simplified moment-curvature relations for low axial loads.

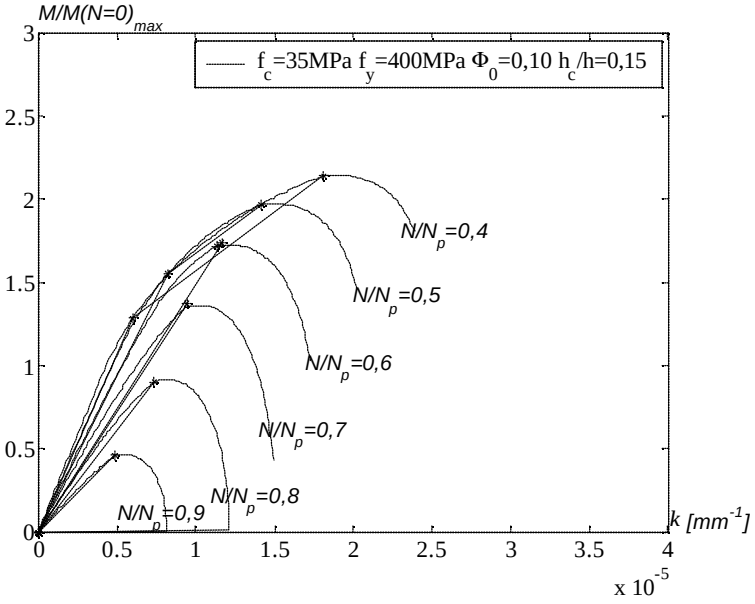

Figure 7.39. Moment-curvature relations and simplified moment-curvature relations for high axial loads.

The simplified moment-curvature relation is used in stead of the correct one as explained previously. Thus the maximum value of the applied moment may be determined for a given

axial load. Examples are shown in Figure 7.40 to Figure 7.43 where calculations are presented for two different *l/h*-ratios and various levels of axial load.

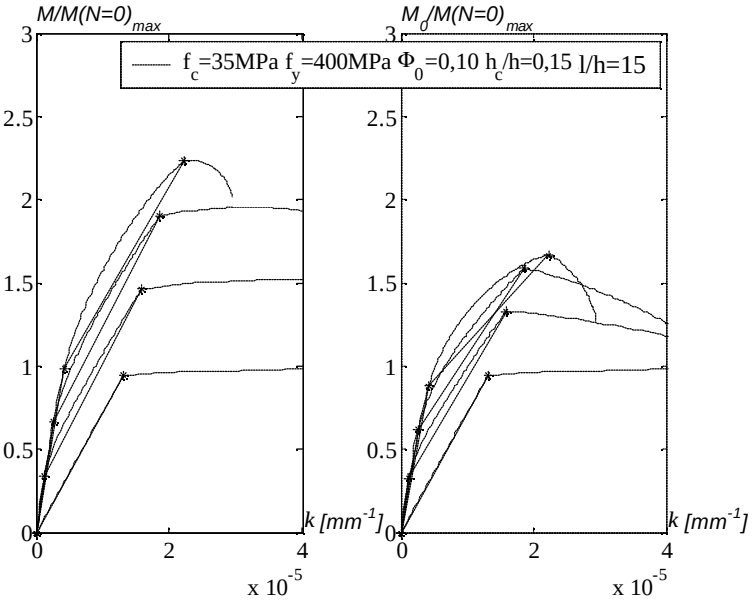

Figure 7.40. Moment-curvature relations (simplified and not simplified) and applied moment-curvature relations (simplified and not simplified).

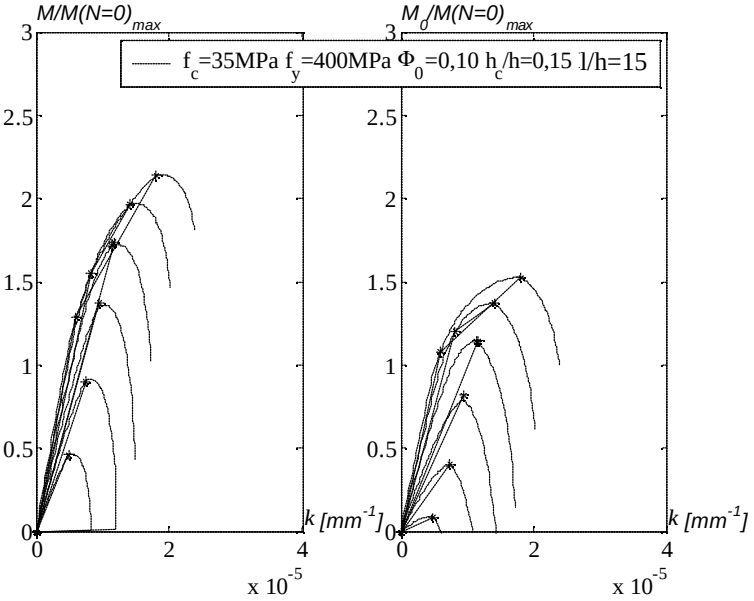

Figure 7.41. Moment-curvature relations (simplified and not simplified) and applied moment-curvature relations (simplified and not simplified).

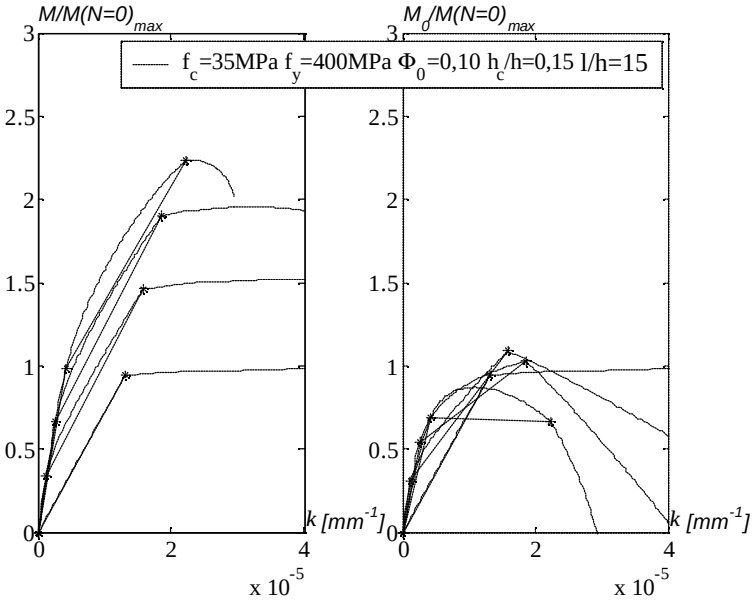

Figure 7.42. Moment-curvature relations (simplified and not simplified) and applied moment-curvature relations (simplified and not simplified).

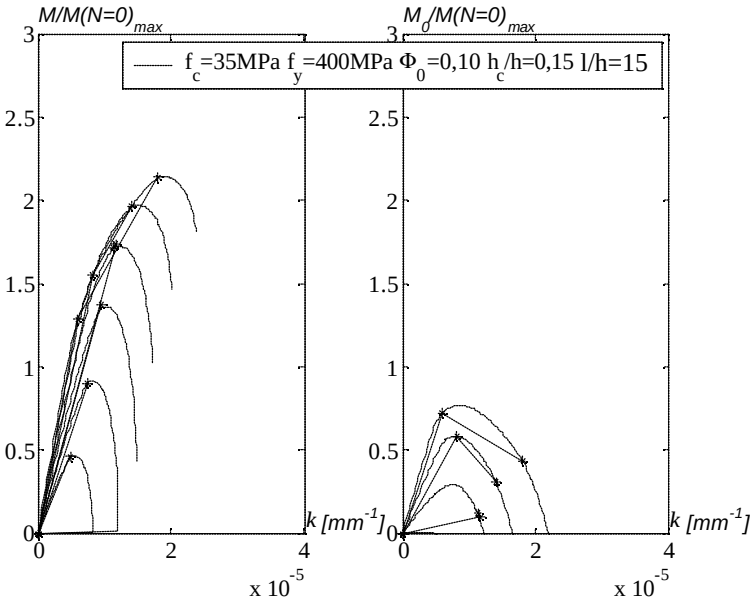

Figure 7.43. Moment-curvature relations (simplified and not simplified) and applied moment-curvature relations (simplified and not simplified).

It appears that the point calculated for zero stress in the bottom reinforcement becomes critical as the slenderness increases.
The accuracy of the proposed approximation seems to be sufficient for most practical purposes.

7.4.6 Interaction diagrams

In practice a beam-column is often subjected to different levels of axial load and applied moment. Therefore, it is convenient if an interaction curve for axial load versus applied moment is available. Such curves may be established by calculating the maximum applied moment for an adequate number of axial loads.
The load-carrying capacity is influenced by the degree of reinforcement and the slenderness ratio, see Figure 7.44 and Figure 7.45.
In Figure 7.44 the length, *l*, is small so instability is of no importance for the load-carrying capacity.

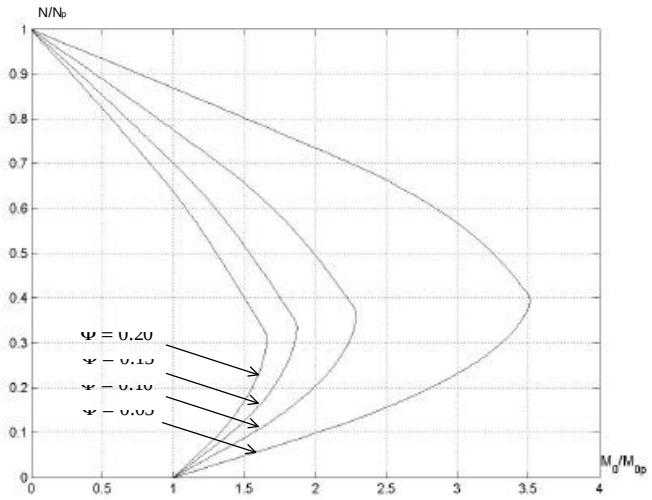

Figure 7.44 Influence of the degree of reinforcement. Other data as in Table 7.1

Figure 7.44 shows that the effect of axial load on the load-carrying capacity is pronounced for low degrees of reinforcement.

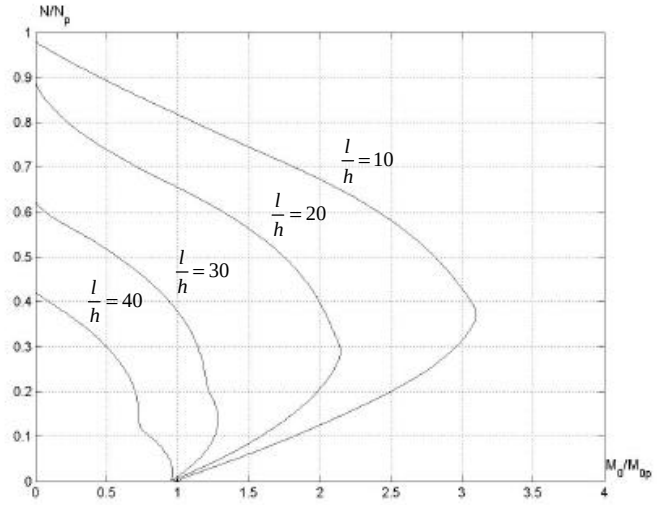

Figure 7.45 Influence of the slenderness ratio. Other data as in Table 7.1.

Figure 7.45, which has been calculated for $\Phi_0 = 0.05$, shows that the load carrying-capacity is also strongly influenced by the slenderness ratio. A radical change in the form of the interaction diagram takes place when the beam-column becomes slender (see for example the curve drawn for $l/h = 30$).

The interaction diagrams in Figure 7.45 are not convex. A convex curve is a curve, which intersects a straight line in only two points. Otherwise the curve is non-convex see Figure 7.46.

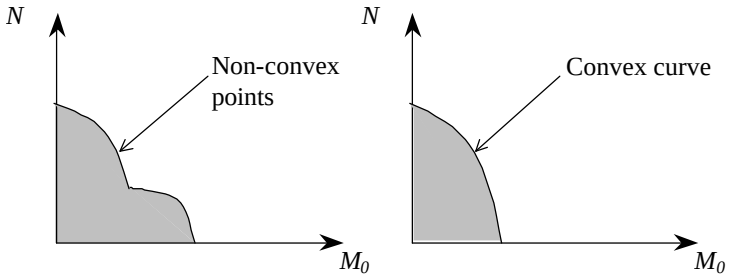

Figure 7.46. Non-convex and convex curves

7.4.7 Simplification of interaction diagrams

The method described above is only suitable for calculations on a computer. For design purposes, a hand calculation method may be desirable. This section sets out to establish a

simplified interaction diagram based on a parabolic stress-strain relationship as above. Further simplifications are made in section 7.4.8.

When establishing a simplified interaction diagram it may be of interest to notice, that, since the moment-curvature relation is a convex curve, a point different from the correct intersection point may always be used to determine the applied moment. This is illustrated in Figure 7.47.

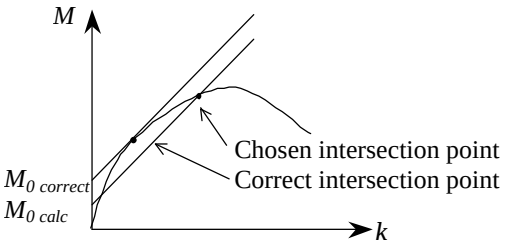

Figure 7.47. Choice of a safe intersection point.

From Figure 7.47, it appears that a calculation of the applied moment from a point different from the correct tangent point always leads to a lover value of the applied load.
This theorem is useful when it comes to determine the interaction diagram. The points used in the calculations do not necessarily have to be the tangent points.

Further simplifications are made by studying moment-curvature relations for a beam-column such as the ones illustrated in Figure 7.48. It is seen that for axial loads lower than approximately 0,3 N_p there is an almost straight part on the curves. The first assumption made is that this part is a straight line and the second assumption is that the straight parts for each level of axial load are parallel, cf. Figure 7.48.

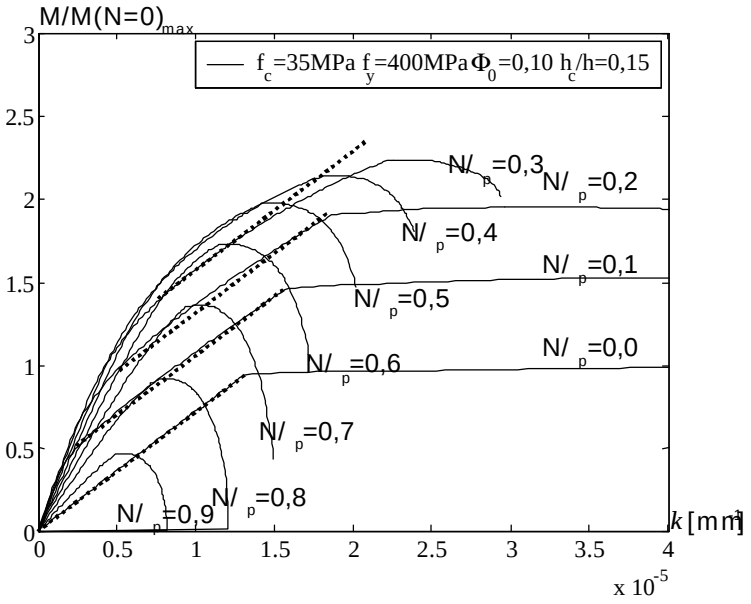

Figure 7.48. Moment-curvature relations.

As seen these simplifications are fairly accurate until the axial load reaches a certain level. This level may be determined by considering the situation where the yield strain is reached at the bottom as well as at the top.

Consider first the situation where the axial load is low (say lower than 0,3 N/N_p). In this case the inclination of the straight part may be set equal to the inclination of the curve valid for pure bending. It appears from Figure 7.49, that the inclination of the line *a* and the inclination of the line *b* is the same and may be calculated as:

$$\frac{dM}{dk} = \frac{M_Y(N=0)}{k_Y(N=0)} \tag{7.61}$$

Here (k_Y,M_Y) is the point where the yield strain is reached at the bottom.

In Figure 7.49 the line *(1)* and the line *(2)* are two load lines for a given beam-column and a given axial load. Since the deflection may be calculated from the curvature in the mid point, the inclination of the load curve may be found as:

$$\frac{dM}{dk} = N\frac{1}{a}l^2 \tag{7.62}$$

If the moment-curvature relation is given by the line *a* or the lines *b* and *c*, there is one level of axial load where the inclination of the load lines are the same as the inclination of the line *b*. In this situation, the applied moment may be found by using any point on the line *b*. For a

slightly higher axial load, the applied moment is found using point *A* and for an infinitesimally lower axial load, the applied load is found using point *B*.
Point *A* and *B* changes along with the axial load. However, since the inclination of the line between these points is constant the applied moment for a steep load line *(1)* is determined by the *A*-point and the specific axial load and the specific length of the beam-column.

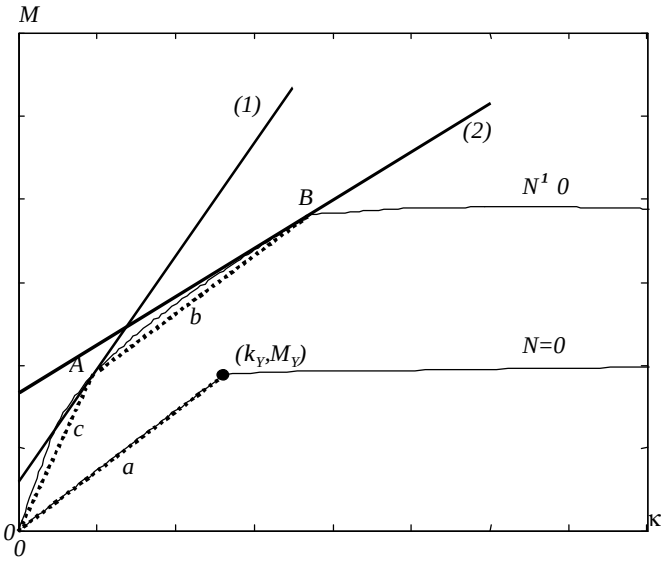

Figure 7.49. Moment-curvature relations composed of straight lines.

The inclination of line the *a* may be used to determine whether the applied moment has to be found from an *A* or a *B*-point. Such a distinction may always be made since it does not effect the calculation of the applied moment directly, but only decides from which point the applied moment has to be calculated. Keeping in mind that a calculation of the applied moment from any other point than the tangent point will lead to a lower value of the applied moment, it appears that the distinction might lead to a poor, but always safe result.
The axial load, which governs whether the calculation of the applied moment has to be found using an *A* or a *B*-points, is named N_i and is determined by inserting (7.61) into (7.62):

$$N_i \frac{1}{a} l^2 = \frac{M_Y\left(N=0\right)}{k_Y\left(N=0\right)}$$
$$N_i = \frac{a\, M_Y\left(N=0\right)}{l^2 k_Y\left(N=0\right)} \qquad (7.63)$$

For an axial load increasing from zero, the load curve will always intersect a *B*-point first since the inclination of the load line is almost zero. As illustrated in Figure 7.51 point *B* is almost on a straight line *(i)* and the vertical distance between the points is almost constant for a constant change in the axial load. If this property is adopted the moment at a *B*-point may be calculated as:

$$M_{B,1} = \left(M_{B,2} - M_{Y(N=0)} \right) \frac{N_1}{N_2} + M_{Y(N=0)} \tag{7.64}$$

This means that the moment at any *B*-point may be calculated from another *B*-point and M_Y. A similar relation may be established for the curvature:

$$k_{B,1} = \left(k_{B,2} - k_{Y(N=0)} \right) \frac{N_1}{N_2} + k_{Y(N=0)} \tag{7.65}$$

From this it may be seen that the applied moment may be calculated as:

$$\begin{aligned} M_{0,1} &= M_{B,1} - \frac{1}{a} l^2 N_1 k_{B,1} \\ M_{0,1} &= \left(\left(M_{B,2} - M_{Y(N=0)} \right) \frac{N_1}{N_2} + M_{Y(N=0)} \right) - \frac{1}{a} l^2 N_1 \left(\left(k_{B,2} - k_{Y(N=0)} \right) \frac{N_1}{N_2} + k_{Y(N=0)} \right) \\ M_{0,1} &= -\frac{1}{a} l^2 \frac{\left(k_{B,2} - k_{Y(N=0)} \right)}{N_2} N_1^{\,2} + \left(\frac{\left(M_{B,2} - M_{Y(N=0)} \right)}{N_2} - \frac{1}{a} l^2 k_{Y(N=0)} \right) N_1 + M_{Y(N=0)} \end{aligned} \tag{7.66}$$

Since $k_{B,2}$ is found from N_2 (N_2 being larger than N_1) it is seen that the coefficient on $N_1^{\,2}$ is negative. This leads to a convex curve in the interaction diagram as illustrated in Figure 7.50.

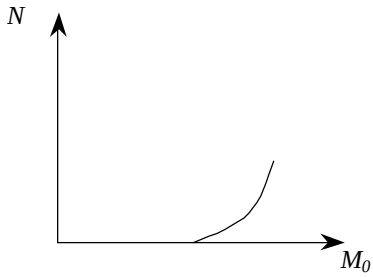

Figure 7.50. Convex form in the interaction diagram.

Thus it is safe to simplify this curve even more, namely with a straight line. This is valid as long as both the moment and the curvature can be assumed to depend linearly with the axial load. A linear relation valid for an axial load varying from zero to the point of yielding in both top and bottom reinforcement, corresponds to the line (*ia)* in Figure 7.51. As seen, the vertical

distance between the intersection points is almost constant which may be introduced as a further assumption.

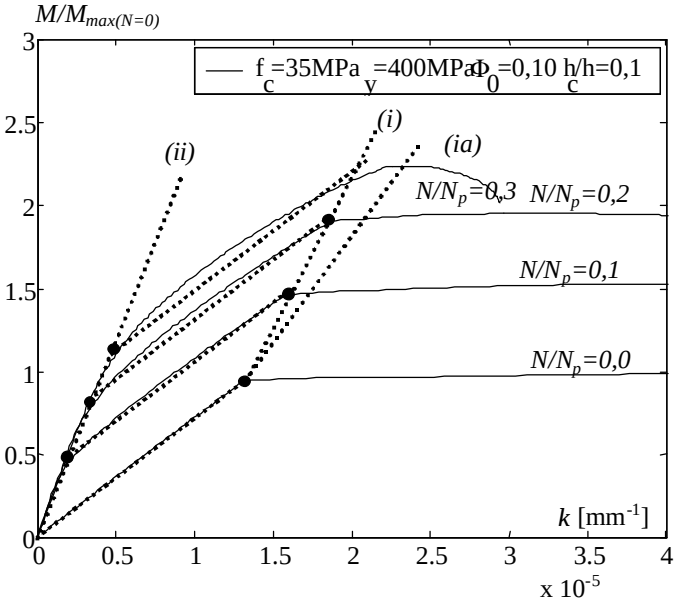

Figure 7.51. Moment curvature relations composed of straight lines.

The relation, (7.66), between M_0 and N means that the interaction curve may be simplified as a straight line as long as the axial load is lower than N_{BB} (the axial load causing yielding in top and bottom) and N_i.

If N_i is lower than N_{BB} a straight line may be drawn from the point corresponding to pure bending to the point corresponding to N_i in the interaction diagram. If N_i is larger than N_{BB} a straight line may be drawn from the point corresponding to pure bending to the point corresponding to N_{BB}.

This criterion is used in what follows to obtain a distinction between short and slender beam-columns. For slender beam-columns N_i is lower than N_{BB}. Thus the inclination of the load line will be steep since l^2 enters in the expression of the inclination, and calculations for N larger than N_i, is therefore made using an A-point.

Similar approximations may be made regarding the *A*-points. As illustrated in Figure 7.51 the *A*-points are almost on a straight line *(ii)* and the distance between the intersections are the same. Using similar simplifications and approximations as for the *B*-points leads to the

conclusion that the interaction diagram is convex and a straight line may therefore be used to simplify the curve, cf. Figure 7.52.

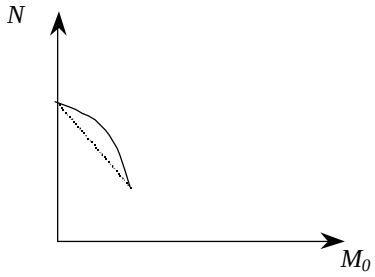

Figure 7.52. Convex form of the interaction diagram.

The linear approximation is safe for all the *A*-points until the critical column load is reached. Therefore, the line may be drawn from the first *A*-point to the critical load.

Three points therefore characterize slender beam-columns.

1. Pure bending
2. Point corresponding to N_i.
3. The critical column load

Between these points, straight lines may be used.

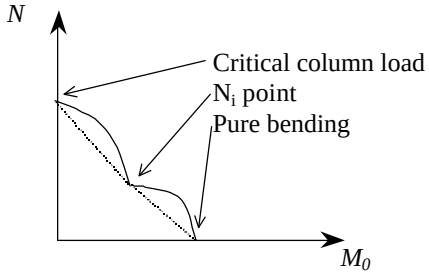

Figure 7.53. Interaction diagram for slender beam-columns.

For short columns the first two points in the interaction diagram correspond to pure bending and N_{BB}. For an axial load larger than N_{BB} the situation becomes a bit more difficult. In Figure 7.54 both the point corresponding to yielding in the top and bottom reinforcement, $M_{BB'}$, and the point corresponding to yielding at the top and zero stress in the bottom $M_{AB'}$ are marked.

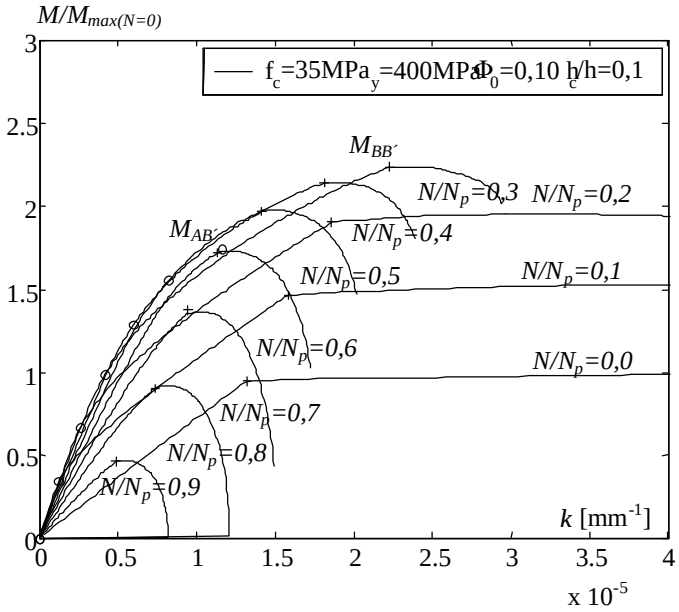

Figure 7.54.Moment-curvature relations.

To prove analytically that it is safe to assume a linear relation in the interaction diagram between these points is not simple. However, from numerical calculations it appears that the curve between these two points are convex and a straight line may therefore be used as a simplification as illustrated in Figure 7.55.

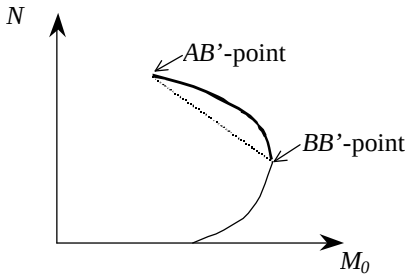

Figure 7.55. Convex form of the interaction diagram.

Numerical calculations also show that for axial loads larger than N_{AB} the interaction curve is concave, which means that a linear simplification is not conservative and this cannot be used.

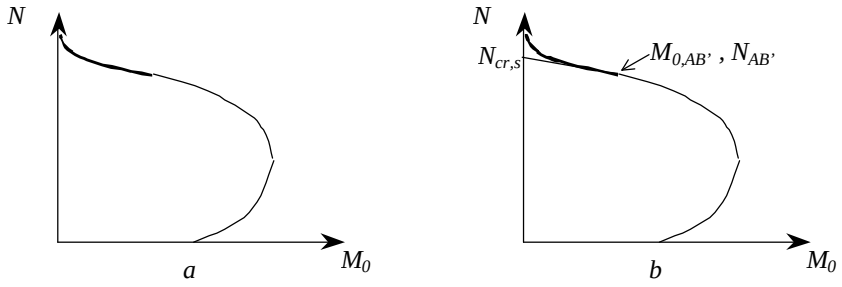

Figure 7.56. Concave form in the interaction diagram.

Instead a conservative simplification would be to calculate the critical column load from the tangent at the *AB'*-point. This is illustrated in Figure 7.56. $N_{cr,s}$ is determined numerically.

Three points therefore characterize short beam-columns

1. Pure bending
2. Point of $N_{BB'}$
3. Point of $N_{AB'}$
4. The critical column load, $N_{cr,s}$

Between these points, straight lines may be used to simplify the curve of the interaction diagram. This is illustrated in Figure 7.57.

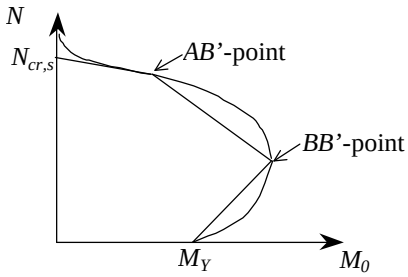

Figure 7.57. Interaction diagram for short beam-columns.

All in all the simplifications made above mean that only five points are of interest when calculating the interaction diagram. These five points are:

1. Pure bending
2. Yielding in the top and bottom reinforcement simultaneously, *BB'*-point
3. Yielding in the top reinforcement and cracking in the concrete simultaneously, *AB'*-point

4. The situation where $N=N_i$
5. The critical column load (calculated in a simplified manner if $N_i>N_{BB'}$).

This is illustrated in Figure 7.58.

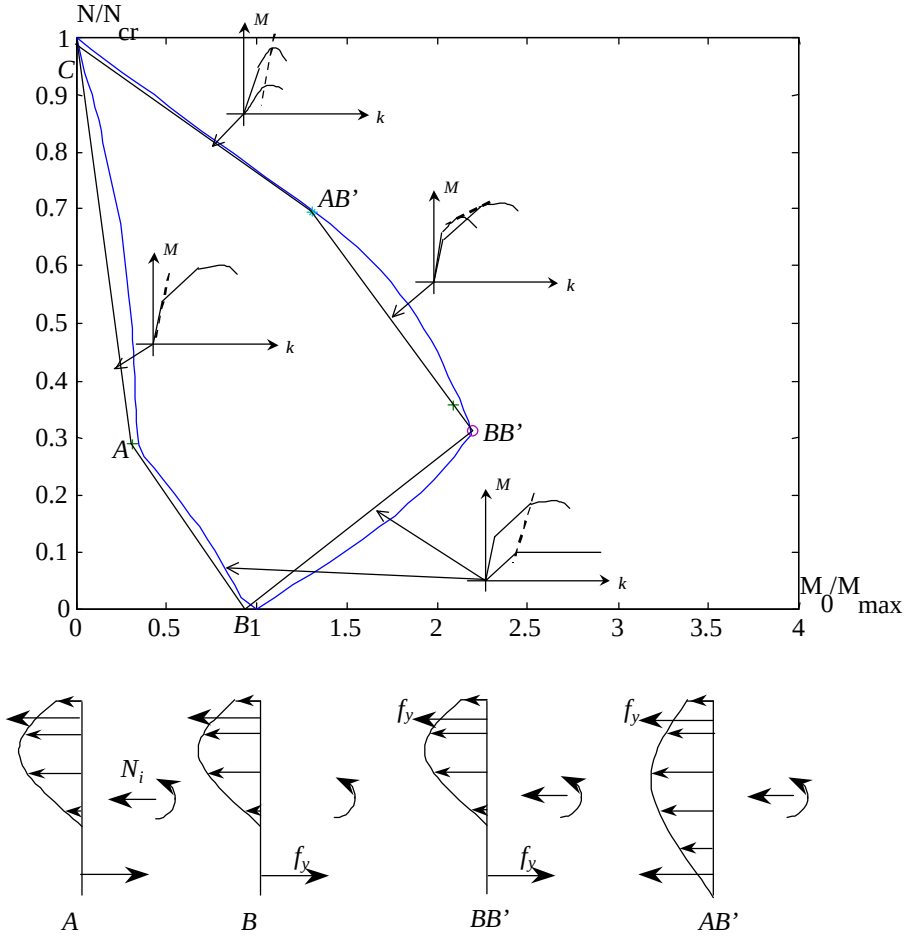

C represents the critical column load N_{cr}
calculated as $N_{cr,s}$ if $N_i>N_{BB}$

Figure 7.58. Review of the simplifications introduced for interaction diagrams.

In Figure 7.59, a flow diagram for the determination of the important points is shown. It is seen that according to the simplifications made, it is only necessary to determine three levels of axial load and from this, three or four points are found.

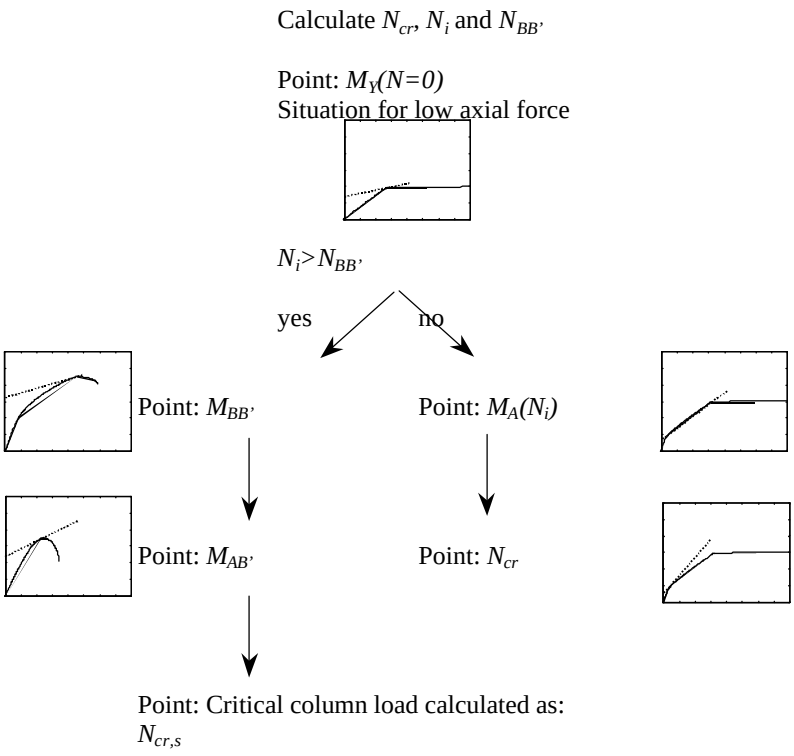

Figure 7.59. Flow diagram for the determination of points used in simplified interaction diagrams.

If the calculations are made as described above and, the simplified interaction curves become as shown in Figure 7.60.

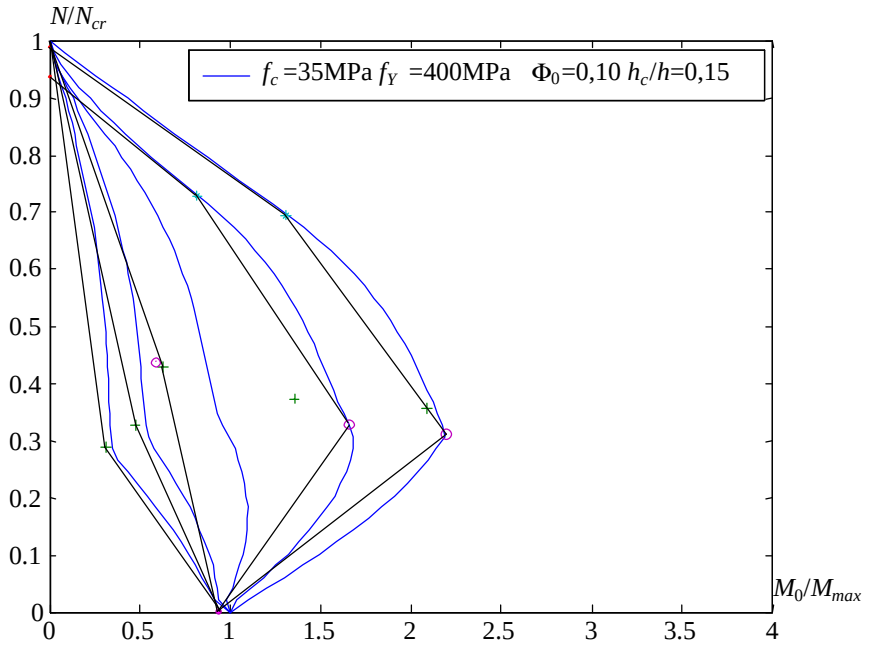

Figure 7.60. Simplified interaction curves for points in the applied moment- axial load diagram.

7.4.8 Practical calculation of beam-columns

7.4.8.1 Interaction diagram

A simple hand calculation method for calculating the load-carrying capacity of a beam-column may be developed on the basis of the investigations made in the previous sections. However the interaction diagram may be simplified even more. The simplified interaction diagram is constructed from 3-4 cross-section analyses as shown in Figure 7.61. In this figure five cases are outlined.

B_{simp}: Pure bending with a max concrete strain equal to 3,5 $^0/_{00}$ and the stress in the stress block is constant at $s_c = f_c$.

BB'_{simp1}: Bending with axial load. Othervise the same as $B_{simp.}$

BB'_{simp2}: Bending with axial load. The concrete is considered linear elastic with a maximum stress equal to 1,25 f_c (as in the Danish Code of Practice) in the concrete and yielding in the bottom reinforcement.

AB'_{simp}: Compression in the entire cross-section, where the stress in the bottom face is zero and the maximum stress at the top face is 1,25 f_c (as in the Danish Code of Practice).

A_{simp}: Bending with axial load, where the concrete is linear elastic and cracked. The bottom reinforcement yields.

In B_{simp}, BB'_{simp1} and BB'_{simp2} the top reinforcement might also yield for certain reinforcement ratios and yield strengths. BB'_{simp1} and BB'_{simp2} are both points, which estimate the point BB' in the previous simplifications this point being a maximum point of the interaction diagram for short columns.

In all cross-section analyses with linear elastic material behaviour, the modulus of elasticity is equal to the secant modulus 500 f_c (as in the Danish Code of Practice).

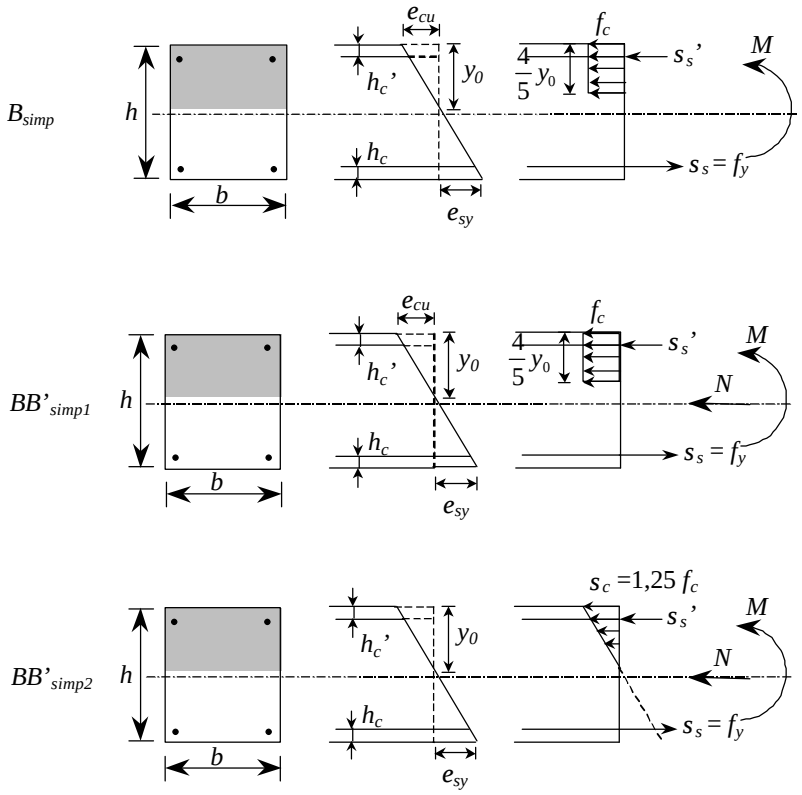

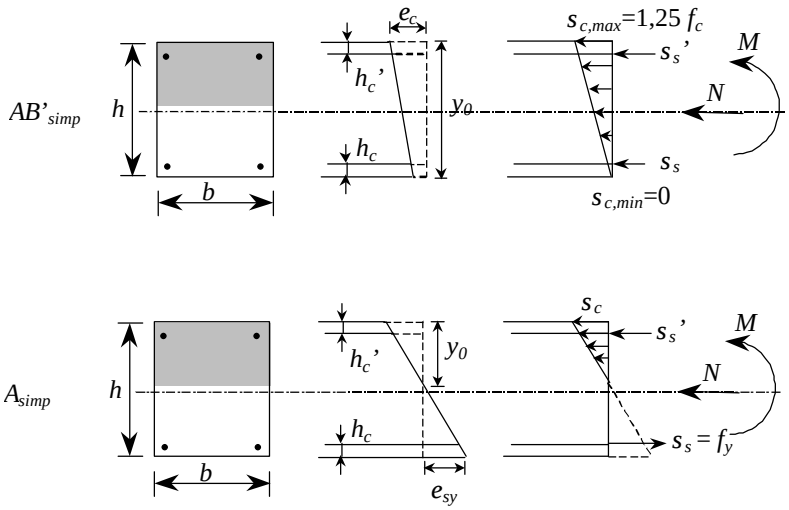

Figure 7.61 Cross-section analyses used to estimate the interaction curve between the applied moment and the axial load.

7.4.8.2 The calculation procedure

1. Determine the critical load by use of Ritter's equation.
2. Calculate the bending moment, applied moment and curvature by the cross-section analysis A_{simp} with $N = 0$ and determine N_i.
3. Calculate the maximum M, N -combination from the cross-section analyses BB'_{simp1} or BB'_{simp2} and determine if the column is slender or short.
4. If the column is short, calculate the point obtained using the cross-section analysis AB'_{simp}; plot this point together with B_{simp}, BB'_{simp1} or BB'_{simp2} and the critical load in an interaction diagram.
5. If the column is slender, calculate the point obtained from the cross-section analysis A_{simp} and plot this point together with the point obtained from the cross-section analysis B_{simp} and the critical load in an interaction diagram.

Re 1.

The critical stress according to the Ritter equation is

$$s_{cr} = \frac{f_c}{1 + \frac{f_c}{p^2 E_{0,cr}} \left(\frac{l}{i} \right)^2} \tag{7.67}$$

where

$$E_{0cr} = \min\begin{cases}1000\, f_c \\ 0{,}75 E_0\end{cases}$$

The maximum axial load is, according to DS411, determined by.

$$N_{cr} = \min\begin{cases} s_{cr} A_c \cdot (1 + n \cdot r) \\ s_{cr} A_c + A_s \cdot f_y \\ 2 \cdot s_{cr} A_c & \text{(Without overlap splices in the reinforcement)} \\ 1.5 \cdot s_{cr} A_c & \text{(With overlap splices in the reinforcement)}\end{cases}$$

Re 2.

Calculate the moment and curvature for the situation A_{simp} when $N = 0$.

Calculate the N_i level from the equation.

$$N_i = \frac{M_{A_{simp}, N=0}}{k_{A_{simp}, N=0}} \frac{a}{l^2}$$

Re 3.

Calculate the N, M_0 -combination from the cross-section analyses BB'_{simp1} or BB'_{simp2}

If N_i > N using BB'_{simp1} or BB'_{simp2}, then the column is short

If N_i < N using BB'_{simp1} or BB'_{simp2}, then the column is slender

Point 4 and 5 do not require any more comments.

7.4.8.3 Interaction diagrams compared with theory

In this section, the simple procedure outlined in the previous section will be compared with calculations using the equilibrium method. First, the results for short columns will be illustrated and then the results for slender columns.

In the calculation the parameters shown in

Table 7.4 are used. The results may be seen in Figure 7.62 where the slenderness ratio is varied between

$$5 \le \frac{l}{h} \le 25$$

with a step of 5.

In Figure 7.64 similar results may be seen. The slenderness ratio is in these plots varied within:

$$25 \le \frac{l}{h} \le 50$$

b [mm]	h [mm]	h_c [mm]	f_c [MPa]	e_{cy} [‰]	Φ_0 []
250	250	20	30	2	0.05

Table 7.4 The data used if other values are not listed.

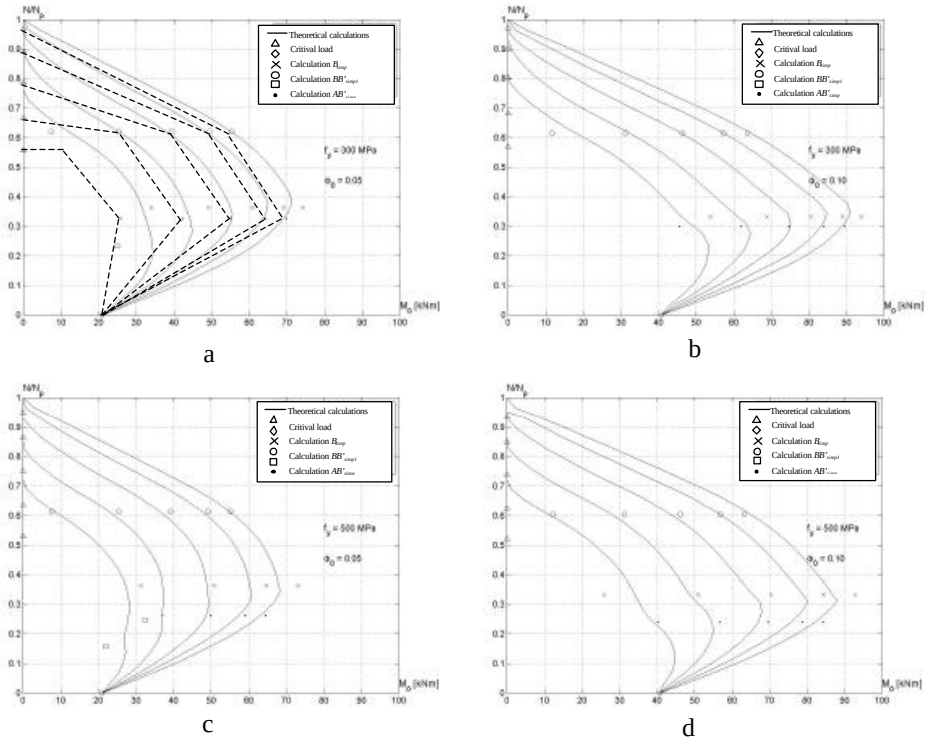

a b c d

Figure 7.62 Interaction diagrams for short columns

In Figure 7.62 a, interaction diagrams using point BB'_{simp2} as the maximum point is shown as the broken lines. It is seen that they fit the theoretical interaction diagram very well. It is also seen that the line between the top point and point AB'_{simp} is cut off by the horizontal line at the critical load (AB'_{simp} is represented by a circle in Figure 7.62 a). Thus a moment may be applied at the critical load. This corresponds to the Danish Code of Practice where a small initial eccentricity is allowed for columns calculated as concentrically loaded columns.

The four figures illustrate the simplified interaction diagram for two different yield strength and two degrees of reinforcement. As seen the result is very good. In Figure 7.63, the difference between using point BB'_{simp1} and BB'_{simp2} is illustrated.
If the columns are slender, the results are shown in Figure 7.64.

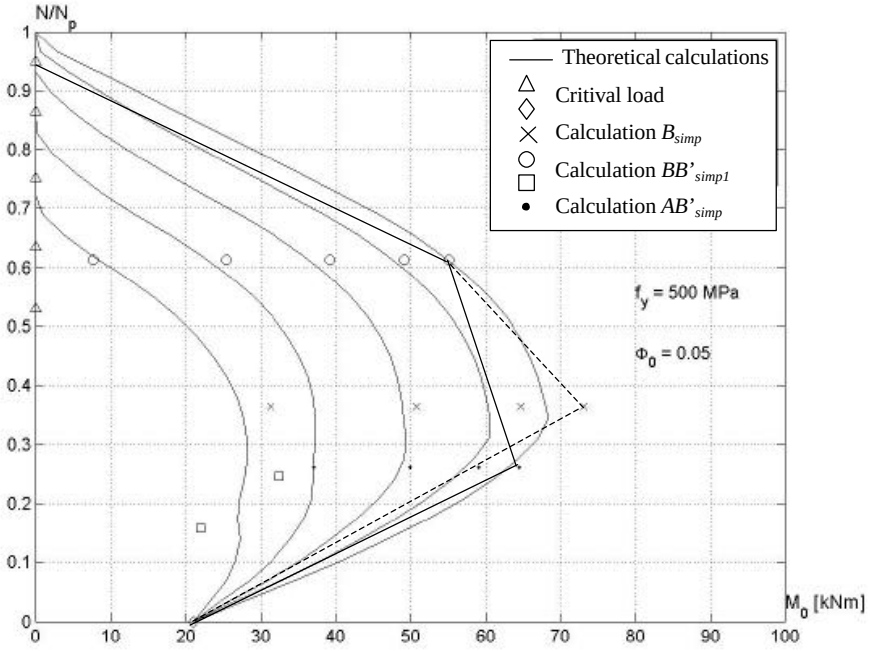

Figure 7.63 Illustration of the difference by using the two top points corresponding to BB'_{simp1} and BB'_{simp2}.

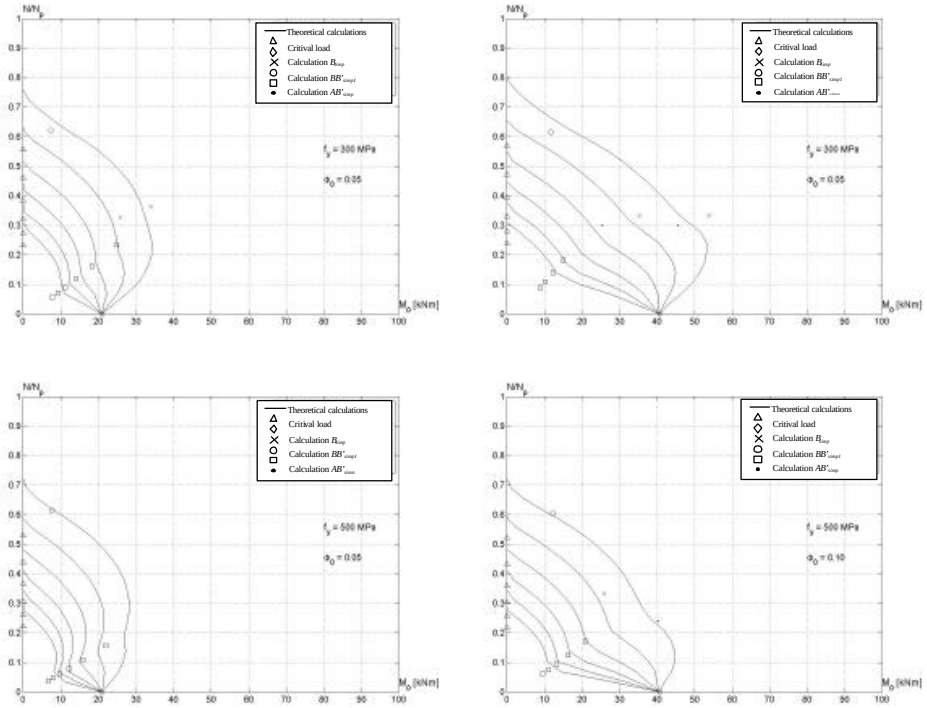

Figure 7.64 Interaction diagrams for slender columns

Figure 7.64 show that a simple and conservative interaction diagram for slender columns may be produced. However, the underestimation by using the approximate curves is in some cases large. This indicates that the stiffness of the column is underestimated. If the modulus of elasticity is set to the initial modulus of elasticity ($1000f_c$) instead of $500f_c$ the interaction diagrams illustrated in Figure 7.65 are obtained.

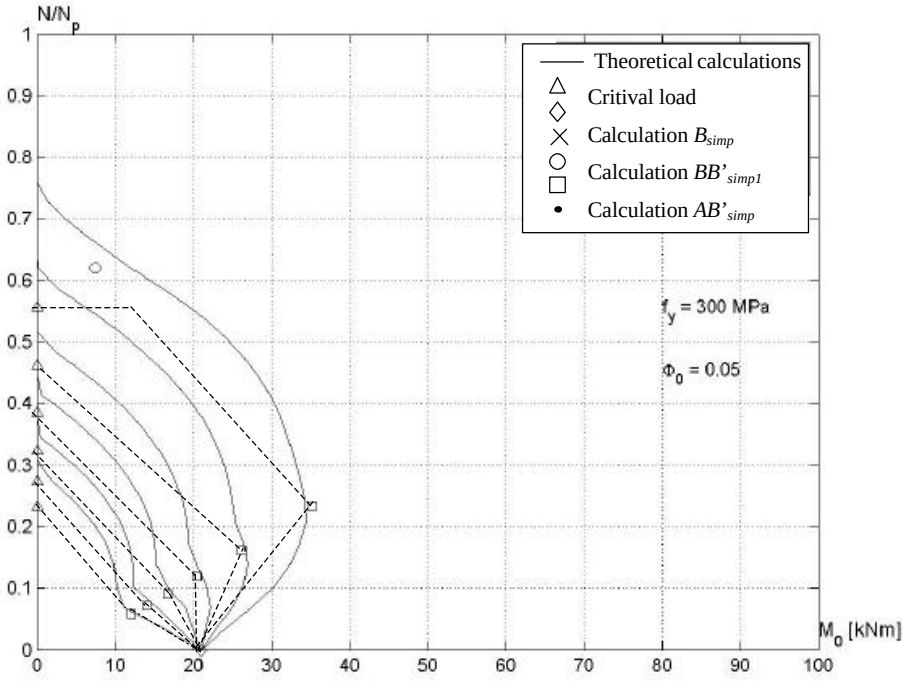

Figure 7.65 Interaction diagram using $E_{o,cr}$ *as the modulus of elasticity*

Figure 7.65 show that this improves the interaction diagram and the simplification leads to interaction diagrams, which, compared with the theoretical ones, are very good.

As mentioned previously, the Danish Code of Practice prescribes that a column can be calculated as concentrically loaded if the eccentricity is smaller than 1/5 of the core radius *k*. The critical load for l/h=25 is $0{,}56N_p$ which gives a maximum applied moment of

$$M_{0,\max,DS} = 0{,}56N_p\frac{k}{5} = 0{,}56bhf_c\left(1+2\Phi_0\right)\frac{h}{30} = 9{,}63\,\text{kNm}$$

since the core radius is $h/6$ for a rectangular cross section.

The values used are listed in

Table 7.4, which justifies the cut off of the interaction curve at the critical load.

8 Comparison with experiments

8.1 Investigators and experiments

In this section the calculations are compared with experiments taken from the literature.
In the calculations a = 10 is used. Regarding the detailed experimental results, see section 12.

Bauman, O. 1935, [13]

The experimental investigation made by Baumann was subdivided into two sections, a pilot series and a main series. Both series consider concentrically as well as eccentrically loaded columns. The pilot series consists of 12 tests and the main series of 31 tests. The columns in the pilot series and in the first 15 tests of the main series were simply supported. In the remaining of the tests in the main series the end conditions were changed. The cross-section was varied in many of the tests, which means that comparison by using interactions diagrams is very cumbersome. The data are presented in the supplements, section 12.1.

Rambøll, B. J. 1951 [14]

The experimental investigation made by Rambøll consisted of 38 tests with columns loaded eccentrically as well as concentrically. The cross section was kept constant. The investigation dealt with four different column-lengths and within each series the eccentricity was varied: $\frac{e}{h} = 0, 0{,}08, 0{,}17, 0{,}33, 0{,}67$ and $0{,}83$. Furthermore, the reinforcement was the same for all columns, except column 35. The data are presented in the supplements, section 12.2.

Ernst, G. C., Hromdik, J. J. and Riveland, A. R. 1953 [15]

This experimental investigation consisted of 16 tests with columns loaded eccentrically as well as concentrically. The eccentricity was $\frac{e}{h} = 0, 0{,}13, 0{,}25$ and $0{,}38$. Eight of the tests were made on elements, which had the same size as the standard compressive specimens. They all failed in compression as reported in the investigation, which is why they are not plotted in the

interaction diagram. The columns were simply supported in both ends and the load was applied through a knife-edge. The data are presented in the supplements, section 12.3.

Gehler, W. and Hütter, A. 1954 [16]

This investigation is a collection of tests carried out over a period of ten years. The first test series was carried out from 1940-41 and contained 18 tests with concentrically loaded columns. The concrete cross-section was kept constant and the reinforcement was either 4 ø 8 or 4ø14. The second test series was carried out from 1951-52. This series contained 12 concentrically loaded columns and 24 laterally loaded columns; the lateral load was applied at the midpoint as a point load. The columns were simply supported in all cases. The data are presented in the supplements, section 12.4.

Gaede, K. 1958 [17]

This investigation contained eight tests on eccentrically loaded, simply supported columns. The length of the columns was varied between, 2,94 m and 3,54 m. Two eccentricities were used, $\frac{e}{h} = 0{,}2$ and $0{,}5$. The load was applied through knife-edges. The deflections were measured and reported for the entire series. The cross-section and reinforcement were kept constant. The data are presented in the supplements, section 12.5.

Chang, W. F. and Ferguson, P. M. 1963 [18]

In this investigation six columns were tested, each simply supported. The load was applied as a concentrically axial load, by two jacks and then the moment was applied by changing the ratio between the loads in the two jacks so that the sum was kept constant. This makes is possible to investigate the moment curvature relationship for the column. The constant level of axial load was according to the investigators very difficult to obtain. The cross-section and the reinforcement were kept constant in each test. The data are presented in the supplements, section 12.6.

Pannell, F. N. and Robinson, J. L. 1968 [19]

This investigation contained 10 columns, 6 of which were concentrically loaded, and 4 laterally loaded. The lateral load was applied at mid point of the column as a point load. The cross-section and the reinforcement were kept constant in each experiment. Each column was simply supported in both ends. The data are presented in the supplements, section 12.7.

Breen, J. E. and Ferguson, P. M. 1969 [20]

This investigation contained 10 tests on columns, which were fixed in one end and free in the other one. The loads applied were axial load and lateral load both applied at the free end. The cross-section and the reinforcement were kept constant in each experiment. The ratio between the lateral load and the axial load was kept at five constant values. The data are presented in the supplements, section 12.8.

Mehmel, A., Schwarz, H., Kasparek, K. H. and Makovi, J. 1969, [21]

This investigation contained 16 tests, 14 of these with the same eccentricity in both ends and two with different eccentricities at the ends. Three different types of reinforcement were used and the cross-section had three different sizes. The deflection at failure was measured together with the deflection during the tests. The data are presented in the supplements, section 12.9.

Kim, J. K and Yang, J. K. 1993 [28]

In this investigation 30 tests on simply supported columns were reported. Two of the columns failed at the ends and are therefore disregarded. The investigation contained three different levels of compressive strength, low, medium and high. Furthermore, two different reinforcement ratios were tested. In the case of a reinforcement ratio of 4 % two of the bars are disregarded, because they were placed at the centre of the cross-section. The deflection at failure was reported. The data are presented in the supplements, section 12.10.

Chuang, P. H. and Kong, F. K. 1997 [29]

In this investigation, 26 eccentrically loaded simply supported columns were tested. Normal strength concrete as well as high strength concrete was used. The concrete cross-section had two different sizes and three types of reinforcement were used. Measurements of the deflection at failure were reported. The data are presented in the supplements, section 12.11.

Foster, S. J. and Attrad, M. M. 1997 [30]

In this investigation 68 tests on simply supported columns were reported. The investigation contained three different levels of compressive strength, low, medium and high. Furthermore, two different reinforcement ratios were tested. In the case of a reinforcement ratio of 4 % two of the bars are neglected, because they were placed at the centre of the cross-section. The deflection at failure was reported. The data were presented in the supplements, section 12.12.

Cleason, C. 1997 [31]

12 experiments were reported in this investigation. Normal as well as high strength concrete was used. Two different cross-sections along with two types of reinforcement were designed. The deflections at failure were measured and reported. The data are presented in the supplements, section 12.13.

In Table 8.1 the types of columns are indicated. These types refer to the columns shown in Figure 8.1. They are named A, B, …, G.

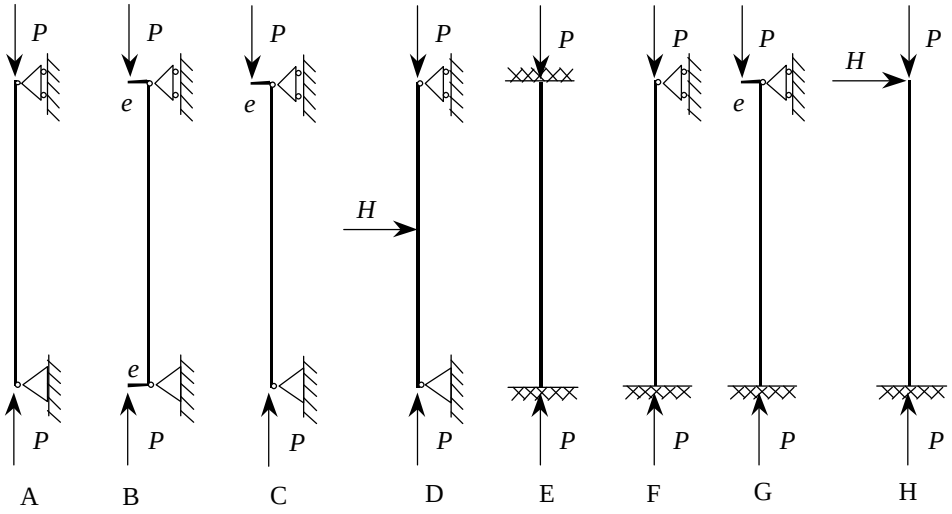

Figure 8.1. Illustration of the different kinds of columns used in the investigations.

In Table 8.1 the number of tests made by each investigator is presented. In the column to the left the mean value, m , and the standard deviation, s, is shown. Subscript "*theory*" and "*DS*" denotes calculations done with the equilibrium method and calculations according to DS411, method I, respectively. The mean value and standard deviation are calculated for the ratio:

$$\frac{N_{\exp}}{N_{calc}} \tag{7.68}$$

where N_{calc} may either be the axial load when using the equivalence method or the axial load calculated by using DS411, method I.

Investigator	Year	References	Number of tests	Mean value and standard deviation
Baumann	1935	[13]	14 A 13 B 4 E 3 F 3 C* 6 G*	$m_{theory} = 0{,}98;\ s_{theory} = 0{,}16$ $m_{DS} = 1{,}14;\ s_{DS} = 0{,}18$
Rambøll	1951	[14]	38 B	$m_{theory} = 1{,}19;\ s_{theory} = 0{,}21$ $m_{DS} = 1{,}30;\ s_{DS} = 0{,}22$
Ernst, G. C., Hromdik, J. J. and Riveland	1953	[15]	2 A 6 B	$m_{theory} = 0{,}92;\ s_{theory} = 0{,}22$ $m_{DS} = 1{,}02;\ s_{DS} = 0{,}25$
Gehler, W. and Hütter, A.	1954	[16]	30 A 24 D	$m_{theory} = 1{,}09;\ s_{theory} = 0{,}19$ $m_{DS} = 1{,}29;\ s_{DS} = 0{,}26$ $m_{theory} = 1{,}12;\ s_{theory} = 0{,}10$ $m_{DS} = 1{,}14;\ s_{DS} = 0{,}11$
Gaede, K.	1958	[17]	8 B	$m_{theory} = 0{,}89;\ s_{theory} = 0{,}05$ $m_{DS} = 0{,}81;\ s_{DS} = 0{,}06$
Chang, W. F. and Ferguson, P. M.	1963	[18]	6 B	$m_{theory} = 0{,}65;\ s_{theory} = 0{,}04$ $m_{DS} = 0{,}66;\ s_{DS} = 0{,}05$
Pannell, F. N. and Robinson, J. L.	1968	[19]	6 A 4 D	$m_{theory} = 1{,}18;\ s_{theory} = 0{,}33$ $m_{DS} = 1{,}22;\ s_{DS} = 0{,}23$
Breen, J. E. and Ferguson, P. M.	1969	[20]	10 H	$m_{theory} = 0{,}77;\ s_{theory} = 0{,}18$ $m_{DS} = 0{,}76;\ s_{DS} = 0{,}14$
Mehmel, A., Schwarz, H., Kasparek, K. H. and Makovi, J.	1969	[21]	14 B 2 C*	$m_{theory} = 0{,}87;\ s_{theory} = 0{,}10$ $m_{DS} = 0{,}96;\ s_{DS} = 0{,}11$

Kim, J. K and Yang, J. K.	1993	[28]	28 B	$m_{theory} = 0,85;\ s_{theory} = 0,08$ $m_{DS} = 1,01;\ s_{DS} = 0,14$
Chuang, P. H. and Kong, F. K.	1997	[29]	26 B	$m_{theory} = 1,57;\ s_{theory} = 0,50$ $m_{DS} = 1,78;\ s_{DS} = 0,54$
Foster, S. J. and Attrad, M. M.	1997	[30]	68 B	$m_{theory} = 0,93;\ s_{theory} = 0,09$ $m_{DS} = 1,13;\ s_{DS} = 0,13$
Cleason, C.	1997	[31]	12 B	$m_{theory} = 0,77;\ s_{theory} = 0,12$ $m_{DS} = 0,89;\ s_{DS} = 0,15$
Total 311 tests			55 A 200 B 5 C* 28 D 4 E 3 F 6 G* 10 H	

*) Theses tests are neglected in the comparison

Table 8.1 Standard deviation and mean value of tests used for comparison with theory.

8.2 Comparison

The difference between theory and experiment for beam-columns are measured by the distance from the measured point and the intersection point between the interaction diagram and the line $M_0 = Ne$. This is illustrated in Figure 8.2. Strictly speaking this method is only fully jusitfied for eccentrically loaded beam-columns.

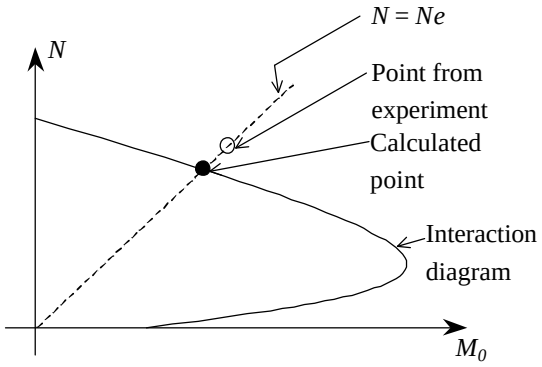

Figure 8.2. Illustration of the method used to compare calculation methods with experiments.

The method is questionable for laterally loaded columns since the loading may not always be proportional loading. Often the loading procedure is unknown. However, the method is used for all tests since the results seam to indicate proportional loading.

8.2.1 Concentrically loaded columns

An unreinforced concrete column is seldom built and is therefore of less interest than a reinforced column. Therefore, no comparison will be made between theory and experiments in this report for this type of column.

In Figure 8.3 and Figure 8.4 the results of 2 test series are compared with the formulas described previously. The data used in these plots may be found in section 12.4 and 12.7.

In the calculations, the modulus of elasticity, in Ritter´s column formula is calculated according to the Danish Code of Practice (see section 7.3.2).

It appears that the formulas show good agreement with the experiments. It should be noted that an ideal column experiment is almost impossible carry out because of imperfections such as initial deflections from casting etc.

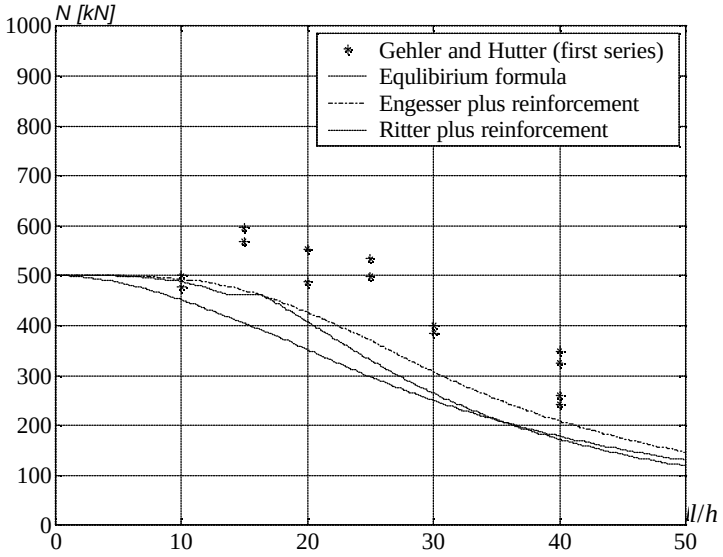

Figure 8.3. Plot of test results versus theory. Details may be found in section 12.4.

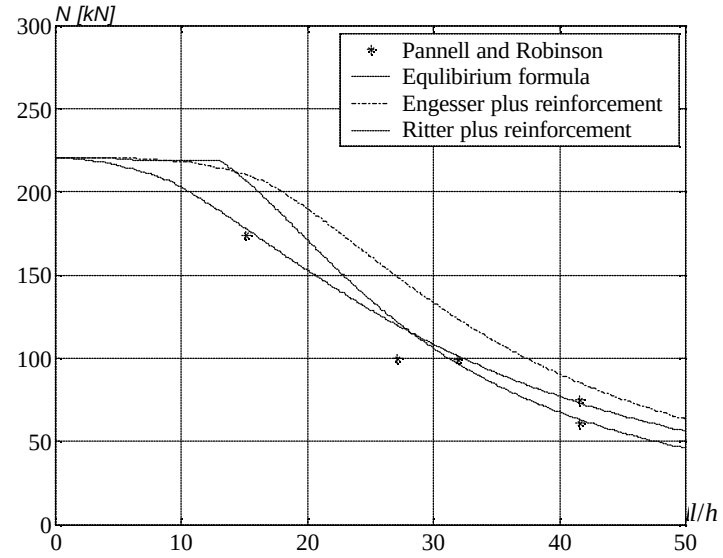

Figure 8.4. Plot of test results versus theory. Details may be found in section 12.7.

The results from all tests on concentrically loaded columns are illustrated in Figure 8.5-Figure 8.8.

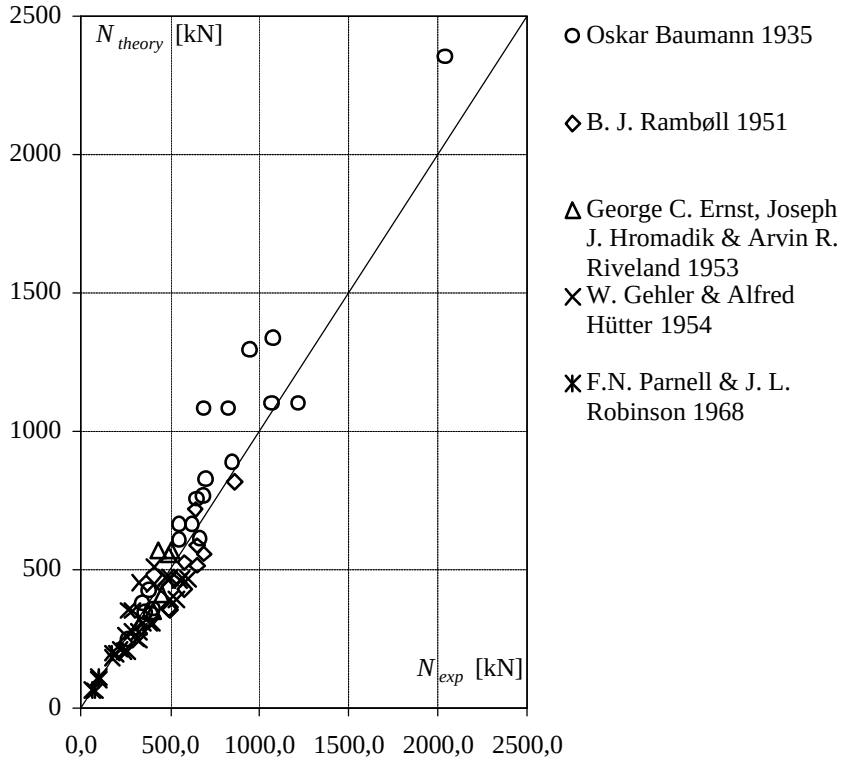

Figure 8.5. The equilibrium method compared with experiments.

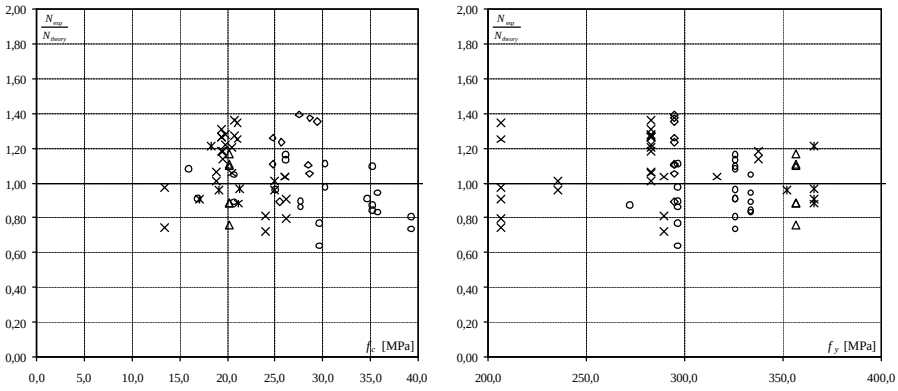

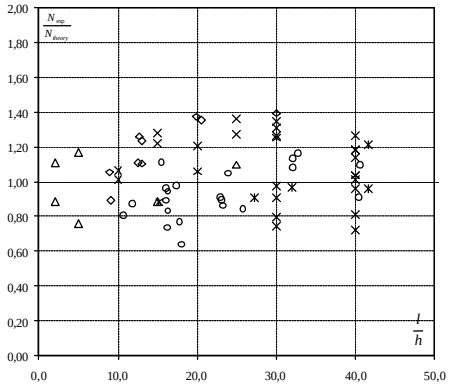

Figure 8.6 The equilibrium method compared with experiments as a function of the compressive strength of the concrete, the yield strength of the reinforcement and the slenderness ratio l/h, respectively.

The agreement between the equilibrium method and experiments is seen to be good for concentrically loaded columns. The mean value and standard deviation are, respectively:

$$m_{theory} = 1{,}06 \text{ and } s_{theory} = 0{,}19$$

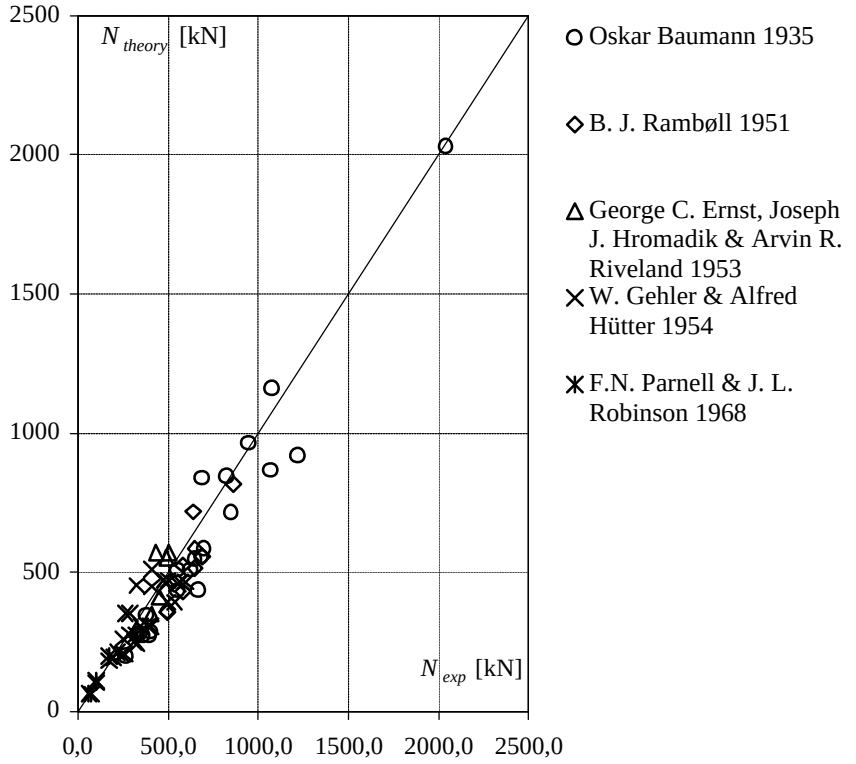

Figure 8.7. The Danish Code of Practice, method I, compared with experiments

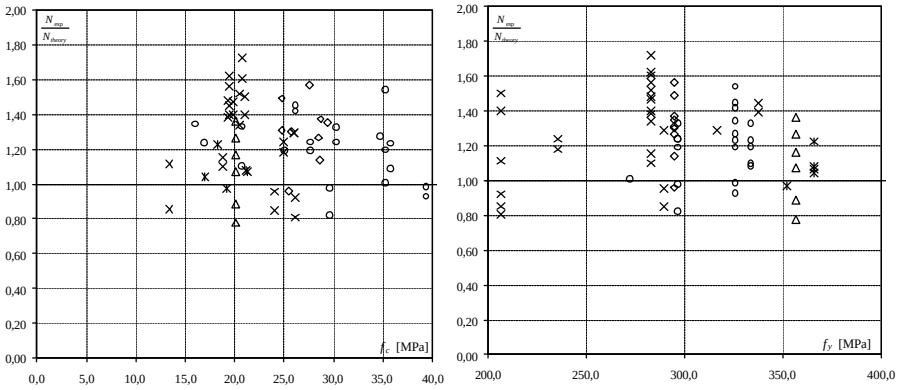

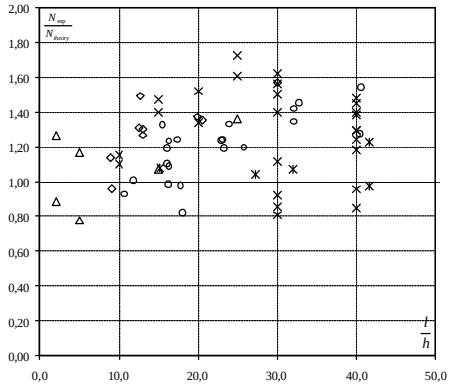

Figure 8.8 The Danish Code of Practice, method I, compared with experiments as a function of the compressive strength of the concrete, the yield strength of the reinforcement and the slenderness ratio l/h, respectively.

The agreement between the Danish Code of Practice, method I, and experiments for concentrically loaded columns is seen to be good. The mean value and standard deviation are, respectively:

$$m_{DS} = 1{,}18 \text{ and } s_{DS} = 0{,}25$$

8.2.2 Eccentrically loaded beam-columns

In this section comparisons are made for eccentrically loaded beam-columns. This includes columns of type B (see Figure 8.1). The interaction diagrams in Figure 8.9 show the statical results from the equilibrium method compared with experiments by Mehmel, A., Schwarz, H., Kasparek, K. H. & Makovi, H. (section 12.9). It appears that the tests fit the theoretical curve well. In section 12 the tests are plotted in interaction diagrams for each test series using the equilibrium method.

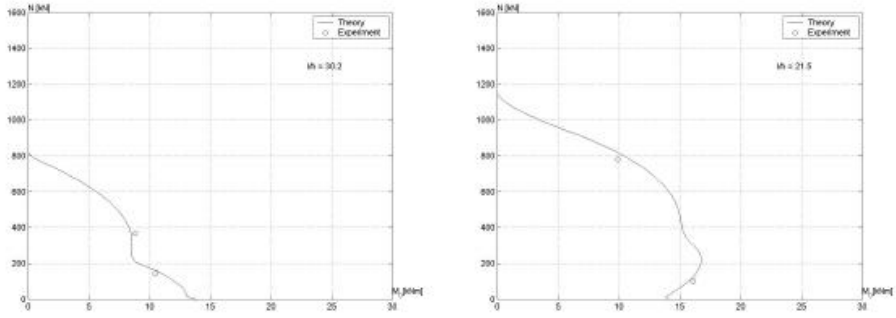

Figure 8.9 Interaction diagram where the equilibrium method is compared with experiments by Mehmel, A., Schwarz, H., Kasparek, K. H. & Makovi, H.(section 12.9).

The test points in Figure 8.9 are for all investigations where beam-columns of the type B are tested. Similar diagrams are produced in section 12 for each test series.

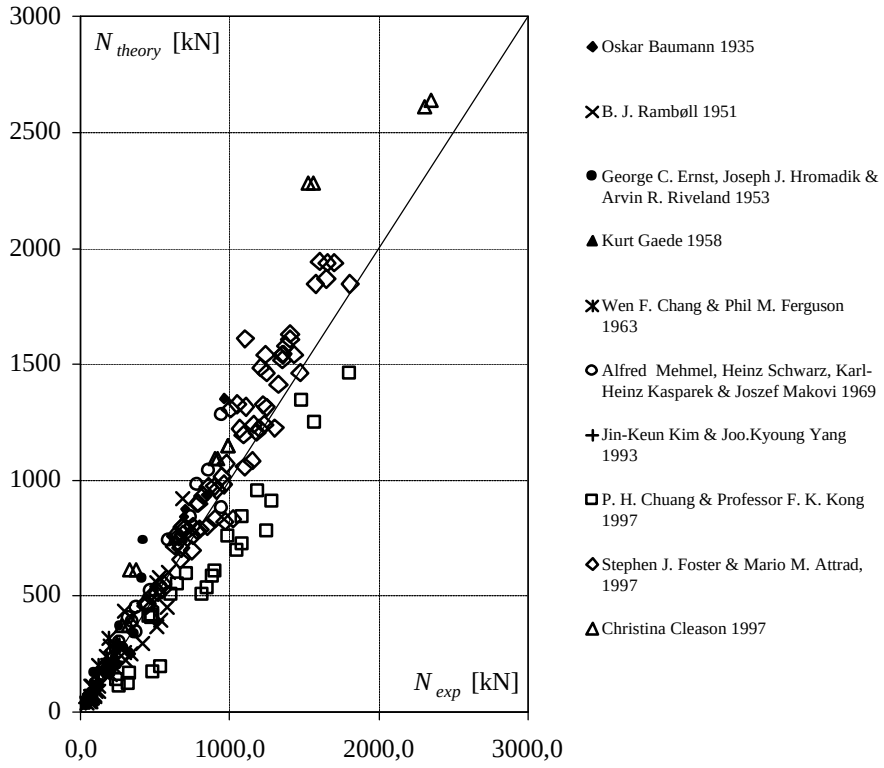

Figure 8.10 The equilibrium method compared with experiments

Furthermore in Figure 8.11, the results from the calculations are compared with experimental values as a function of the eccentricity, the compressive strength of the concrete, the yield strength of the reinforcement and the slenderness ratio *l*/*h*, respectively

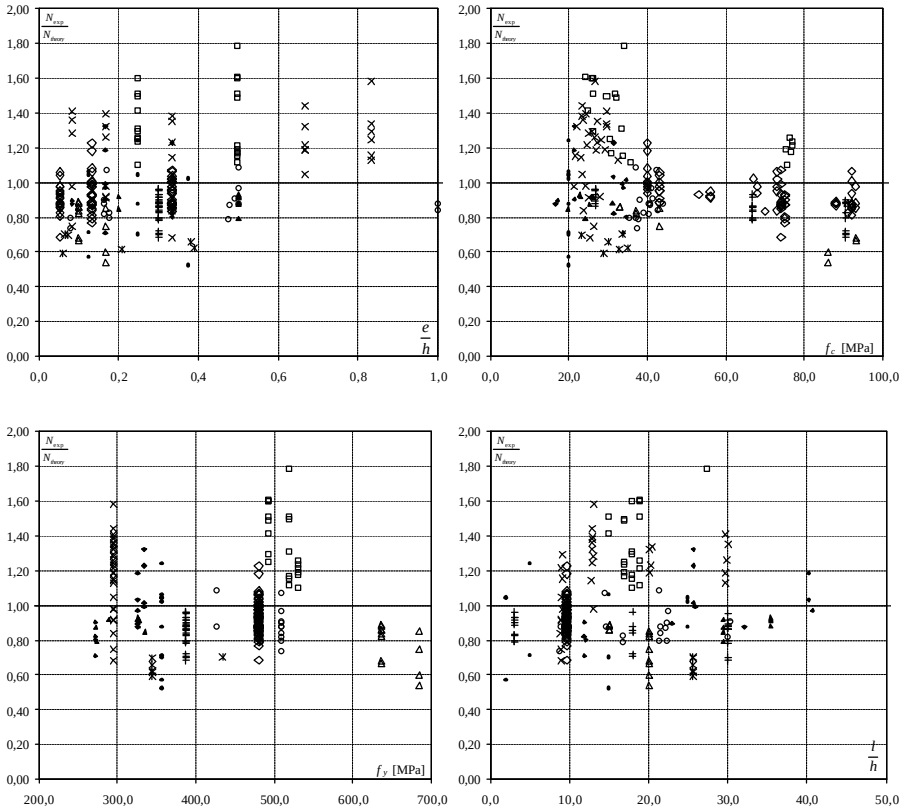

Figure 8.11. The equilibrium method compared with experiments as a function of the eccentricity, the compressive strength of the concrete, the yield strength of the reinforcement and the slenderness ratio l/h, respectively.

The agreement between the equilibrium method and experiments made on eccentrically loaded beam-columns is very good. The mean value and standard deviation are, respectively:

$$m_{theory} = 1{,}08 \text{ and } s_{theory} = 0{,}23$$

To compare with the Danish Code of Practice similar plots have been made. These are shown in Figure 8.12and Figure 8.13.

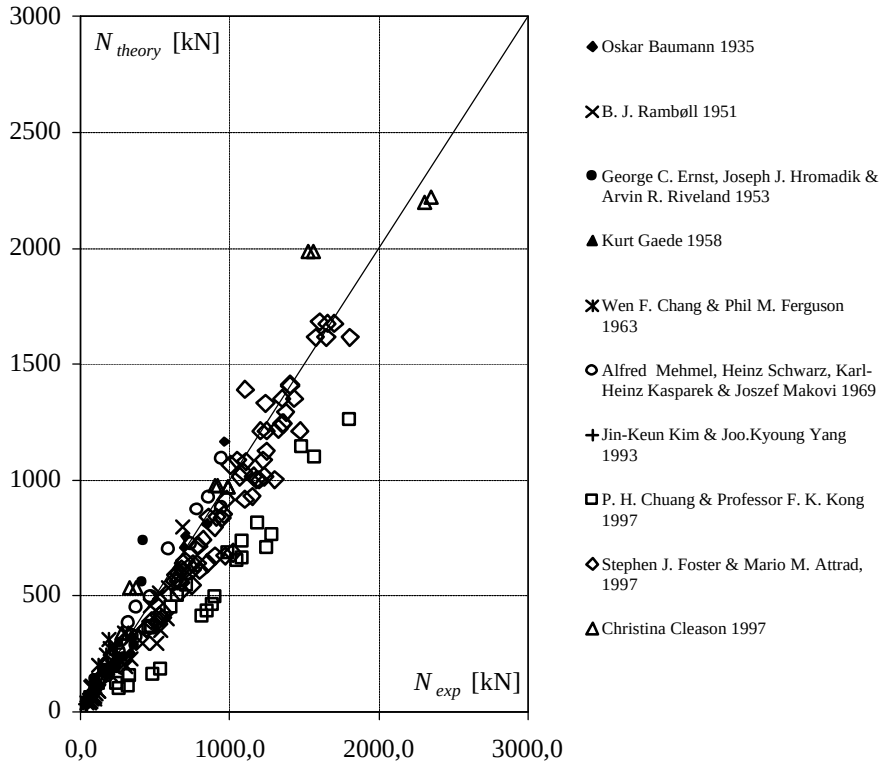

Figure 8.12. The Danish Code of Practice, method I, compared with experiments

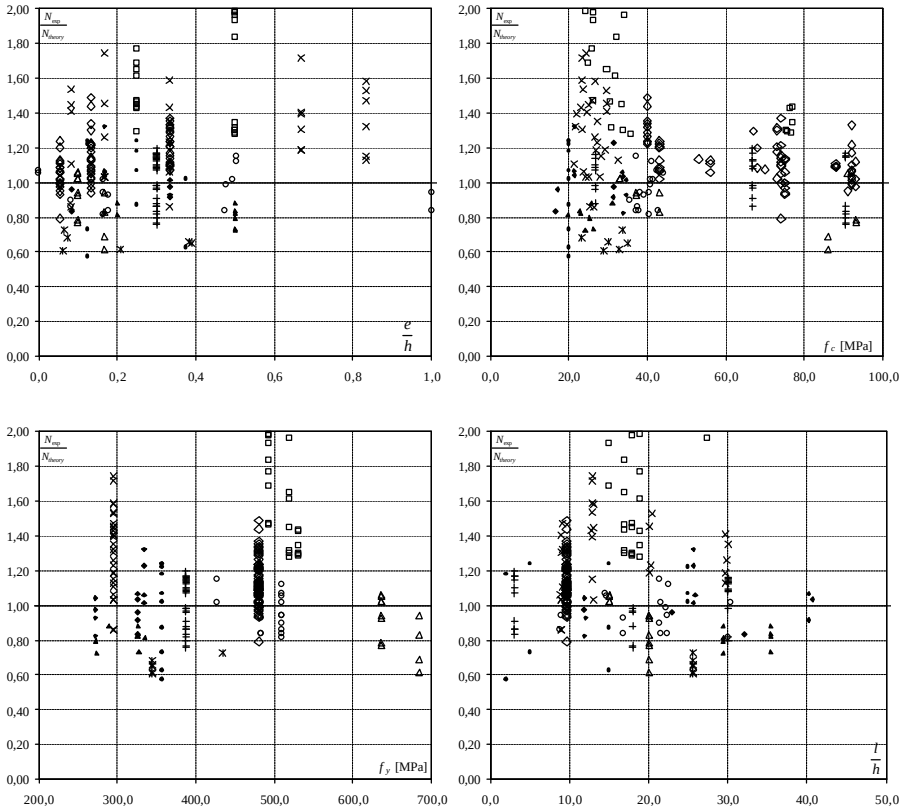

Figure 8.13. The Danish Code of Practice, method I, compared with experiments as a function of the eccentricity, the compressive strength of the concrete, the yield strength of the reinforcement and the slenderness ratio l/h, respectively.

The agreement between the Danish Code of Practice and experiments is relatively good. It appears that the method is a bit conservative, which is clearly demonstrated by the mean value. The mean value and the standard deviation are, respectively:

$$m_{DS} = 1{,}19 \text{ and } s_{DS} = 0{,}27$$

8.2.3 Laterally loaded beam-columns

Similar comparison as for eccentrically loaded beam-columns has been made in the case of laterally loaded beam-columns. The types of beam-columns, which are used for in the comparisons, are of type D and H. The interaction diagram in Figure 8.14 illustrates how the equilibrium method compares with the experiments by Gehler, W. and Hütter, A. (section 12.4).

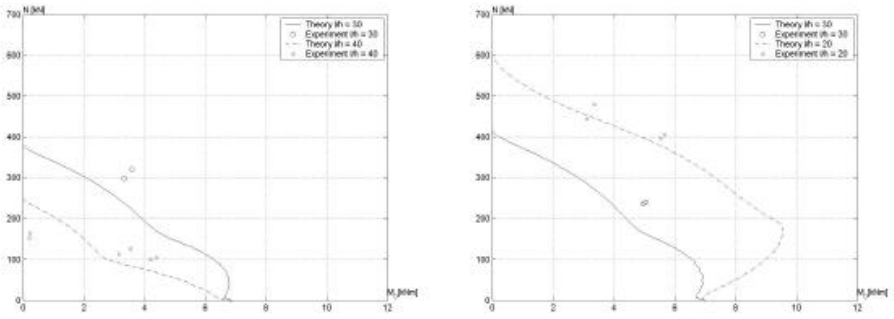

Figure 8.14. Interaction diagrams comparing the equilibrium method with experiments taken from the investigation by Gehler, W. and Hütter, A. (section 12.4).

In Figure 8.15 and Figure 8.16 all tests with lateral load are compared with the equilibrium method.

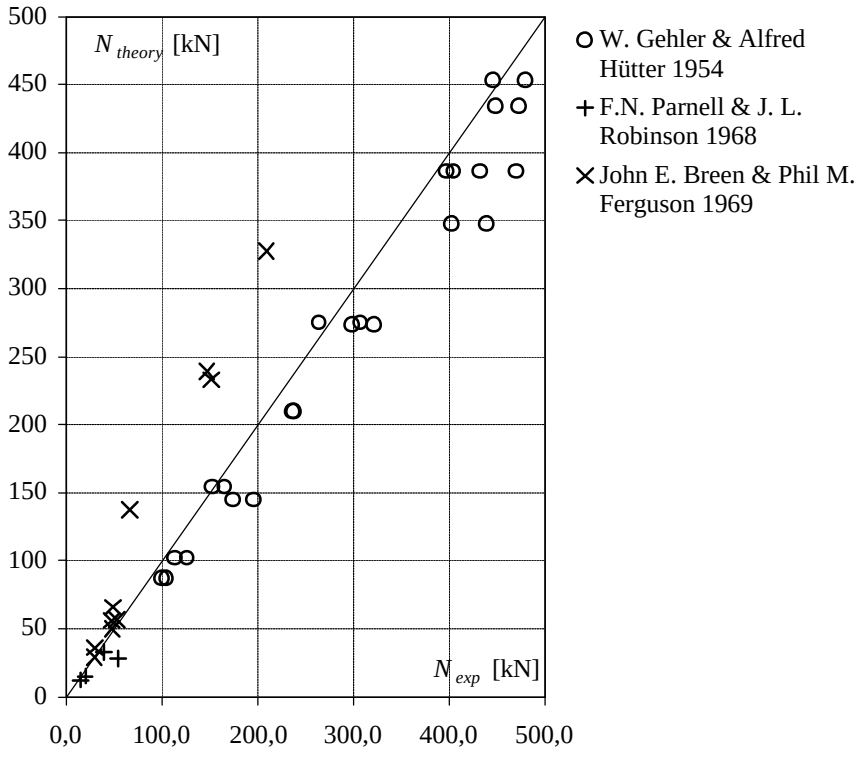

Figure 8.15. The equilibrium method compared with experiments

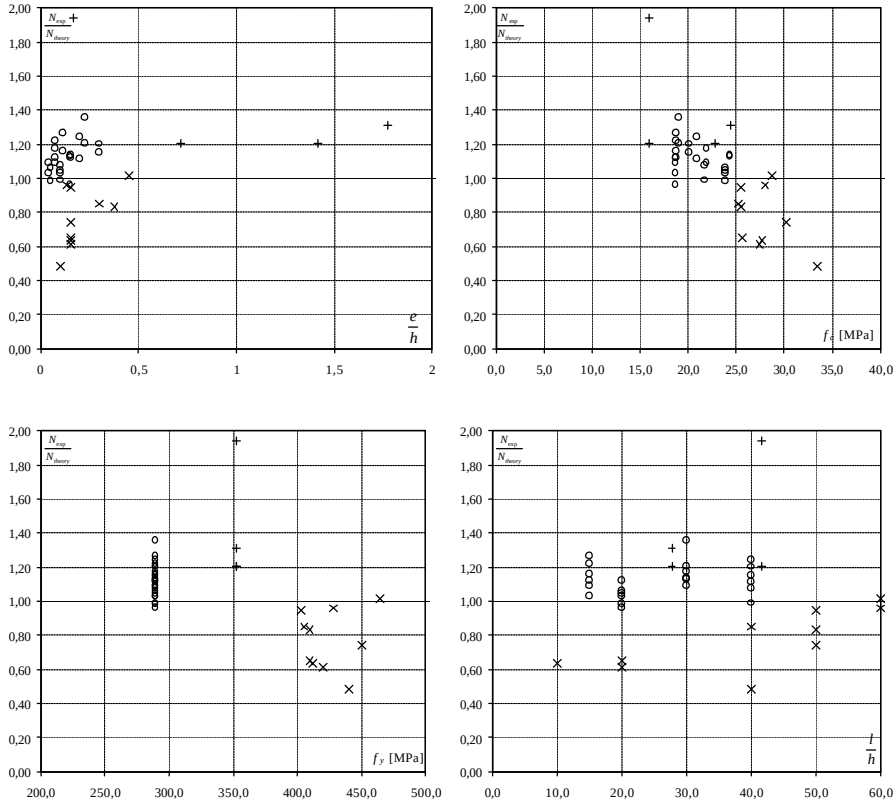

Figure 8.16. The equilibrium method compared with experiments as a function of the the eccentricity, the compressive strength of the concrete, the yield strength of the reinforcement and the slenderness ratio l/h, respectively.

The agreement between the equilibrium method and experiments is relatively good also for laterally loaded beam-columns too. The mean value and standard deviation are, respectively:

$$m_{theory} = 1{,}06 \text{ and } s_{theory} = 0{,}25$$

The method used in the Danish Code of Practice has been compared with experiments as well. The results are shown in Figure 8.17 and Figure 8.18.

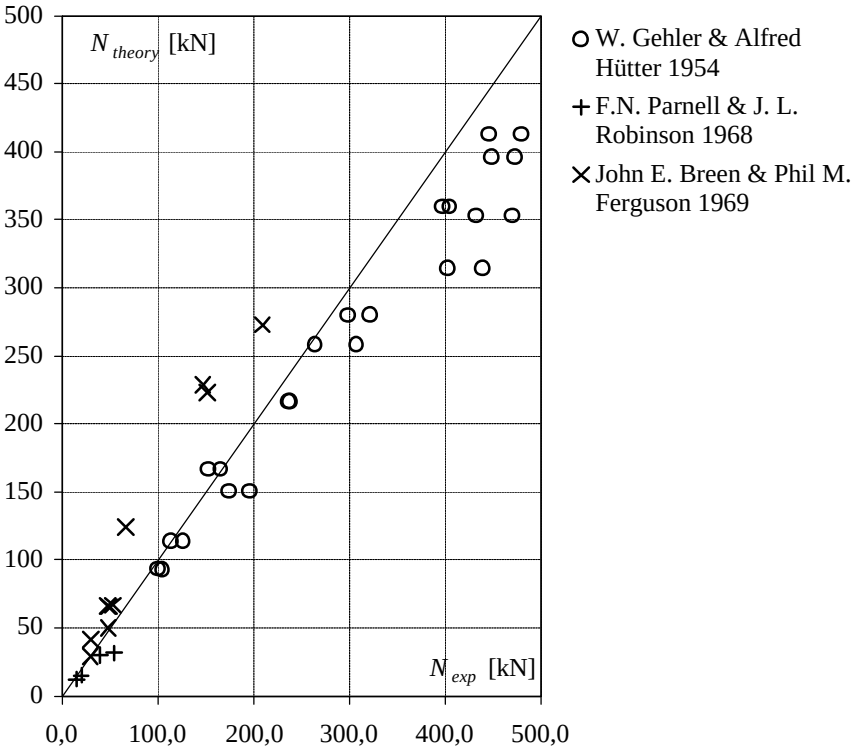

Figure 8.17. The Danish Code of Practice, method I, compared with experiments

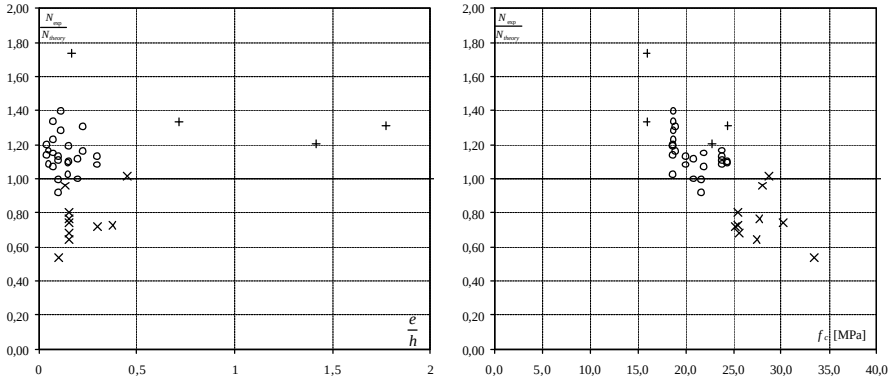

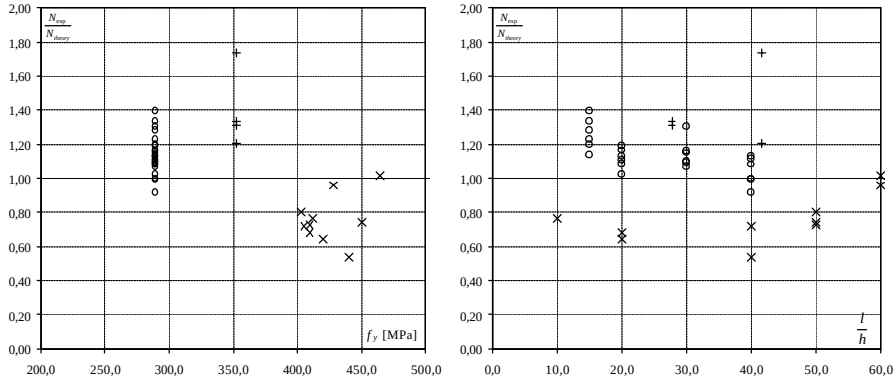

Figure 8.18. The Danish Code of Practice, method I, compared with experiments as a function of the eccentricity, the compressive strength of the concrete, the yield strength of the reinforcement and the slenderness ratio l/h, respectively.

The eccentricity used in the comparisons in Figure 8.16 and Figure 8.18 is calculated as the moment from the applied lateral load divided by the axial load.

The agreement between the Danish Code of Practice and experiments is seen to be good and it appears that the method is a bit conservative. The mean value and standard deviation are, respectively:

$$m_{DS} = 1{,}07 \text{ and } s_{DS} = 0{,}24$$

9 Conclusion

This paper provides a theoretical verification of calculation methods in the Danish Code of Practice DS411, using the equilibrium method. Furthermore, comparisons with experiments both the Danish Code method and a more theoretically correct approach have been made.
The equilibrium method is based on a parabolic stress-strain relation of concrete in compression. The tensile strength is set equal to zero. Furthermore the reinforcement bars are assumed linear elastic-perfectly plastic in both compression and tension.

Since the calculation procedures are iterative in the case of beam-columns, a simplified calculation procedure has been suggested. The simplified method provides an interaction diagram for short and slender columns by calculating 4 or 3 points dependent on whether the column is short or slender, respectively.
The procedure has been compared with the equilibrium method and good agreement has been found.

A number of 311 experiments have been collected from the literature. Among these 200 experiments were made on eccentrically loaded columns, 73 with concentrically loaded columns and 38 with laterally loaded columns. In each case the Danish Code of Practice and the equilibrium method show good agreement. However, as expected, the Danish Code of Practice is a bit conservative. In all cases, the standard deviation between theory and experiments is about 25%, which is relatively high when compared with standard derivations for theories on concrete in general. The large values of the standard derivations may be explained as an effect of unavoidable imperfections.

The conclusion is that the Danish Code of Practice provides a conservative but sufficiently good procedure for calculating both concentrically loaded columns and eccentrically and laterally loaded beam-columns.

10 Literature

The list is ordered by year.

General literature:

[1] SHANLEY, F. R.: Inelastic Column Theory, *Journal of the Aeronautical Sciences, Vol. 4, No. 5, May 1947.*

[2] EULER, L.: On the Strength of Columns (Translation by J.A. Van den Broek), *American journal of physics, pp. 315-318, July - August 1947.*

[3] TIMOSHENKO, S. P. and GERE, J. M.: Theory of Elastic Stability, *International student edition, MaGraw-Hill. 1961.*

[4] HUTCHINSON, J. W.: On the Postbuckling Behaviour of Imperfection-Sensitive Structures in the Plastic Range, *Journal of Applied Mechanics, March 1972.*

[5] NIELSEN, M. P. and HANSEN, L. P.: Mekanik 3.2. Søjler og Bjælkesøjler, *Danmarks Ingeniørakademi, Bygningsafdelingen Aalborg, Den Private Ingeniørfond, 1973.*

[6] NIELSEN, M. P. and RATHKJEN, A.: Mekanik 2.1. Plane spændings og deformationstilstande, *Danmarks Ingeniørakademi, Bygningsafdelingen Aalborg, Den Private Ingeniørfond, 1979.*

[7] NIELSEN, M. P.: Beton 1 del 3, 2. foreløbige, rettede udgave,*Lyngby (DTH), 1993*

[8] JÖNSSON, J.: Continuum Mechanics of Beam and Plate Flexure, *Aalborg University, July 1995.*

[9] NIELSEN, M. P.: Limit Analysis and Concrete Plasticity, *Second Edition, CRC Press, 1998*

[10] DANSK STANDARD: Norm for betonkonstruktioner DS411 (4.1) (Code of Practice for the structural use of concrete), *Dansk Standard, 4.udgave/1.oplag 1999-03-03.*

[11] NIELSEN, M. P., HANSEN, L. P. and RATHKJEN, A.: Mekanik 2.2 del 1. Rumlige spændings og deformationstilstande, *Danmarks Tekniske Universitet, Institut for Bærende Konstruktioner og Materialer København/Aalborg, 2001.*

[12] NIELSEN, M. P., HANSEN, L. P. and RATHKJEN, A.: Mekanik 2.2 del 2. Rumlige spændings og deformationstilstande, *Danmarks Tekniske Universitet Institut for Bærende Konstruktioner og Materialer København/Aalborg, 2001*.

Literature on concrete columns tests:

[13] BAUMANN, O.: "Die Knickung der Eisenbeton-Säulen", *ETH, Zürich,1935*

[14] RAMBØLL, B. J.: "Reinforced Concrete Columns, Concentrically and Eccentrically loaded", *Teknisk forlag, København 1951.*

[15] ERNST, G. C., HROMADIK, J. J. and RIVELAND, A. R.: "Inelastic Buckling of Plain and Reinforced Concrete Columns, Plates and Shells", *University of Nebraska, Bulletin No. 3. August 1953.*

[16] GEHLER, W. and HÜTTER, A.: “Knichkversuche mit Stahlbetonsäulen”. (Buckling tests on reinforced concrete columns.), Berlin, Wilhelm Ernst und Sohn, *Deutscher Ausschuss für Stahlbeton. Heft 133. pp.1-56, 1954.*

[17] GAEDE, K.: “Knicken von Stahlbetonstäben unter Kurtz- und Langzeitbelastung”, Berlin, *Deutscher Ausschuss für Stahlbeton. Heft 129. pp.1-82, 1958.*

[18] CHANG, W. F. and FERGUSON, P. M.: "Long Hinged Reinforced Concrete Columns", *Journal of ACI, Proceedings V. 60, No. 1, Jan. 63.*

[19] PANNELL, F. N. and ROBINSON, J. L.: “Slender reinforced concrete columns with biaxial eccentricity of loading”. *Magazine of concrete research. Vol. 20, No. 65 pp. 195-204, December 1968.*

[20] BREEN, J. E. and FERGUSON, P. M.: "Long Cantilever Columns Subject to Lateral loads", *ACI Journal, November 1969.*

[21] MEHMEL, A., SCHWARZ, H., KASPAREK, K. H. and MAKOVI, J.: "Tragverhalten ausmittig beanspruchter Stahlbetondruckglieder", *Berlin 1969.*

[22] CRANSTON, W. B.: A Computer method for the Analysis of Restrained Columns, *London, Cement and Concrete Association, April 1967, pp. 20. Technical Report TRA 402*

[23] CRANSTON, W. B.: "Analysis and design of reinforced concrete columns", *Cement and Concrete Association, research report 20, 1972.*

[24] OLSEN, P: C.: Beregning af søjle og rammeforsøg efter DS411’s metoder, *Institut for Ren og Anvendt Mekanik DIAB, 1972, Report No. 76:69.*

[25] LENSCHOW, R.: Betongkonstruktjoner, Grunnkurs, *Universitet i Tronheim, Tapir, 1977.*

[26] MACGREGOR, J. G.: Reinforced Concrete, Mechanics & Design, *Department of Civil Engineering University of Alberta, Prentice Hall, 1992.*

[27] NIELSEN, M. P.: “Beton 1 del 3”, *2. foreløbige, rettede udgave, Lyngby (DTH), 1993.*

[28] KIM, J. K. and YANG, J. K.: "Buckling behaviour of slender high-strength concrete columns", *Engng Struct, Volume 17, Number 1., 1993.*

[29] CHUANG, P. H. and KONG, F. K.: "Large-scale tests on slender reinforced concrete columns", *The Structural Engineer, Volume 75, Nos 23 & 24, December 1997.*

[30] FORSTER, S. J. and ATTRAD, M. M.: "Experimental Tests on Eccentrically Loaded High-Strength Concrete Columns", *ACI Structural Journal, V.94, No. 3, May-June* 1997.

[31] CLEASON, C.: "Behavior of slender reinforced concrete columns subjected to Eccentric loading", *Annual Conference of the Canadian Society for Civil Engineering, Sherbrooke, Québec, May 1997*

[32] CHUANG, P. H. and KONG, F. K.: Large-scale tests on slender, reinforced concrete columns, *The Structural Engineer, Volume 75/Nos 23 & 24, December 1997.*

[33] NIELSEN, M. P.: Beton 2 del 1 og 4. *1. Udgave, Lyngby (DTU), 2000.*

[34] NAWY, E. G.: Reinforced Concrete, A Fundamental Approach, *Prentice Hall, 2000.*

11 Appendix

11.1 Author contribution list

Since this paper has been written by two authors the following list of the contributions by the two authors has been made.

Tim Gudmand-Høyer

Sections:

7.3.3 The equilibrium method

7.4.4 Deflection shape and comparison with simplified method

7.4.5 Simplification of the moment-curvature relationship

7.4.6 Interaction diagrams

7.4.7 Simplification of interaction diagrams

7.4.8 Practical calculation of beam-columns

Lars Zenke Hansen

Sections:

8 Comparison with experiments

12 Supplement: Experimental results for concrete beam-columns

12 Supplement: Experimental results for concrete beam-columns

Investigations used to compare theory with experiments:

Oskar Baumann 1935

B. J. Rambøll 1951

George C. Ernst, Joseph J. Hromadik & Arvin R. Riveland 1953

W. Gehler & Alfred Hütter 1954

Kurt Gaede 1958

Wen F. Chang & Phil M. Ferguson 1963

F.N. Parnell & J. L. Robinson 1968

John E. Breen & Phil M. Ferguson 1969

Alfred Mehmel, HeinzSchwarz, Karl-Heinz Kasparek & Joszef Makovi 1969

Jin-Keun Kim & Joo.Kyoung Yang 1993

P. H. Chuang & F. K. Kong 1997

Stephen J. Foster & Mario M. Attrad, 1997

Christina Cleason 1997

The compressive strength is the compressive strength of a Danish standard cylinder (diameter 150 mm and height 300mm).

In the interaction diagrams the compressive strength used for plotting the theoretical curves is taken as a mean value within the individual series.

12.1Baumann, O. 1935

Test No.	b	h	d/h	100ρ	f_c	f_y	$e_{1,u}/h$	$e_{1,0}/h$	l/h	N_{exp}	u_m	Type	N_{exp}	N_{exp}
	[mm]	[mm]			[MPa]	[MPa]				[kN]	[mm]		N_{teo}	N_{DS}
I	200,0	100,0	0,9	1,6	16,0	326,0	0,0	0,0	32,1	265,1	-	A	1,08	1,34
Ia	200,0	100,0	0,9	1,6	16,6	326,0	0,1	0,1	32,1	152,2	-	B	0,88	0,83
III	140,0	140,0	0,9	1,6	16,9	326,0	0,0	0,0	22,9	343,7	-	A	0,91	1,23
IIIa	140,0	140,0	0,9	1,6	17,1	326,0	0,1	0,1	22,9	235,7	-	B	0,90	0,96
V	177,0	139,0	0,9	2,5	27,7	296,6	0,0	0,0	23,3	648,1	-	A	0,86	1,19
Va	178,0	140,0	0,9	2,5	27,7	296,6	0,0	0,0	23,1	685,4	-	A	0,90	1,24
VI	198,0	98,0	0,9	1,6	26,2	326,0	0,0	0,0	32,8	392,8	-	A	1,16	1,45
Via	200,0	100,0	0,9	1,6	26,2	326,0	0,0	0,0	32,1	402,6	-	A	1,13	1,42
VII	182,0	178,0	0,9	1,9	29,7	296,6	0,0	0,0	18,0	687,4	-	A	0,64	0,82
VIIa	180,0	180,0	0,9	1,9	29,7	296,6	0,0	0,0	17,8	824,9	-	A	0,76	0,98
VIII	182,0	178,0	0,9	1,9	30,3	296,6	0,0	0,0	17,5	1070,4	-	A	0,97	1,24
VIIIa	180,0	180,0	0,9	1,9	30,3	296,6	0,0	0,0	15,6	1217,7	-	A	1,11	1,32
1	250,0	250,0	1,0	1,3	35,3	272,0	0,0	0,0	11,9	2042,6	-	A	0,87	1,01
2	250,0	125,0	0,9	0,6	35,3	333,9	0,0	0,0	25,8	697,2	-	A	0,84	1,19
3	250,0	160,0	0,9	0,8	35,3	326,0	0,0	0,0	40,7	667,8	-	A	1,09	1,54
4	250,0	250,0	1,0	1,3	33,8	272,0	0,2	0,2	11,9	962,4	-	B	0,71	0,83
5	250,0	125,0	0,9	0,6	33,6	333,9	0,2	0,2	25,8	343,7	-	B	0,99	1,06
6	250,0	160,0	0,9	0,8	33,8	326,0	0,2	0,2	40,7	225,9	-	B	0,97	1,03
7	250,0	250,0	1,0	1,3	21,4	272,0	0,2	0,2	11,9	844,5	-	B	0,90	1,04
8	250,0	126,0	0,9	0,6	21,4	333,9	0,2	0,2	25,6	333,9	-	B	1,32	1,32
9	250,0	162,0	0,9	0,8	21,3	326,0	0,2	0,2	40,2	206,2	-	B	1,19	1,07
10	253,0	251,0	1,0	1,3	31,4	272,0	0,3	0,3	11,8	692,3	-	B	0,82	0,98
11	252,0	126,0	0,9	0,6	31,4	333,9	0,3	0,3	25,6	196,4	-	B	1,23	1,23
12	250,0	162,0	0,9	0,8	31,2	326,0	0,3	0,3	40,2	112,9	-	B	1,03	0,92
13	251,0	247,0	0,9	1,3	34,5	272,0	0,3	0,3	12,0	701,1	-	B	0,80	0,93
14	248,0	126,0	0,9	0,6	34,5	333,9	0,3	0,3	25,6	163,0	-	B	1,02	1,02
15	247,0	161,0	0,9	0,8	34,7	326,0	0,0	0,0	40,4	549,9	-	A	0,91	1,27
17	200,0	90,0	0,9	1,1	20,7	333,9	0,0	0,0	16,2	378,1	-	E	0,89	1,10
18	201,0	91,0	0,9	1,1	20,7	333,9	0,0	0,0	23,9	359,4	-	F	1,04	1,33
19	250,0	130,0	0,9	1,0	25,1	326,0	0,2	0,0	24,7	387,9	-	C	1,14	1,14
20	250,0	130,0	0,9	1,0	25,1	326,0	0,0	0,0	16,1	849,4	-	F	0,96	1,19
21	200,0	89,0	0,9	1,1	35,8	333,9	0,0	0,0	16,3	549,9	-	E	0,83	1,08
22	200,0	89,0	0,9	1,1	35,8	333,9	0,0	0,0	16,3	623,6	-	E	0,94	1,23
23	248,0	129,0	0,9	1,0	39,4	326,0	0,0	0,0	10,7	1075,3	-	E	0,81	0,93
24	248,0	129,0	0,9	1,0	39,4	326,0	0,0	0,0	16,2	947,6	-	F	0,73	0,98
25	248,0	250,0	1,0	1,0	31,2	296,6	0,2	0,0	8,1	1306,1	-	G	0,99	1,18
26	252,0	250,0	1,0	1,0	31,2	296,6	0,2	0,0	12,6	1325,7	-	C	1,08	1,26
27	201,0	92,0	0,9	1,7	32,2	326,0	0,2	0,0	23,7	338,8	-	G	1,25	1,31
28	200,0	89,0	0,9	1,8	30,2	326,0	0,2	0,0	24,5	289,7	-	G	1,22	1,22
29	250,0	130,0	0,9	1,9	33,5	296,6	0,2	0,0	16,0	736,5	-	G	1,07	1,21
30	250,0	132,0	0,9	1,9	33,5	296,6	0,2	0,0	15,8	770,9	-	G	1,11	1,25

31	250,0	250,0	1,0	2,0	28,9	282,8	0,2	0,0	8,1	1433,7	-	G	1,19	1,33
32	250,0	250,0	1,0	2,0	28,9	282,8	0,2	0,0	12,6	1350,3	-	C	0,86	0,96

Table 12.1 Data used for calculations, taken from [13]

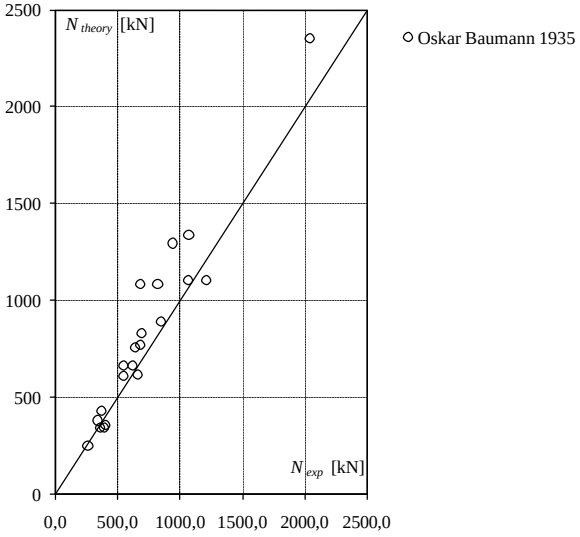

Figure 12.1 The results of calculations by the equilibrium method compared with experiments for e=0

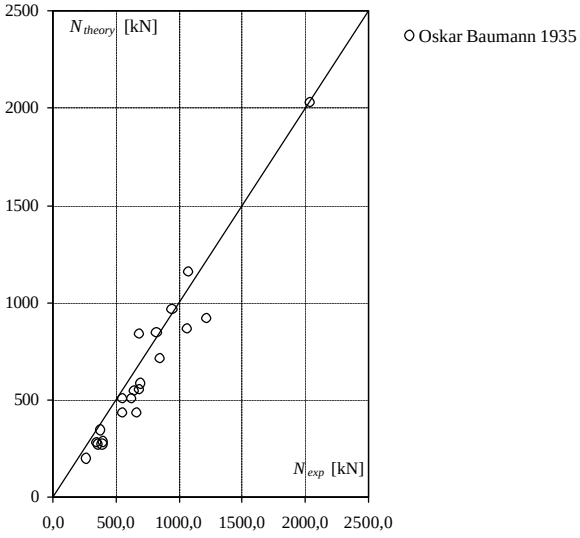

Figure 12.2 The results of calculations by the Danish Code of Practice compared with experiments for e=0

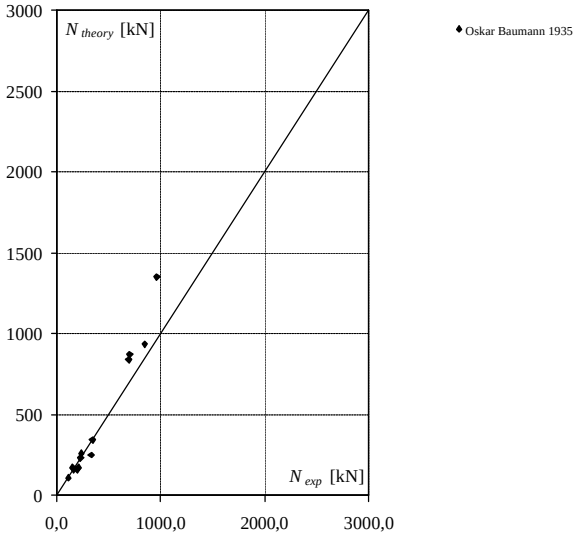

Figure 12.3 The results of calculations by the equilibrium method compared with experiments for eccentrically loaded beam-columns

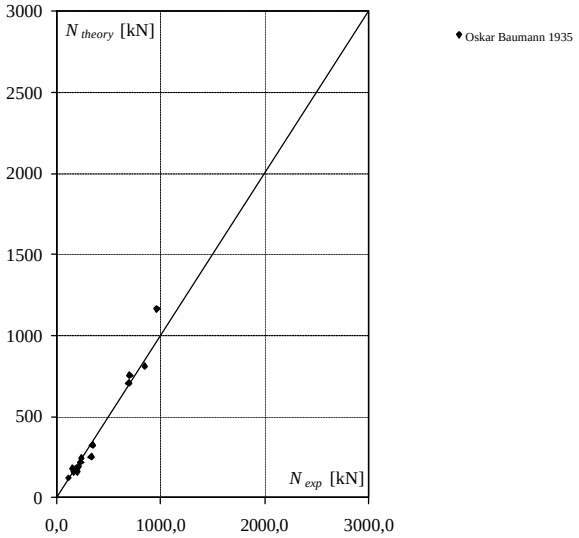

Figure 12.4 The resulst of calculations by the equilibrium method compared with experiments for eccentrically loaded beam-columns

12.2Rambøll, B. J. 1951

Test No.	b	h	d/h	100ρ	f_c	f_y	$e_{t,t}/h$	$e_{t,b}/h$	l/h	N_{exp}	u_m	Type	N_{exp}	N_{exp}
	[mm]	[mm]			[MPa]	[MPa]				[kN]	[mm]		N_{teo}	N_{DS}
1	182,0	144,0	0,8	1,0	28,6	294,6	0,0	0,0	8,9	859,3	-	A	1,05	1,14
2	181,0	141,0	0,8	1,0	25,5	294,6	0,0	0,0	9,1	638,3	-	A	0,89	0,96
3	182,0	143,0	0,8	1,0	26,5	294,6	0,1	0,1	9,0	687,4	-	B	0,75	0,86
4	181,0	141,0	0,8	1,0	21,2	294,6	0,1	0,1	9,1	589,2	-	B	0,98	1,11
5	181,0	143,0	0,8	1,0	27,8	294,6	0,2	0,2	9,0	510,6	-	B	0,92	1,03
6	181,0	143,0	0,8	1,0	25,1	294,6	0,2	0,2	9,0	530,3	-	B	0,92	1,03
7	180,0	145,0	0,8	1,0	23,7	294,6	0,3	0,3	8,8	338,8	-	B	0,84	1,06
8	181,0	144,0	0,8	1,0	25,4	294,6	0,3	0,3	8,9	294,6	-	B	0,68	0,86
9	181,0	142,0	0,8	1,0	23,4	294,6	0,7	0,7	9,0	117,8	-	B	1,05	1,30
10	181,0	144,0	0,8	1,0	24,5	294,6	0,7	0,7	8,9	106,1	-	B	1,22	1,41
11	181,0	141,0	0,8	1,0	25,8	294,6	0,8	0,8	9,1	78,6	-	B	1,29	1,47
12	181,0	141,0	0,8	1,0	21,6	294,6	0,8	0,8	9,1	78,6	-	B	1,15	1,32
13	181,0	142,0	0,8	1,0	28,5	294,6	0,0	0,0	13,0	579,4	-	A	1,10	1,27
14	181,0	142,0	0,8	1,0	25,7	294,6	0,0	0,0	13,0	687,4	-	A	1,23	1,30
15	181,0	147,0	0,8	1,0	24,7	294,6	0,0	0,0	12,6	648,1	-	A	1,11	1,31
16	183,0	146,0	0,8	1,0	24,7	294,6	0,0	0,0	12,7	648,1	-	A	1,26	1,49
17	180,0	142,0	0,8	1,0	25,1	294,6	0,1	0,1	13,0	579,4	-	B	1,28	1,45
18	181,0	144,0	0,8	1,0	23,6	294,6	0,1	0,1	12,8	534,2	-	B	1,36	1,53
19	180,0	142,0	0,8	1,0	24,2	294,6	0,2	0,2	13,0	471,4	-	B	0,98	1,03
20	182,0	143,0	0,8	1,0	24,4	294,6	0,2	0,2	12,9	510,6	-	B	1,39	1,74
21	183,0	145,0	0,8	1,0	23,1	294,6	0,3	0,3	12,8	294,6	-	B	1,14	1,43
22	182,0	144,0	0,8	1,0	23,3	294,6	0,3	0,3	12,8	306,4	-	B	1,38	1,59
23	181,0	144,0	0,8	1,0	23,5	294,6	0,7	0,7	12,8	94,3	-	B	1,44	1,72
24	181,0	144,0	0,8	1,0	22,0	294,6	0,7	0,7	12,8	94,3	-	B	1,32	1,39
25	182,0	144,0	0,8	1,0	28,2	294,6	0,8	0,8	12,8	68,7	-	B	1,25	1,15
26	181,0	141,0	0,8	1,0	26,8	294,6	0,8	0,8	13,1	66,8	-	B	1,58	1,58
27	182,0	141,0	0,8	1,0	29,4	294,6	0,0	0,0	20,6	579,4	-	A	1,35	1,35
28	183,0	146,0	0,8	1,0	28,7	294,6	0,0	0,0	19,9	491,0	-	A	1,37	1,37
29	182,0	144,0	0,8	1,0	29,6	294,6	0,2	0,2	20,1	333,9	-	B	1,32	1,45
30	182,0	143,0	0,8	1,0	27,2	294,6	0,3	0,3	20,3	196,4	-	B	1,23	1,23
31	183,0	144,0	0,8	1,0	29,2	294,6	0,7	0,7	20,1	72,7	-	B	1,19	1,19
32	183,0	142,0	0,8	1,0	29,5	294,6	0,8	0,8	20,4	57,0	-	B	1,34	1,53
33	183,0	143,0	0,8	1,0	27,6	294,6	0,0	0,0	30,1	494,9	-	A	1,39	1,57
34	182,0	145,0	0,8	1,0	29,6	294,6	0,1	0,1	29,7	412,4	-	B	1,41	1,41
35	183,0	144,0	0,8	1,7	26,6	294,6	0,2	0,2	29,9	235,7	-	B	1,26	1,26
36	183,0	143,0	0,8	1,0	27,3	294,6	0,3	0,3	30,1	117,8	-	B	1,35	1,35
37	182,0	145,0	0,8	1,0	26,9	294,6	0,7	0,7	29,7	56,0	-	B	1,18	1,18
38	182,0	145,0	0,8	1,0	32,5	294,6	0,8	0,8	29,7	44,2	-	B	1,13	1,13

Table 12.2 Data used for calculations, taken from [14]

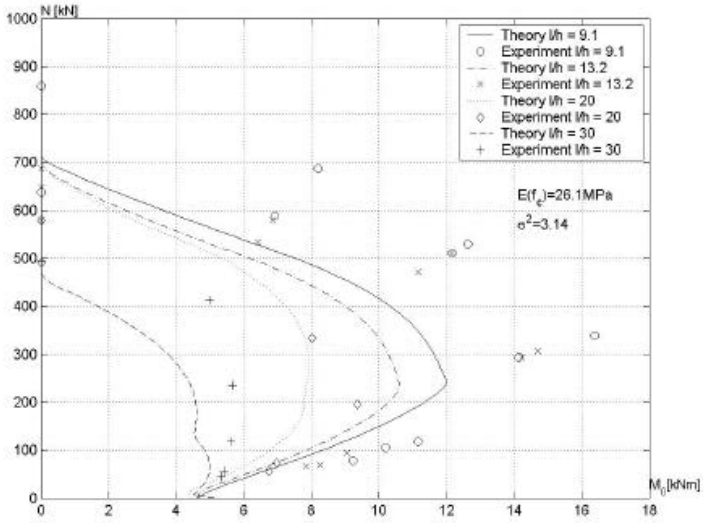

Figure 12.5 The result of calculations plotted in an interaction diagram.

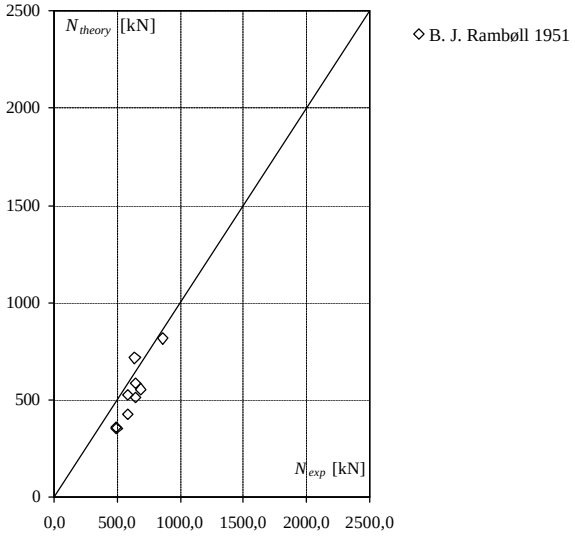

Figure 12.6 The results of calculations by the equilibrium method compared with experiments for e=0

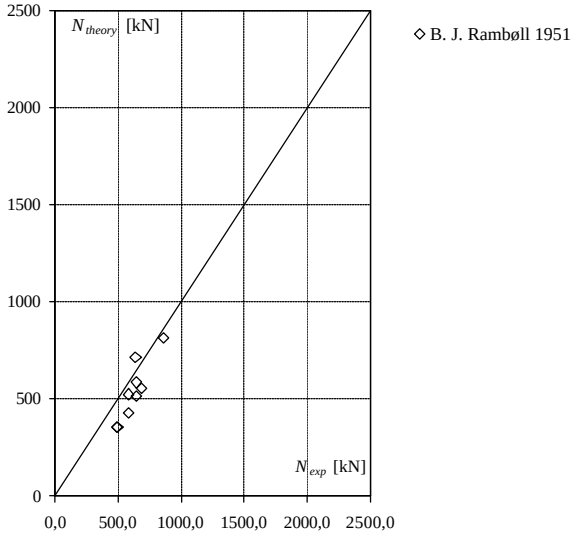

Figure 12.7 The results of calculations by Danish Code of Practice compared with experiments for e=0

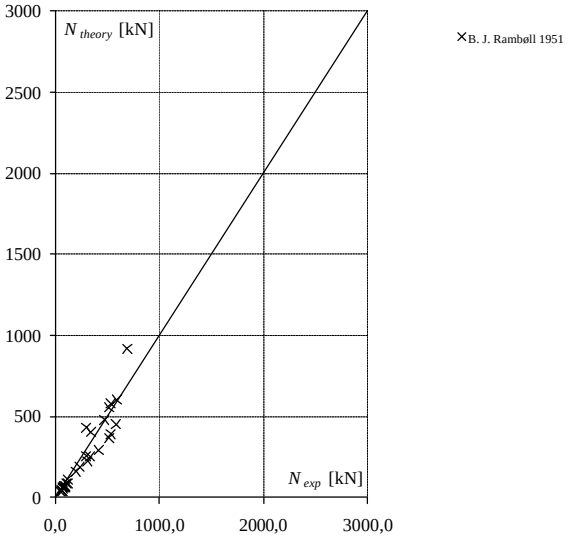

Figure 12.8 The results of calculations by the equilibrium method compared with experiments for eccentrically loaded beam-columns

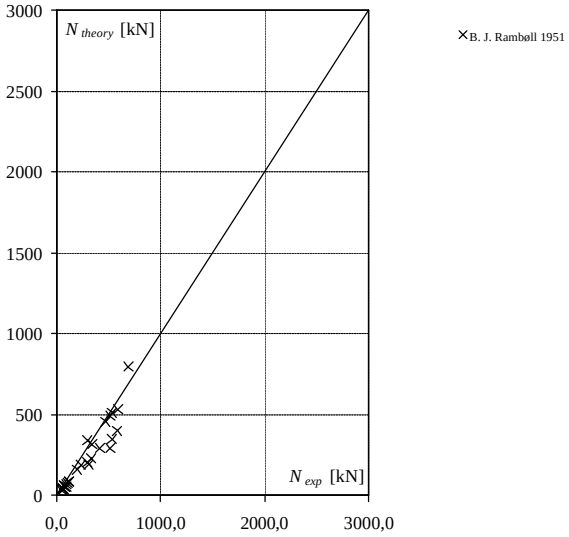

Figure 12.9 The results of calculations by the Danish Code of Practice compared with experiments for eccentrically loaded beam-columns

12.3Ernst, G. C, Hromadik, J. J. & Riveland, A. R. 1953

Test No.	b	h	d/h	100ρ	f_c	f_y	$e_{i,t}/h$	$e_{i,b}/h$	l/h	N_{exp}	u_m	Type	N_{exp}	N_{exp}
	[mm]	[mm]			[MPa]	[MPa]				[kN]	[mm]		N_{teo}	N_{DS}
1	152,4	152,4	0,8	1,2	20,1	356,8	0,0	0,0	2,0	503,3	-	A	0,88	0,89
2	152,4	152,4	0,8	1,2	20,1	356,8	0,0	0,0	5,0	432,1	-	A	0,76	0,78
3	152,4	152,4	0,8	1,2	20,1	356,8	0,0	0,0	15,0	490,0	-	A	0,89	1,07
4	152,4	152,4	0,8	1,2	20,1	356,8	0,0	0,0	25,0	449,9	-	A	1,10	1,36
5	152,4	152,4	0,8	1,2	20,1	356,8	0,1	0,1	2,0	423,2	-	B	0,57	0,57
6	152,4	152,4	0,8	1,2	20,1	356,8	0,1	0,1	5,0	409,8	-	B	0,71	0,73
7	152,4	152,4	0,8	1,2	20,1	356,8	0,1	0,1	15,0	356,3	-	B	1,06	1,24
8	152,4	152,4	0,8	1,2	20,1	356,8	0,1	0,1	25,0	289,5	-	B	1,04	1,22
9	152,4	152,4	0,8	1,2	20,1	356,8	0,3	0,3	2,0	203,6	-	B	1,04	1,18
10	152,4	152,4	0,8	1,2	20,1	356,8	0,3	0,3	5,0	249,4	-	B	1,24	1,24
11	152,4	152,4	0,8	1,2	20,1	356,8	0,3	0,3	15,0	259,2	-	B	0,70	0,87
12	152,4	152,4	0,8	1,2	20,1	356,8	0,3	0,3	25,0	172,4	-	B	0,88	1,07
13	152,4	152,4	0,8	1,2	20,1	356,8	0,0	0,0	2,0	325,2	-	A	1,11	1,26
14	152,4	152,4	0,8	1,2	20,1	356,8	0,0	0,0	5,0	405,3	-	A	1,16	1,16
15	152,4	152,4	0,8	1,2	20,1	356,8	0,4	0,4	15,0	89,1	-	B	0,52	0,63
16	152,4	152,4	0,8	1,2	20,1	356,8	0,4	0,4	25,0	110,5	-	B	1,02	1,02

Table 12.3 Data used for calculations, taken from [15]

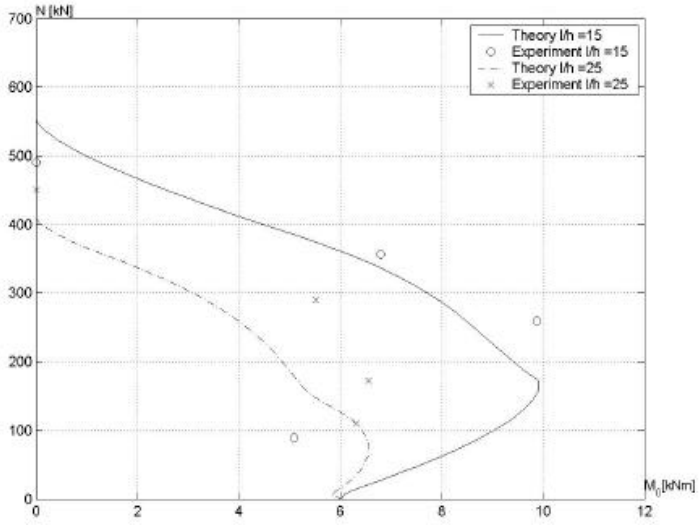

Figure 12.10 The results of calculations plotted in an interaction diagram, $f_{c,cylinder}$ *= 20.1 MPa*

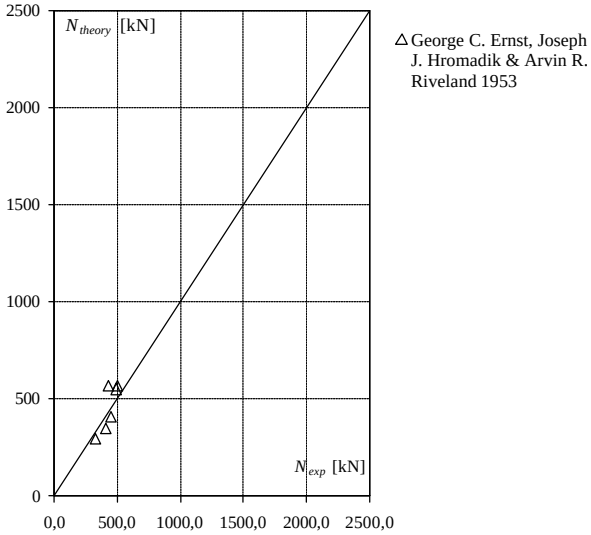

Figure 12.11 The resulst of calculations by the equilibrium method compared with experiments for e=0

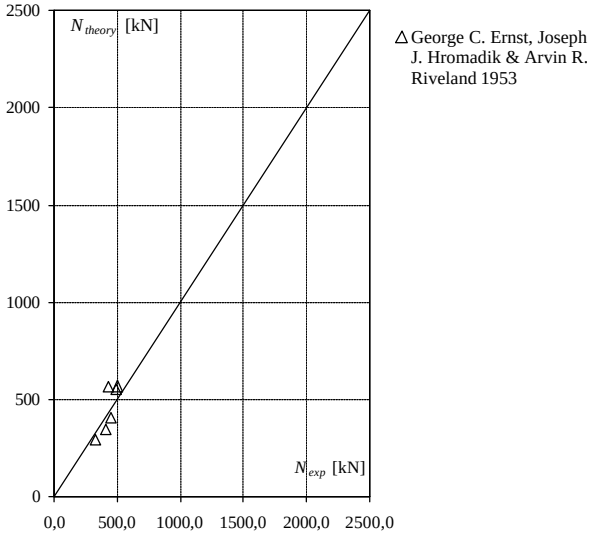

Figure 12.12 The results of calculations by the Danish Code of Practice compared with experiments for e=0

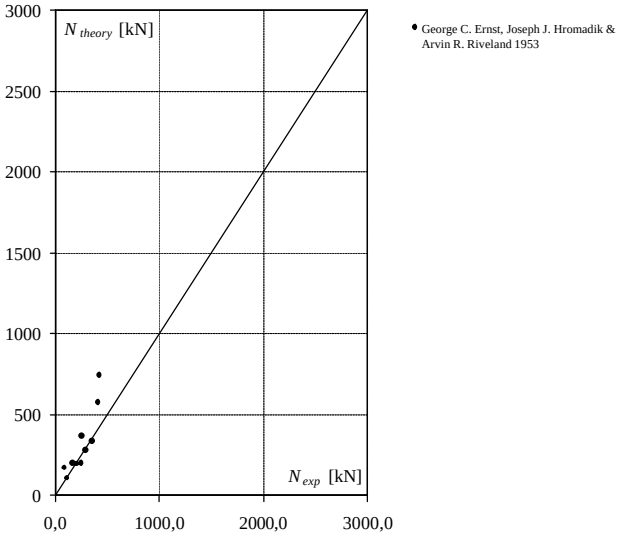

Figure 12.13 The results of calculations by the equilibrium method compared with experiments for eccentrically loaded beam-columns

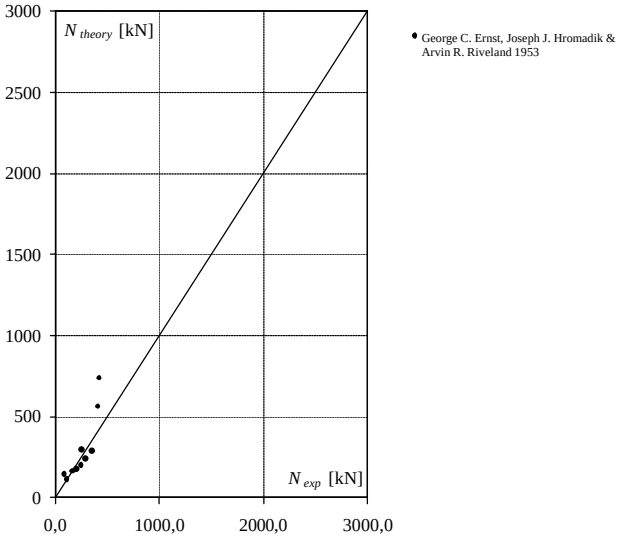

Figure 12.14 The results of calculations by the Danish Code of Practice compared with experiments for eccentrically loaded beam-columns

12.4Gehler, W. & Hütter, A. 1954

Test No.	b	h	d/h	100ρ	f_c	f_y	$e_{i,v}/h$	$e_{i,0}/h$	l/h	N_{exp}	u_m	Type	N_{exp}	N_{exp}
	[mm]	[mm]			[MPa]	[MPa]				[kN]	[mm]		N_{teo}	N_{DS}
Ia	160,0	140,0	0,9	0,9	19,3	282,8	0,0	0,0	40,0	241,0	-	A	1,18	1,38
Ia	160,0	140,0	0,9	0,9	19,3	282,8	0,0	0,0	40,0	258,1	-	A	1,26	1,48
Ib	160,0	140,0	0,9	0,9	19,4	282,8	0,0	0,0	30,0	384,6	-	A	1,26	1,56
Ib	160,0	140,0	0,9	0,9	19,4	282,8	0,0	0,0	30,0	399,2	-	A	1,31	1,62
Ic	160,0	140,0	0,9	0,9	20,7	282,8	0,0	0,0	25,0	497,4	-	A	1,27	1,61
Ic	160,0	140,0	0,9	0,9	20,7	282,8	0,0	0,0	25,0	533,8	-	A	1,36	1,72
Id	160,0	140,0	0,9	0,9	20,5	282,8	0,0	0,0	20,0	486,5	-	A	1,06	1,34
Id	160,0	140,0	0,9	0,9	20,5	282,8	0,0	0,0	20,0	552,0	-	A	1,20	1,52
Ie	160,0	140,0	0,9	0,9	19,8	282,8	0,0	0,0	15,0	595,7	-	A	1,28	1,47
Ie	160,0	140,0	0,9	0,9	19,8	282,8	0,0	0,0	15,0	566,5	-	A	1,22	1,40
If	160,0	140,0	0,9	0,9	18,8	282,8	0,0	0,0	10,0	475,3	-	A	1,01	1,10
If	160,0	140,0	0,9	0,9	18,8	282,8	0,0	0,0	10,0	498,4	-	A	1,06	1,15
Iia	160,0	140,0	0,8	2,8	19,5	337,8	0,0	0,0	40,0	324,6	-	A	1,18	1,45
Iia	160,0	140,0	0,8	2,8	19,5	337,8	0,0	0,0	40,0	348,2	-	A	1,14	1,40
1	160,0	140,0	0,9	0,5	25,0	235,2	0,0	0,0	40,0	174,3	-	A	0,96	1,18
1	160,0	140,0	0,9	0,5	25,0	235,2	0,0	0,0	40,0	196,3	-	A	1,01	1,24
2	160,0	140,0	0,8	2,0	26,0	316,2	0,0	0,0	40,0	218,6	-	A	1,04	1,29
2	160,0	140,0	0,8	2,0	26,0	289,4	0,0	0,0	40,0	285,4	-	A	1,04	1,29
3	160,0	140,0	0,8	5,6	24,0	289,4	0,0	0,0	40,0	326,0	-	A	0,72	0,85
3	160,0	140,0	0,8	5,6	24,0	289,4	0,0	0,0	40,0	285,4	-	A	0,81	0,96
4	160,0	140,0	0,9	0,9	13,4	206,5	0,0	0,0	30,0	262,3	-	A	0,75	0,85
4	160,0	140,0	0,9	0,9	13,4	206,5	0,0	0,0	30,0	253,1	-	A	0,97	1,12
5	160,0	140,0	0,9	0,9	21,1	206,5	0,0	0,0	30,0	311,3	-	A	1,25	1,40
5	160,0	140,0	0,9	0,9	21,1	206,5	0,0	0,0	30,0	327,0	-	A	1,34	1,50
6	160,0	140,0	0,9	0,9	26,2	206,5	0,0	0,0	30,0	405,7	-	A	0,91	0,92
6	160,0	140,0	0,9	0,9	26,2	206,5	0,0	0,0	30,0	405,7	-	A	0,79	0,81

Test No.	b	h	d/h	100r	f_c	f_y	H	l/h	N_{exp}	u_m	Type	N_{exp}	N_{exp}
	[mm]	[mm]			[MPa]	[MPa]	[kN]		[kN]	[mm]	D	N_{teo}	N_{DS}
7	160,0	140,0	0,8	2,0	18,7	289,4	4,7	15,0	473,3	-	D	1,09	1,20
7	160,0	140,0	0,8	2,0	18,7	289,4	4,5	15,0	448,8	-	D	1,03	1,13
8	160,0	140,0	0,8	2,0	23,9	289,4	4,8	20,0	480,2	-	D	1,06	1,16
8	160,0	140,0	0,8	2,0	23,9	289,4	4,5	20,0	446,5	-	D	0,99	1,08
9	160,0	140,0	0,8	2,0	21,9	289,4	3,2	30,0	321,4	-	D	1,17	1,15
9	160,0	140,0	0,8	2,0	21,9	289,4	3,0	30,0	298,7	-	D	1,09	1,07
10	160,0	140,0	0,8	2,0	21,7	289,4	1,5	40,0	152,6	-	D	0,99	0,92
10	160,0	140,0	0,8	2,0	21,7	289,4	1,7	40,0	165,7	-	D	1,07	1,00
11	160,0	140,0	0,8	2,0	18,8	289,4	8,7	15,0	433,0	-	D	1,12	1,23
11	160,0	140,0	0,8	2,0	18,8	289,4	9,4	15,0	470,3	-	D	1,22	1,33
12	160,0	140,0	0,8	2,0	23,9	289,4	7,9	20,0	397,5	-	D	1,03	1,11

12	160,0	140,0	0,8	2,0	23,9	289,4	8,1	20,0	405,1	-	D	1,05	1,13
13	160,0	140,0	0,8	2,0	24,4	289,4	4,7	30,0	236,4	-	D	1,13	1,09
13	160,0	140,0	0,8	2,0	24,4	289,4	4,8	30,0	238,1	-	D	1,14	1,10
14	160,0	140,0	0,8	2,0	20,9	289,4	2,5	40,0	126,6	-	D	1,24	1,11
14	160,0	140,0	0,8	2,0	20,9	289,4	2,3	40,0	113,5	-	D	1,11	1,00
15	160,0	140,0	0,8	2,0	18,8	289,4	12,1	15,0	402,6	-	D	1,16	1,28
15	160,0	140,0	0,8	2,0	18,8	289,4	13,2	15,0	439,2	-	D	1,26	1,40
16	160,0	140,0	0,8	2,0	18,7	289,4	7,9	20,0	264,5	-	D	0,96	1,02
16	160,0	140,0	0,8	2,0	18,7	289,4	9,2	20,0	307,8	-	D	1,12	1,19
17	160,0	140,0	0,8	2,0	19,0	289,4	5,9	30,0	196,3	-	D	1,36	1,31
17	160,0	140,0	0,8	2,0	19,0	289,4	5,2	30,0	174,3	-	D	1,20	1,16
18	160,0	140,0	0,8	2,0	20,1	289,4	3,1	40,0	104,8	-	D	1,20	1,13
18	160,0	140,0	0,8	2,0	20,1	289,4	3,0	40,0	100,5	-	D	1,15	1,08

Table 12.4 Data used for calculations, taken from [16]

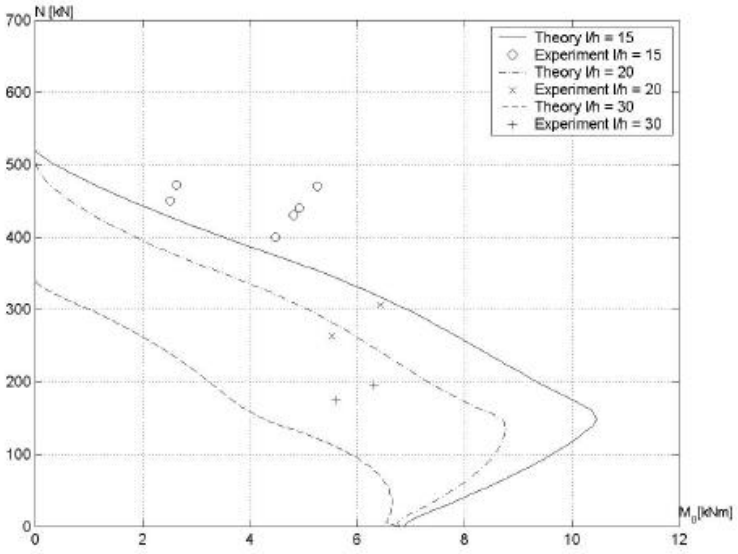

Figure 12.15 The results of calculations plotted in an interaction diagram, $f_{c,cylinder}$ = 18.6 MPa

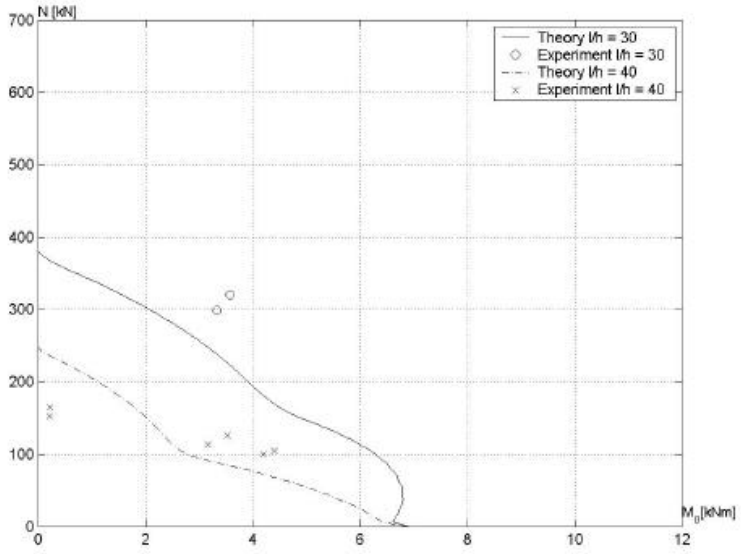

Figure 12.16 The results of calculations plotted in an interaction diagram, $f_{c,cylinder}$ *= 21.8 MPa and* $f_{c,cylinder}$ *= 20.9 MPa respectively*

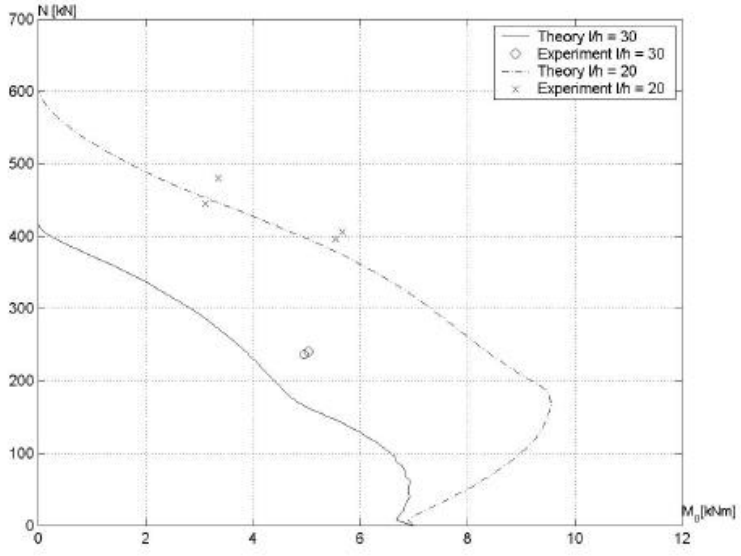

Figure 12.17 The results of calculations plotted in an interaction diagram, $f_{c,cylinder}$ *= 24.3 MPa and* $f_{c,cylinder}$ *= 23.8 MPa respectively*

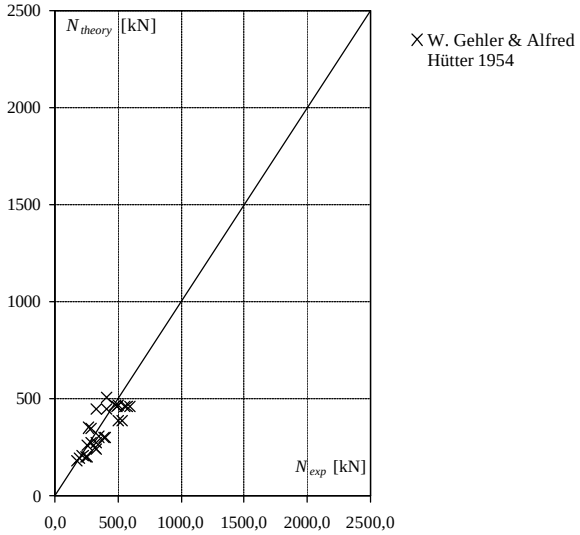

Figure 12.18 The results of calculations by the equilibrium method compared with experiments for e=0

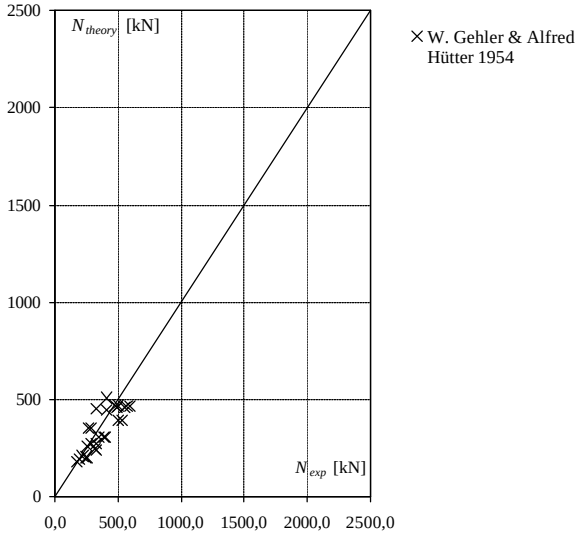

Figure 12.19 The results of calculations by the Danish Code of Practice compared with experiments for e=0

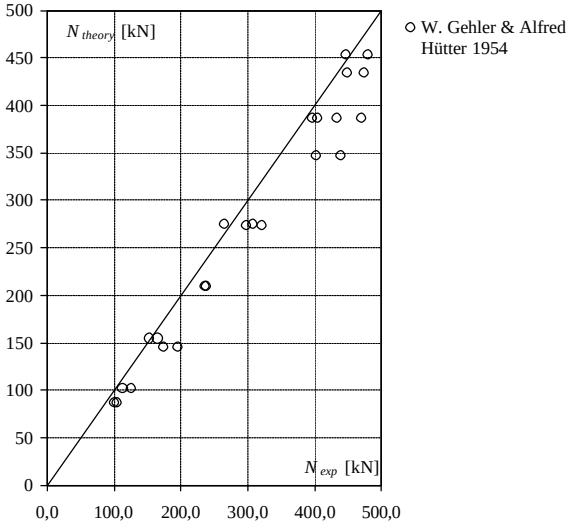

Figure 12.20 The results of calculations by the equilibrium method compared with experiments for laterally loaded beam-columns

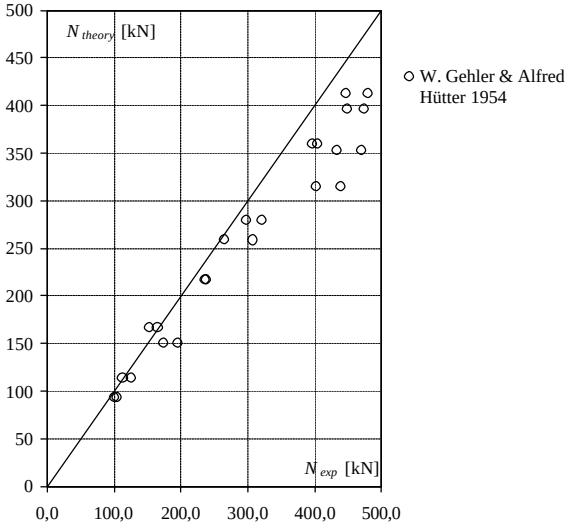

Figure 12.21 The results of calculations by the Danish Code of Practice compared with experiments for laterally loaded beam-columns

12.5Gaede, K. 1958

Test No.	b	h	d/h	100ρ	f_c	f_y	$e_{i,t}/h$	$e_{i,b}/h$	l/h	N_{exp}	u_m	Type	N_{exp}	N_{exp}
	[mm]	[mm]			[MPa]	[MPa]				[kN]	[mm]		N_{teo}	N_{DS}
I/1	154,0	100,0	0,9	1,0	19,8	335,4	0,2	0,2	29,4	75,6	-	B	0,85	0,82
I/5	154,0	100,0	0,9	1,0	25,7	288,9	0,2	0,2	29,4	97,0	-	B	0,92	0,88
II/4	154,0	100,0	0,9	1,0	24,1	273,7	0,5	0,5	29,4	36,1	28,0	B	0,79	0,73
II/5	154,0	100,0	0,9	1,0	25,3	272,6	0,5	0,5	29,4	37,8	23,5	B	0,88	0,80
III/1	154,0	100,0	0,9	1,0	26,3	327,3	0,5	0,5	35,4	33,4	33,0	B	0,92	0,73
III/2	154,0	100,0	0,9	1,0	22,9	326,0	0,5	0,5	35,4	33,4	43,0	B	0,92	0,83
III/3	154,0	100,0	0,9	1,0	22,8	326,5	0,5	0,5	35,4	33,6	45,0	B	0,93	0,84
III/4	154,0	100,0	0,9	1,0	31,1	326,6	0,5	0,5	35,4	37,3	38,5	B	0,88	0,88

Table 12.5 Data used for calculations, taken from [17]

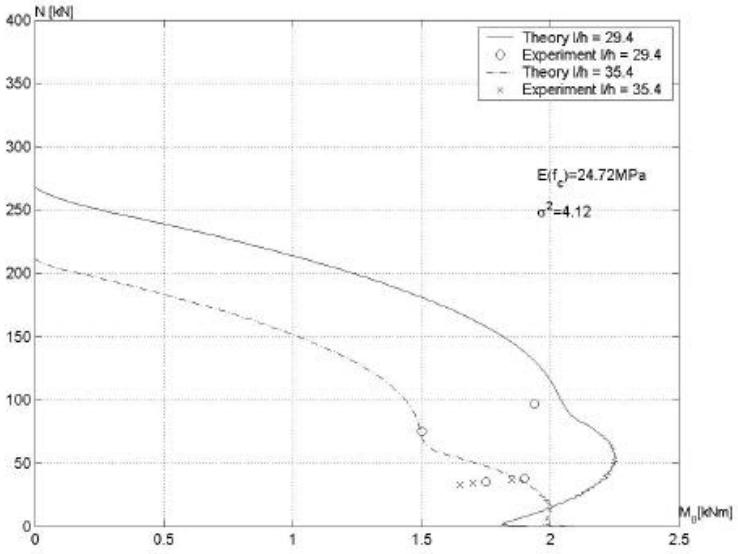

Figure 12.22 The results of calculations plotted in an interaction diagram

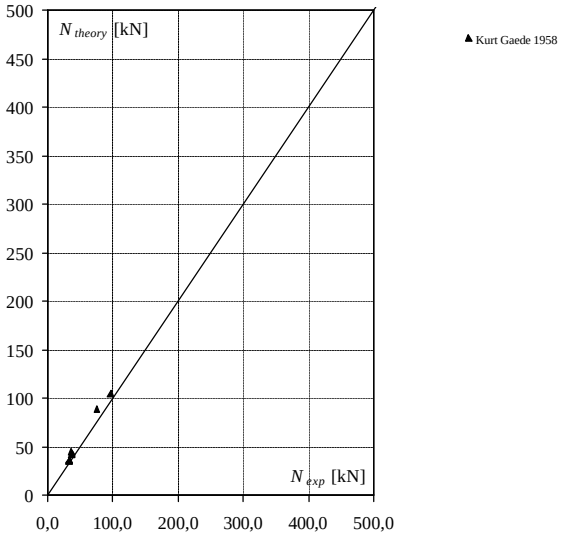

Figure 12.23 The results of calculations by the equilibrium method compared with experiments for eccentrically loaded beam-columns

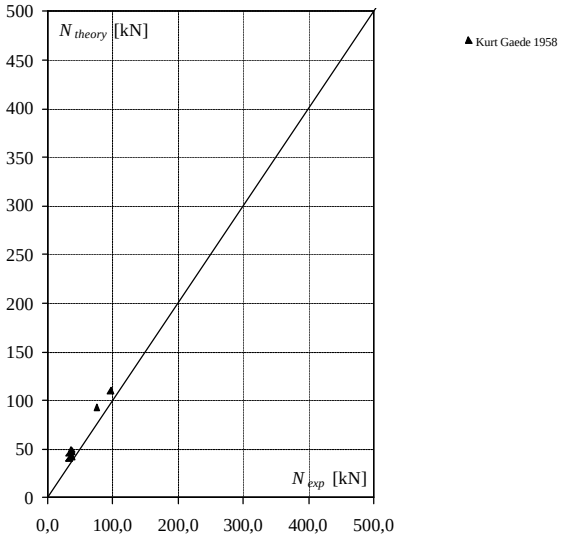

Figure 12.24 The results of calculations by the Danish Code of Practice compared with experiments for eccentrically loaded beam-columns

12.6 Chang, W. F. & Ferguson, P. M. 1963

Test No.	b	h	d/h	100ρ	f_c	f_y	$e_{i,t}/h$	$e_{i,b}/h$	l/h	N_{exp}	u_m	Type	N_{exp}	N_{exp}
	[mm]	[mm]			[MPa]	[MPa]				[kN]	[mm]		N_{teo}	N_{DS}
1	155,6	103,2	0,8	1,8	23,3	344,8	0,1	0,1	25,6	168,1	-	B	0,70	0,68
2	155,6	103,2	0,8	1,8	35,0	344,8	0,4	0,4	25,6	68,9	-	B	0,62	0,65
3	155,6	103,2	0,8	1,8	28,9	344,8	0,1	0,1	25,6	189,5	-	B	0,60	0,61
4	155,6	103,2	0,8	1,8	30,1	344,8	0,4	0,4	25,6	72,5	-	B	0,66	0,66
5	155,6	103,2	0,8	1,8	32,8	344,8	0,2	0,2	25,6	122,8	-	B	0,62	0,62
6	155,6	103,2	0,8	1,8	33,6	434,4	0,1	0,1	25,6	197,5	-	B	0,703	0,729

Table 12.6 Data used for calculations, taken from [18]

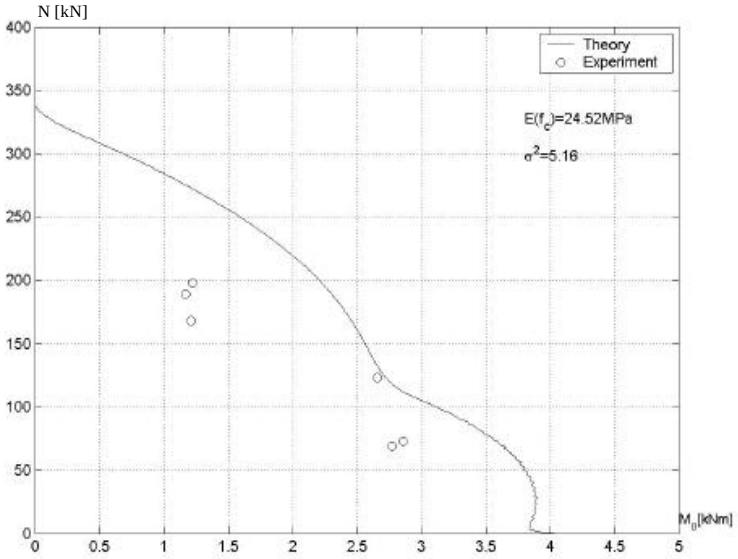

Figure 12.25 The results of calculations plotted in an interaction diagram, l/h = *30*

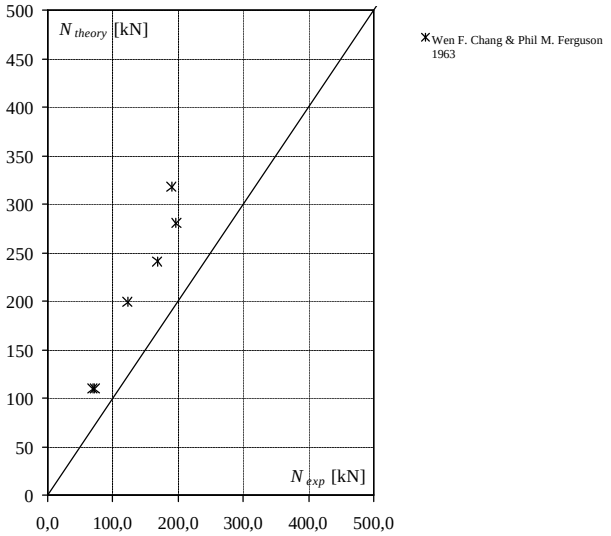

Figure 12.26 The results of calculations by the equilibrium method compared with experiments for eccentrically loaded beam-columns

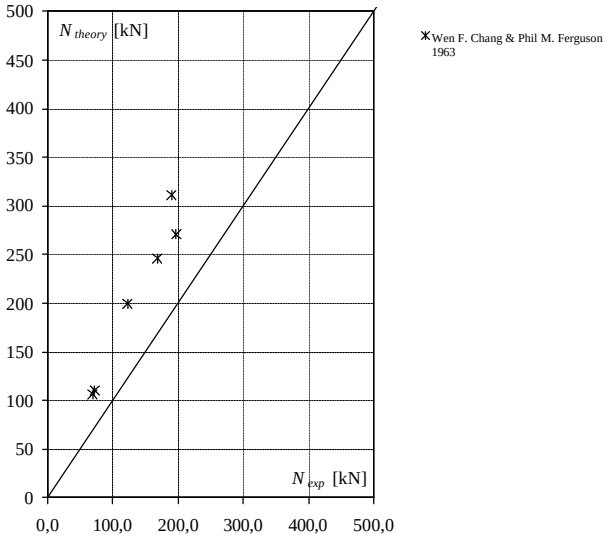

Figure 12.27 The results of calculations by the Danish Code of Practice compared with experiments for eccentrically loaded beam-columns

12.7Panell , F. N. & Robinson, J. L. 1969

Test No.	b	h	d/h	100ρ	f_c	f_y	$e_{i,t}/h$	$e_{i,b}/h$	l/h	N_{exp}	u_m	Type	N_{exp}	N_{exp}
	[mm]	[mm]			[MPa]	[MPa]				[kN]	[mm]		N_{teo}	N_{DS}
1A	95,3	63,5	0,8	3,3	19,1	352,1	0,0	0,0	41,6	60,9	-	A	0,96	0,97
2A	95,3	63,5	0,8	3,3	18,3	365,9	0,0	0,0	41,6	74,7	-	A	1,21	1,23
3A	95,3	63,5	0,8	3,3	17,0	365,9	0,0	0,0	27,2	99,6	-	A	0,91	1,04
4A	95,3	63,5	0,8	3,3	21,2	365,9	0,0	0,0	15,2	174,4	-	A	0,88	1,08
5A	95,3	63,5	0,8	3,3	21,3	365,9	0,0	0,0	32,0	98,7	-	A	0,96	1,07
6B	95,3	63,5	0,8	3,3	22,8	352,1	1,4	1,4	41,6	14,9	-	D	1,20	1,20
7B	63,5	95,3	0,9	3,3	24,5	352,1	1,8	1,8	27,7	19,9	-	D	1,31	1,31
8B	95,3	63,5	0,8	3,3	15,9	352,1	0,2	0,2	41,6	54,7	-	D	1,94	1,74
9B	63,5	95,3	0,9	3,3	15,9	352,1	0,7	0,7	27,7	39,9	-	D	1,20	1,34

Table 12.7 Data used for calculations, taken from [19]

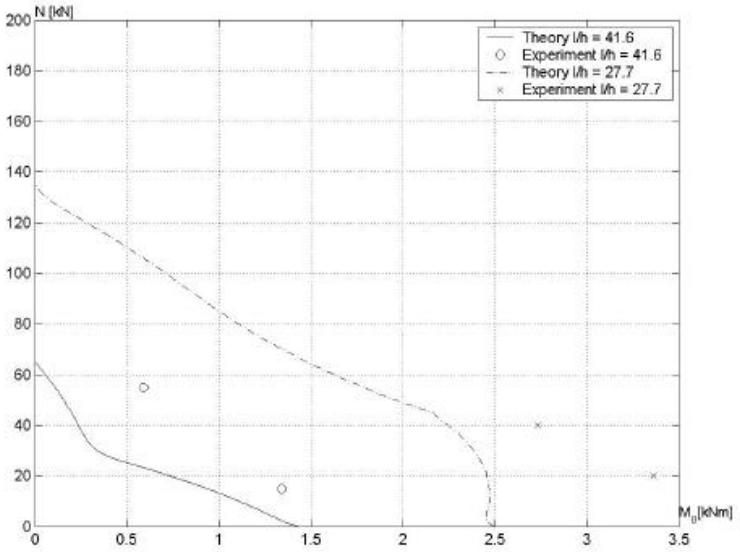

Figure 12.28 The results of calculations plotted in an interaction diagram, the compressive strength is calculated as a mean of the values given in the table above

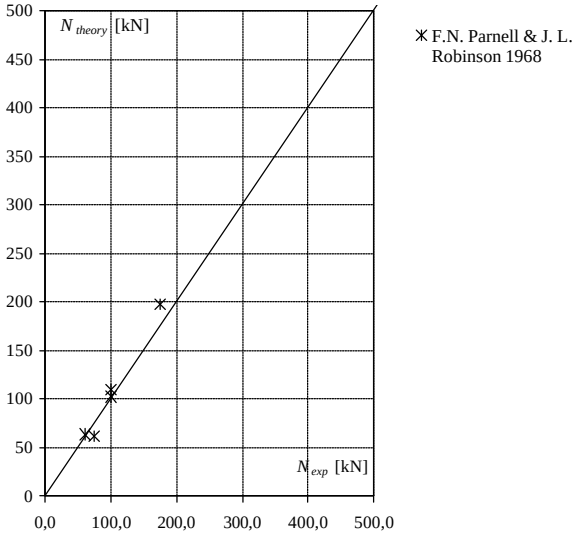

Figure 12.29 The results of calculations by the equilibrium method compared with experiments for e=0

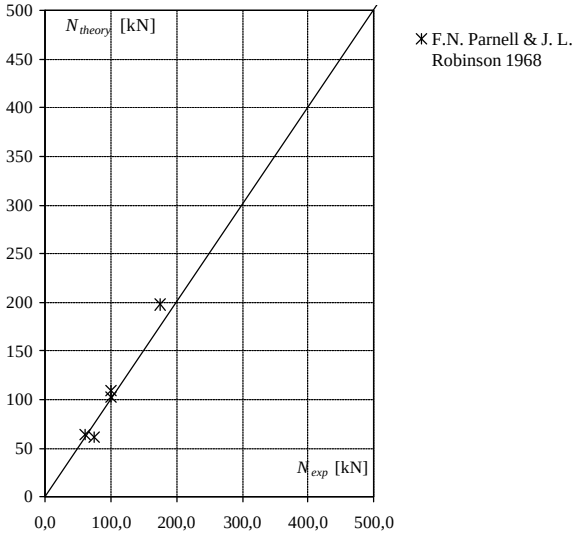

Figure 12.30 The results of calculations by the Danish Code of Practice compared with experiments for e=0

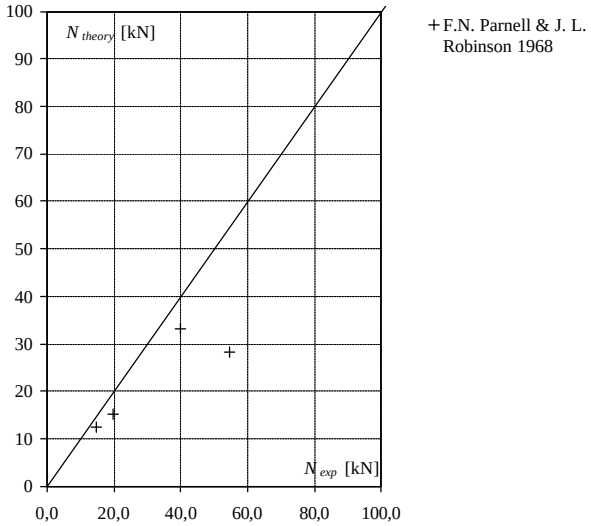

Figure 12.31 The results of calculations by the equilibrium method compared with experiments for laterally loaded beam-columns

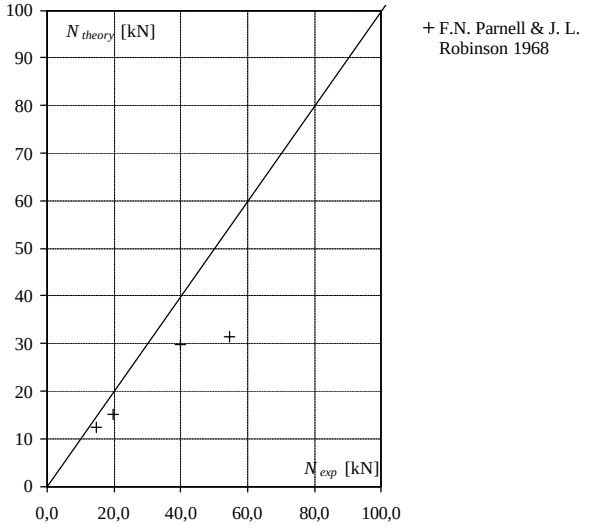

Figure 12.32 The results of calculations by the Danish Code of Practice compared with experiments for laterally loaded beam-columns

12.8Breen, J. E. & Ferguson, P. M. 1969

Test No.	b	h	d/h	100ρ	f_c	f_y	H	l/h	N_{exp}	u_m	Type	N_{exp}	N_{exp}
	[mm]	[mm]			[MPa]	[MPa]	[kN]		[kN]	[mm]		N_{teo}	N_{DS}
G1	155,6	100,6	0,8	1,8	25,6	409,6	4,5	20,0	151,2	-	D	0,65	0,68
G2	154,0	101,6	0,8	1,8	25,2	405,4	1,4	40,0	47,8	-	D	0,85	0,72
G3	153,2	102,0	0,8	1,8	25,5	409,6	0,9	50,0	30,0	-	D	0,83	0,73
G4	153,6	101,6	0,8	1,8	25,5	402,7	0,6	50,0	53,4	-	D	0,95	0,80
G5	152,8	101,6	0,8	1,8	28,7	464,7	0,9	60,0	29,4	-	D	1,02	1,02
G6	153,2	101,6	0,8	1,8	30,2	450,2	0,6	50,0	48,9	-	D	0,74	0,74
G7	154,8	102,2	0,8	1,8	33,4	440,6	0,7	40,0	66,7	-	D	0,49	0,54
G8	152,4	101,8	0,8	1,8	28,0	428,2	0,4	60,0	48,0	-	D	0,96	0,96
G9	152,6	101,4	0,8	1,8	27,4	419,9	4,4	20,0	146,8	-	D	0,61	0,64
G10	152,2	101,6	0,8	1,8	27,7	411,6	12,5	10,0	209,1	-	D	0,64	0,77

Table 12.8 Data used for calculations, taken from [20]

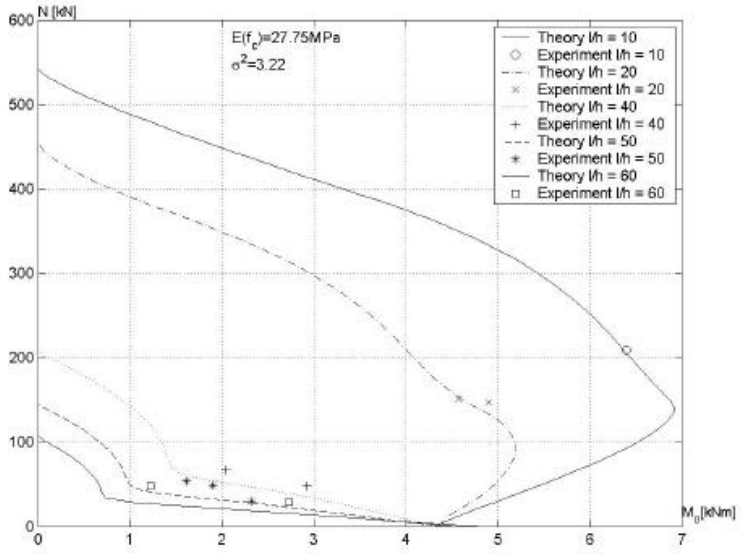

Figure 12.33 The results of calculations plotted in an interaction diagram

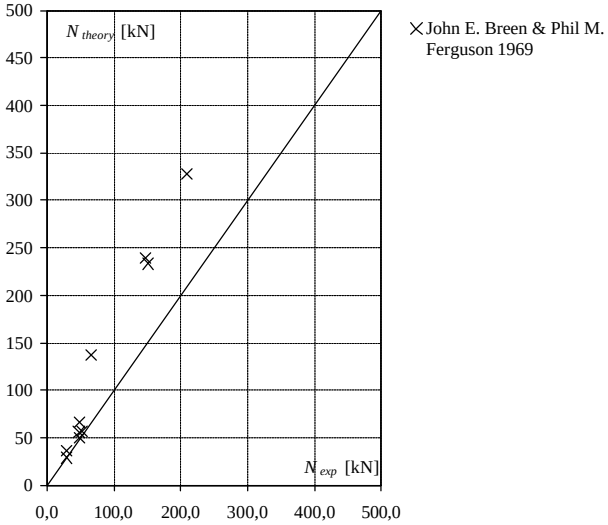

Figure 12.34 The results of calculations by the equilibrium method compared with experiments for laterally loaded beam-columns

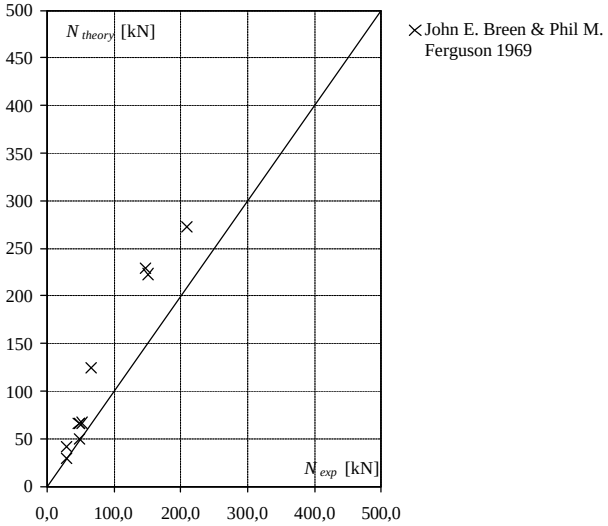

Figure 12.35 The results of calculations by the Danish Code of Practice compared with experiments for laterally loaded beam-columns

12.9 Mehmel, A., Schwartz, H., Kasparek, K. H. & Makovi, J. 1969

Test No.	b	h	d/h	100ρ	f_c	f_y	$e_{1,u}/h$	$e_{1,l}/h$	l/h	N_{exp}	u_m	Type	N_{exp}	N_{exp}
	[mm]	[mm]			[MPa]	[MPa]				[kN]	[mm]		N_{teo}	N_{DS}
0.1	253,0	159,0	0,9	1,1	37,4	509,9	0,1	0,1	8,8	942,7	5,0	B	0,73	0,86
0.2	254,0	156,0	0,9	1,1	40,6	509,9	1,0	1,0	9,0	137,3	12,0	B	0,87	0,94
1.1	253,0	203,0	0,8	1,2	39,3	483,4	0,2	0,2	16,7	857,4	22,0	B	0,82	0,93
1.2	253,0	202,0	0,8	1,2	37,8	483,4	0,5	0,5	16,8	319,8	43,0	B	0,79	0,84
2.1	252,0	202,0	0,9	1,2	37,3	483,4	0,2	0,2	22,3	588,6	43,0	B	0,79	0,84
2.2	252,0	203,0	0,8	1,2	40,8	483,4	0,5	0,5	22,2	259,0	60,0	B	0,87	0,99
3.1	252,0	152,0	0,8	1,2	38,3	509,9	0,2	0,2	22,4	470,9	30,0	B	0,90	0,95
3.2	252,0	151,0	0,8	1,2	41,1	509,9	0,5	0,5	22,5	176,6	48,0	B	0,96	1,12
3.3	254,0	159,0	0,8	1,1	35,4	509,9	0,1	0,1	21,4	782,8	24,0	B	0,80	0,90
3.4	253,0	158,0	0,8	1,1	42,8	509,9	1,0	1,0	21,5	102,0	45,0	B	0,84	0,84
4.1	253,0	150,0	0,8	1,2	40,6	509,9	0,2	0,2	30,0	367,9	35,0	B	0,82	0,82
4.2	253,0	148,0	0,8	1,2	41,5	509,9	0,5	0,5	30,4	145,2	70,0	B	0,90	1,02
5.1	253,0	158,0	0,8	3,1	40,7	426,8	0,2	0,2	21,5	735,8	32,0	B	0,87	1,02
5.2	252,0	159,0	0,8	3,1	37,0	426,8	0,5	0,5	21,4	369,8	52,0	B	1,08	1,15
6.1	254,0	159,0	0,8	1,1	42,5	509,9	0,2	0,0	14,5	939,8	12,0	B	1,07	1,07
6.2	253,0	157,0	0,8	1,1	44,2	509,9	0,5	0,0	14,6	343,4	28,0	B	0,88	1,05

Table 12.9 Data used for calculations, taken from [21]

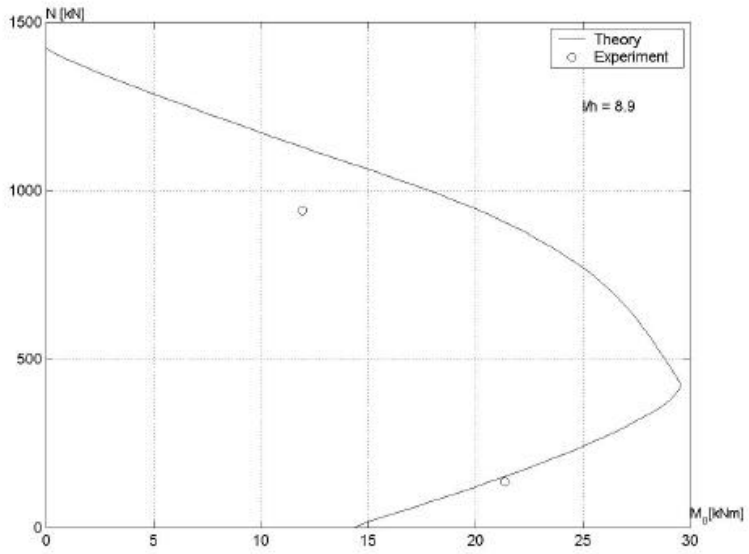

Figure 12.36 The results of calculations plotted in an interaction diagram, $f_{c,cylinder}$ *= 31.2 MPa*

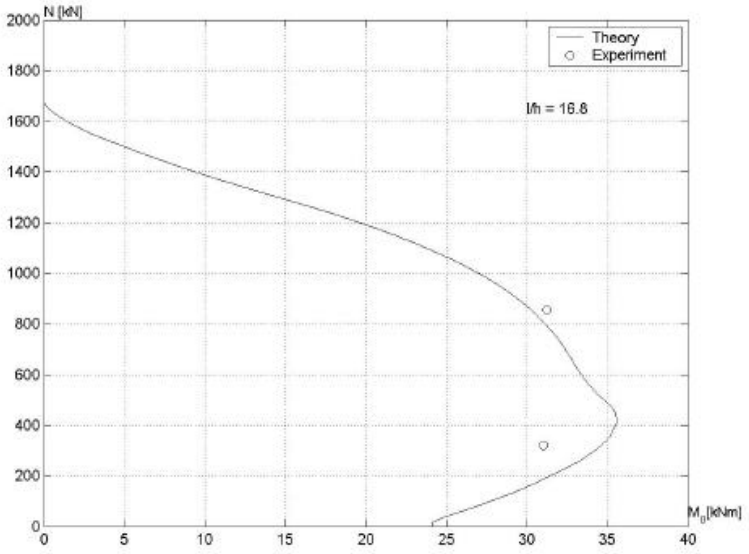

Figure 12.37 The results of calculations plotted in an interaction diagram, $f_{c,cylinder}$ = 30.9 MPa

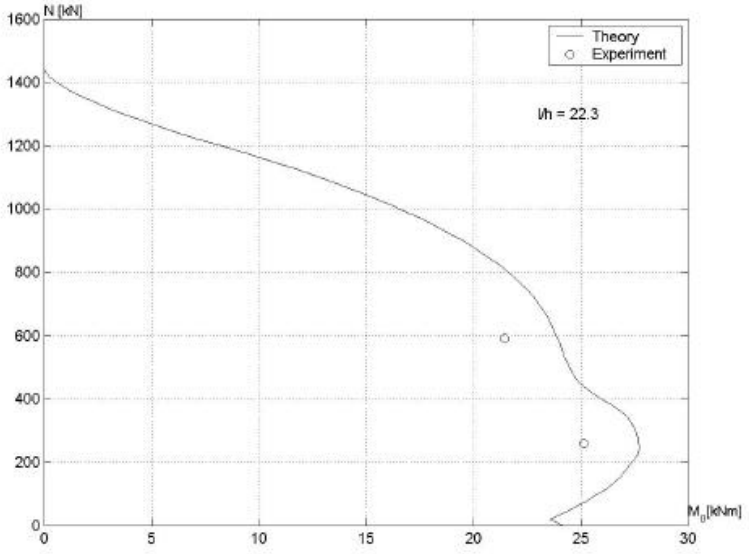

Figure 12.38 The results of calculations plotted in an interaction diagram, $f_{c,cylinder}$ = 31.2 MPa

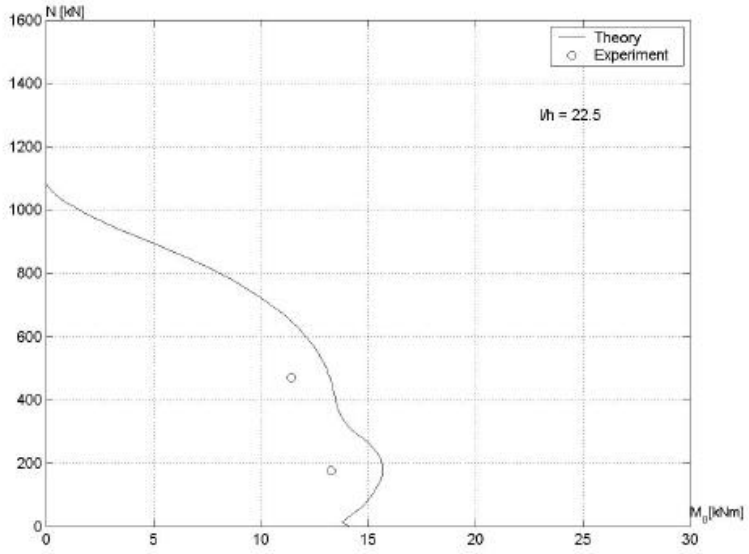

Figure 12.39 The results of calculations plotted in an interaction diagram, $f_{c,cylinder}$ *= 31.7 MPa*

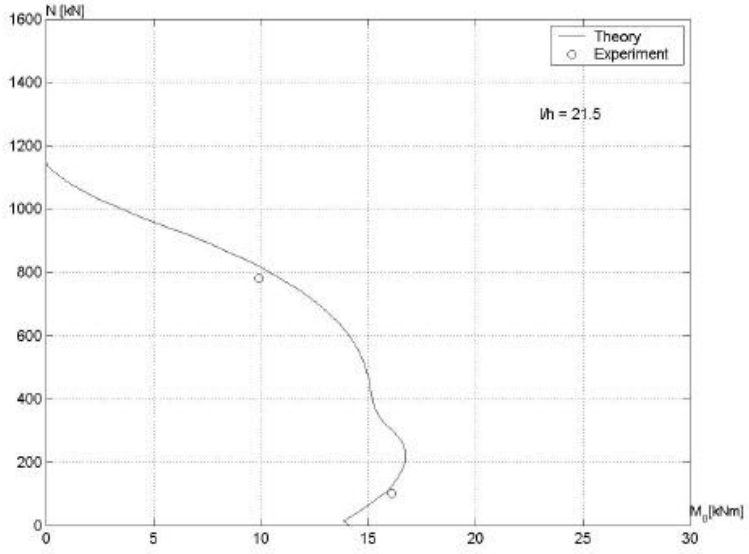

Figure 12.40 The results of calculations plotted in an interaction diagram, $f_{c,cylinder}$ *= 31.2 MPa*

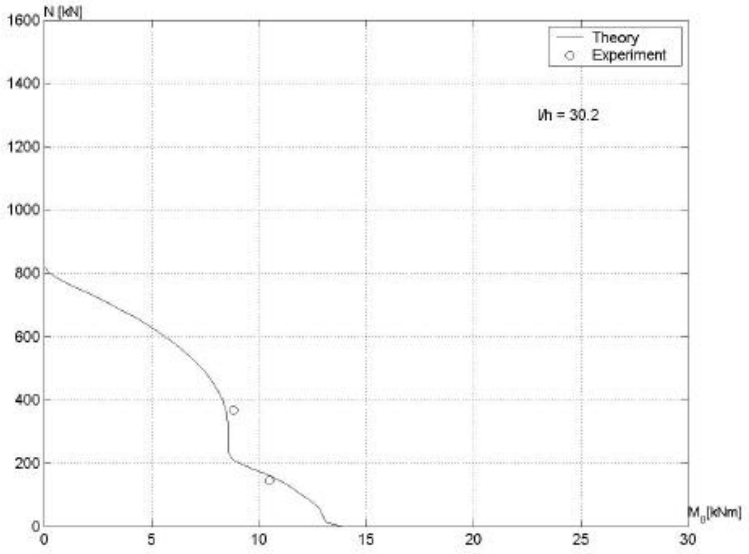

Figure 12.41 The results of calculations plotted in an interaction diagram, $f_{c,cylinder}$ = 32.8 MPa

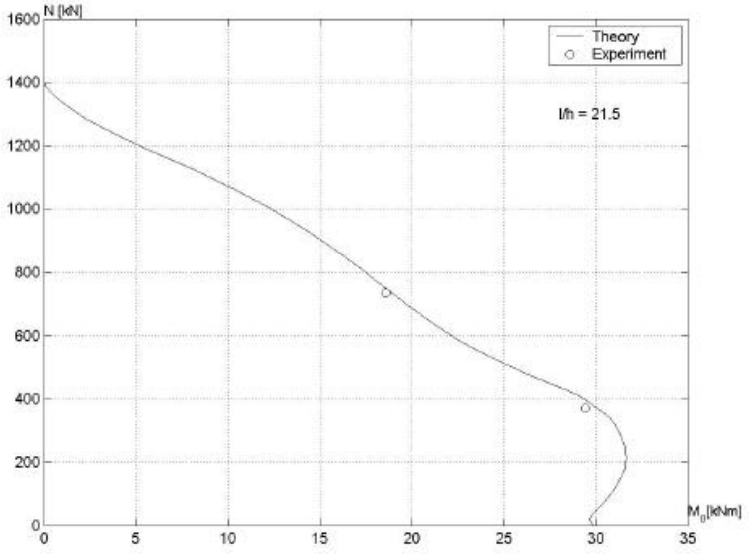

Figure 12.42 The results of calculations plotted in an interaction diagram, $f_{c,cylinder}$ = 31.0 MPa

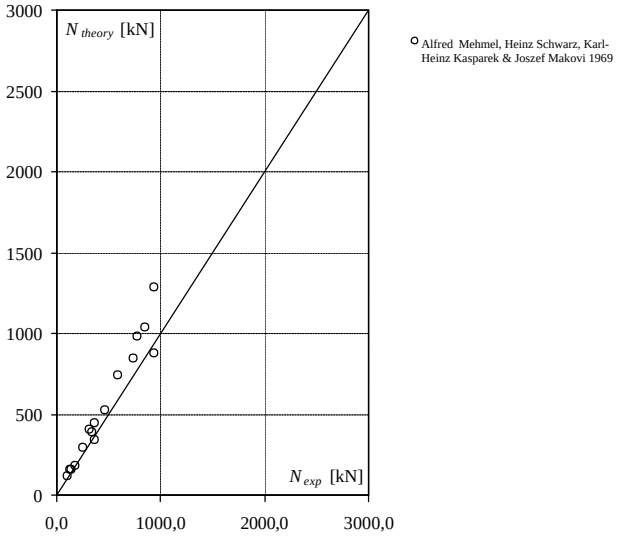

Figure 12.43 The results of calculations by the equilibrium method compared with experiments for eccentrically loaded beam-columns

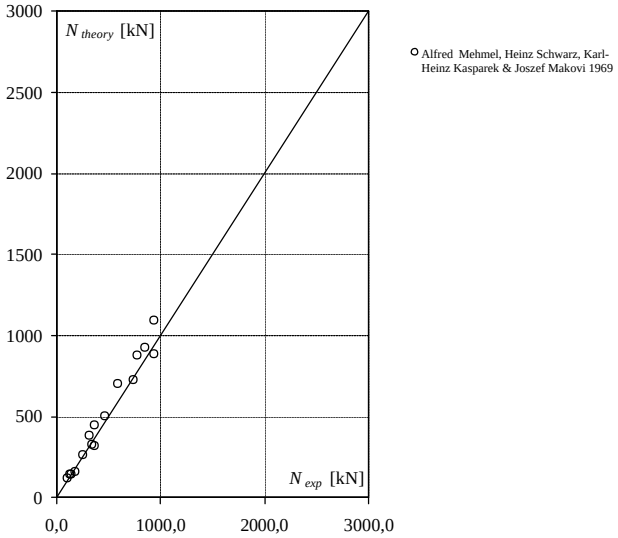

Figure 12.44 The results of calculations by the Danish Code of Practice compared with experiments for eccentrically loaded beam-columns

12.10 Kim, J.-K. & Yang, J.-K. 1993

Test No.	b	h	d/h	100ρ	f_c	f_y	$e_{i,t}/h$	$e_{i,b}/h$	l/h	N_{exp}	u_m	Type	N_{exp}	N_{exp}
	[mm]	[mm]			[MPa]	[MPa]				[kN]	[mm]		N_{teo}	N_{DS}
10L4-1	80,0	80,0	0,8	4,0	26,8	387,0	0,3	0,3	3,0	109,5	0,4	B	0,93	1,07
10L4-2	80,0	80,0	0,8	4,0	26,8	387,0	0,3	0,3	3,0	109,3	0,4	B	0,96	1,10
60L2-1	80,0	80,0	0,8	2,0	26,8	387,0	0,3	0,3	18,0	63,7	14,9	B	0,96	0,96
60L2-2	80,0	80,0	0,8	2,0	26,8	387,0	0,3	0,3	18,0	65,7	16,2	B	0,88	0,88
100L2-1	80,0	80,0	0,8	2,0	26,8	387,0	0,3	0,3	30,0	38,2	29,8	B	0,90	1,14
100L2-2	80,0	80,0	0,8	2,0	26,8	387,0	0,3	0,3	30,0	35,0	32,7	B	0,91	1,16
100L4-1	80,0	80,0	0,8	4,0	26,8	387,0	0,3	0,3	30,0	49,0	38,2	B	0,86	0,98
100L4-2	80,0	80,0	0,8	4,0	26,8	387,0	0,3	0,3	30,0	47,0	36,2	B	0,95	1,08
10M2-1	80,0	80,0	0,8	2,0	66,7	387,0	0,3	0,3	3,0	179,0	0,4	B	0,79	0,86
10M2-2	80,0	80,0	0,8	2,0	66,7	387,0	0,3	0,3	3,0	182,8	0,4	B	0,83	0,91
10M4-1	80,0	80,0	0,8	4,0	66,7	387,0	0,3	0,3	3,0	207,7	0,4	B	0,91	1,17
10M4-2	80,0	80,0	0,8	4,0	66,7	387,0	0,3	0,3	3,0	204,6	0,5	B	0,93	1,20
60M2-1	80,0	80,0	0,8	2,0	66,7	387,0	0,3	0,3	18,0	102,8	20,3	B	0,84	0,97
60M2-2	80,0	80,0	0,8	2,0	66,7	387,0	0,3	0,3	18,0	113,5	18,1	B	0,86	0,98
100M2-1	80,0	80,0	0,8	2,0	66,7	387,0	0,3	0,3	30,0	45,2	26,2	B	0,79	1,08
100M2-2	80,0	80,0	0,8	2,0	66,7	387,0	0,3	0,3	30,0	47,6	27,2	B	0,79	1,09
100M4-1	80,0	80,0	0,8	4,0	66,7	387,0	0,3	0,3	30,0	59,6	31,1	B	0,87	1,13
100M4-2	80,0	80,0	0,8	4,0	66,7	387,0	0,3	0,3	30,0	60,5	34,2	B	0,86	1,13
10H2-1	80,0	80,0	0,8	2,0	90,5	387,0	0,3	0,3	3,0	235,3	0,5	B	0,83	0,87
10H2-2	80,0	80,0	0,8	2,0	90,5	387,0	0,3	0,3	3,0	240,4	0,4	B	0,79	0,83
10H4-1	80,0	80,0	0,8	4,0	90,5	387,0	0,3	0,3	3,0	255,8	0,5	B	0,90	1,16
10H4-2	80,0	80,0	0,8	4,0	90,5	387,0	0,3	0,3	3,0	257,7	0,5	B	0,89	1,15
60H2-1	80,0	80,0	0,8	2,0	90,5	387,0	0,3	0,3	18,0	122,1	15,4	B	0,71	0,76
60H2-2	80,0	80,0	0,8	2,0	90,5	387,0	0,3	0,3	18,0	123,7	16,7	B	0,72	0,77
100H2-1	80,0	80,0	0,8	2,0	90,5	387,0	0,3	0,3	30,0	54,3	24,3	B	0,88	1,14
100H2-2	80,0	80,0	0,8	2,0	90,5	387,0	0,3	0,3	30,0	54,9	23,7	B	0,89	1,15
100H4-1	80,0	80,0	0,8	4,0	90,5	387,0	0,3	0,3	30,0	66,6	32,4	B	0,70	0,82
100H4-2	80,0	80,0	0,8	4,0	90,5	387,0	0,3	0,3	30,0	64,7	33,3	B	0,68	0,80

Table 12.10 Data used for calculations, taken from [28]

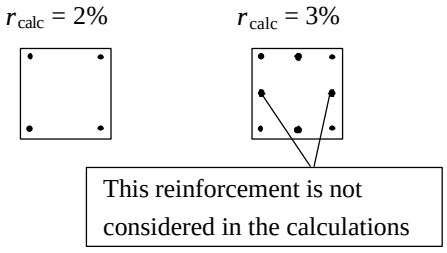

Figure 12.45 The reinforcement in the middle of the section is not considered in the calculations

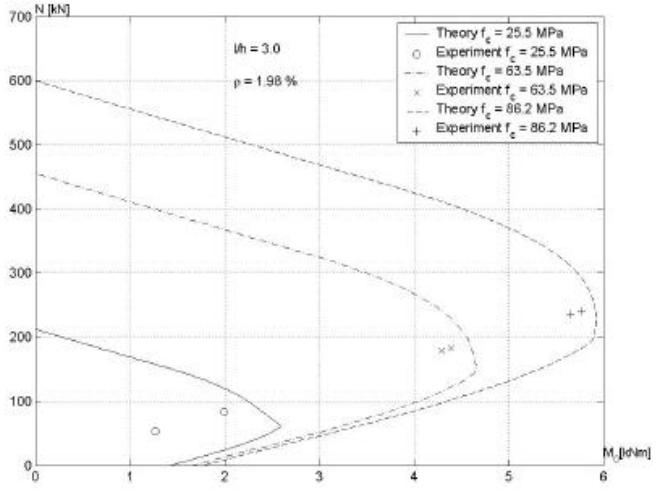

Figure 12.46 The results of calculations plotted in an interaction diagram

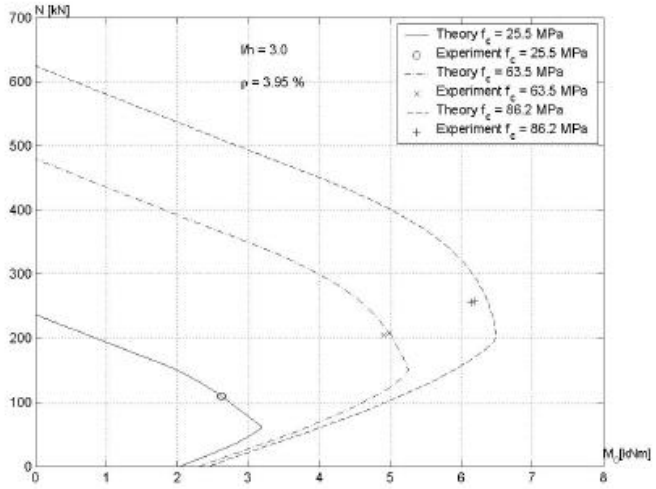

Figure 12.47 The results of calculations plotted in an interaction diagram

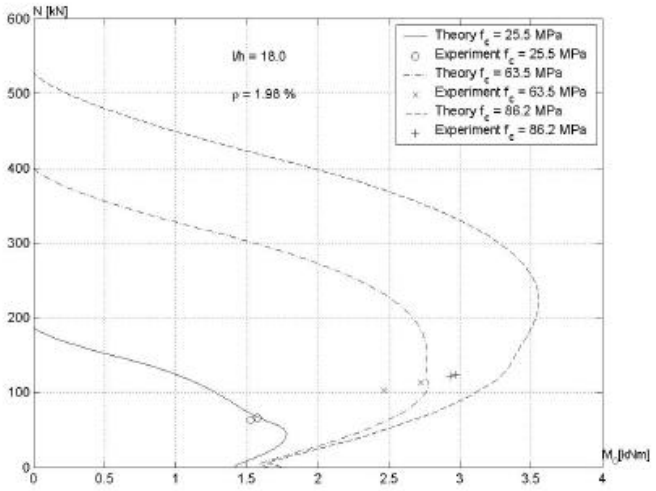

Figure 12.48 The results of calculations plotted in an interaction diagram

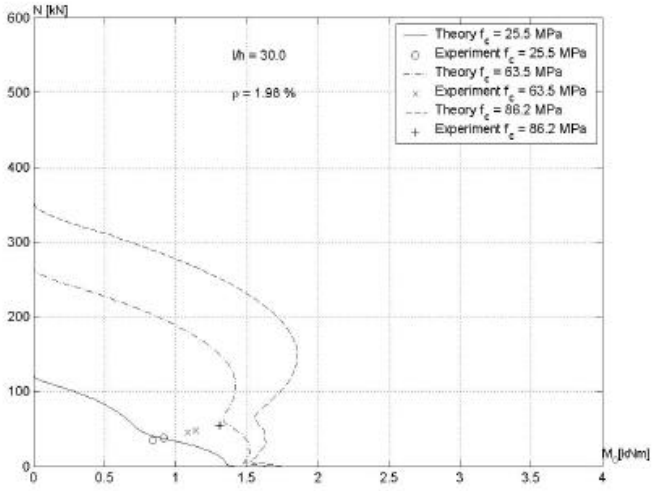

Figure 12.49 The results of calculations plotted in an interaction diagram

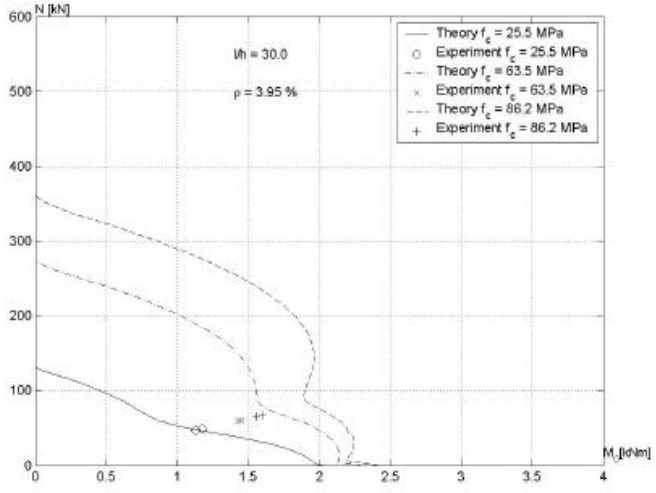

Figure 12.50 The results of calculations plotted in an interaction diagram

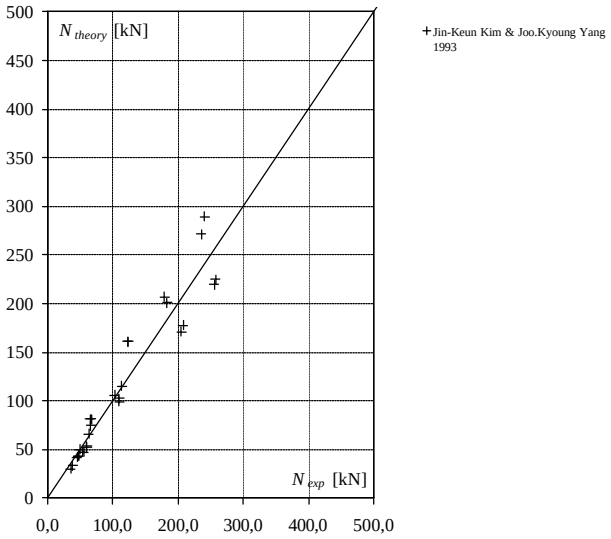

Figure 12.51 The results of calculations by the equilibrium method compared with experiments for eccentrically loaded beam-columns

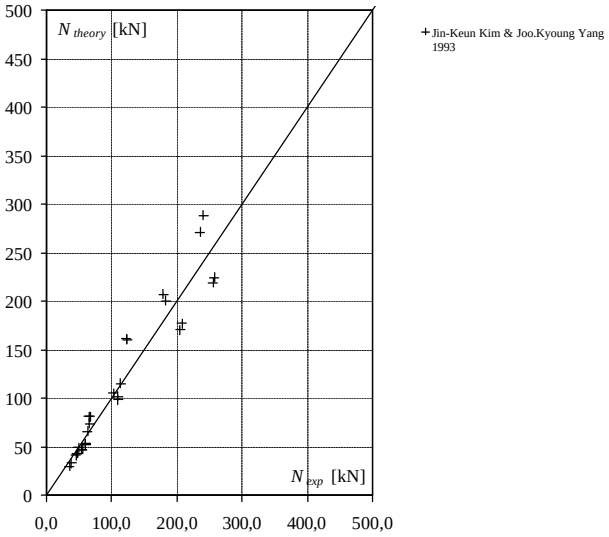

Figure 12.52 The results of calculations by the Danish Code of Practice compared with experiments for eccentrically loaded beam-columns

12.11 Chuang, P. H. & Kong, F. K. 1997

Test No.	b	h	d/h	100ρ	f_c	f_y	$e_{i,v}/h$	$e_{i,0}/h$	l/h	N_{exp}	u_m	Type	N_{exp}	N_{exp}
	[mm]	[mm]			[MPa]	[MPa]				[kN]	[mm]		N_{teo}	N_{DS}
A-15-0.25	300,0	200,0	0,8	3,3	24,9	493,0	0,3	0,3	15,0	1286,2	29,0	B	1,41	1,69
A-17-0.25	300,0	200,0	0,8	3,3	30,6	493,0	0,3	0,3	17,0	1185,0	41,0	B	1,24	1,46
A-18-0.25	300,0	200,0	0,8	3,3	26,2	493,0	0,3	0,3	18,0	1084,1	39,0	B	1,29	1,47
A-19-0.25	300,0	200,0	0,8	3,3	25,8	493,0	0,3	0,3	19,0	1246,6	43,0	B	1,60	1,77
A-15-0.50	300,0	200,0	0,8	3,3	26,4	493,0	0,5	0,5	15,0	886,2	31,0	B	1,51	1,93
A-17-0.50	300,0	200,0	0,8	3,3	32,2	493,0	0,5	0,5	17,0	904,5	55,0	B	1,48	1,83
A-18-0.50	300,0	200,0	0,8	3,3	26,2	493,0	0,5	0,5	18,0	851,6	58,0	B	1,60	1,97
A-19-0.50	300,0	200,0	0,8	3,3	24,2	493,0	0,5	0,5	19,0	816,3	45,0	B	1,60	1,98
B-17-0.25	300,0	200,0	0,8	1,3	29,8	519,0	0,3	0,3	17,0	1086,8	23,0	B	1,49	1,64
B-18-0.25	300,0	200,0	0,8	1,3	33,7	519,0	0,3	0,3	18,0	989,1	25,0	B	1,31	1,45
B-19-0.25	300,0	200,0	0,8	1,3	31,8	519,0	0,3	0,3	19,0	1048,0	26,0	B	1,50	1,61
B-17-0.50	300,0	200,0	0,8	1,3	30,9	519,0	0,5	0,5	17,0	476,7	38,0	B	1,17	1,31
B-18-0.50	300,0	200,0	0,8	1,3	34,0	519,0	0,5	0,5	18,0	479,7	37,0	B	1,15	1,30
B-19-0.50	300,0	200,0	0,8	1,3	36,0	519,0	0,5	0,5	19,0	459,8	37,0	B	1,12	1,27
C-27.5-0.25	200,0	120,0	0,7	3,4	33,7	520,0	0,3	0,3	27,5	531,3	17,0	B	2,71	2,89
C-30.0-0.25	200,0	120,0	0,7	3,4	34,1	520,0	0,3	0,3	30,0	484,8	24,0	B	2,80	3,02
C-31.7-0.25	200,0	120,0	0,7	3,4	35,5	520,0	0,3	0,3	31,7	332,3	45,0	B	2,01	2,18
C-27.5-0.50	200,0	120,0	0,7	3,4	34,1	520,0	0,5	0,5	27,5	242,3	72,0	B	1,78	1,96
C-30.0-0.50	200,0	120,0	0,7	3,4	33,2	520,0	0,5	0,5	30,0	319,7	60,0	B	2,63	2,92
C-31.7-0.50	200,0	120,0	0,7	3,4	35,0	520,0	0,5	0,5	31,7	254,9	94,0	B	2,25	2,53
HB-17-0.25	300,0	200,0	0,8	1,3	77,0	531,0	0,3	0,3	17,0	1802,6	35,0	B	1,23	1,43
HB-18-0.25	300,0	200,0	0,8	1,3	75,8	531,0	0,3	0,3	18,0	1478,4	30,0	B	1,10	1,29
HB-19-0.25	300,0	200,0	0,8	1,3	76,3	531,0	0,3	0,3	19,0	1569,8	15,0	B	1,25	1,43
HB-17-0.50	300,0	200,0	0,8	1,3	75,3	531,0	0,5	0,5	17,0	706,2	34,0	B	1,19	1,30
HB-18-0.50	300,0	200,0	0,8	1,3	76,7	531,0	0,5	0,5	18,0	646,4	40,0	B	1,17	1,29
HB-19-0.50	300,0	200,0	0,8	1,3	76,9	531,0	0,5	0,5	19,0	608,8	39,0	B	1,21	1,34

Table 12.11 Data used for calculations, taken from [29]

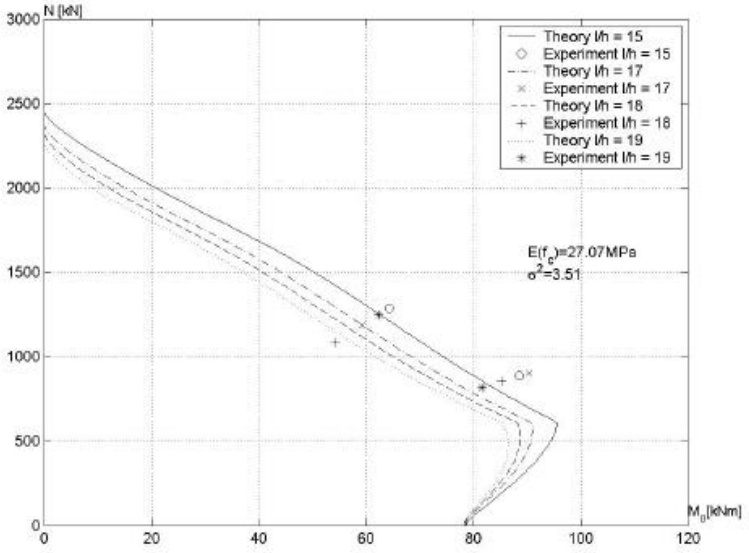

Figure 12.53 The results of calculations plotted in an interaction diagram, ρ = 3.27%

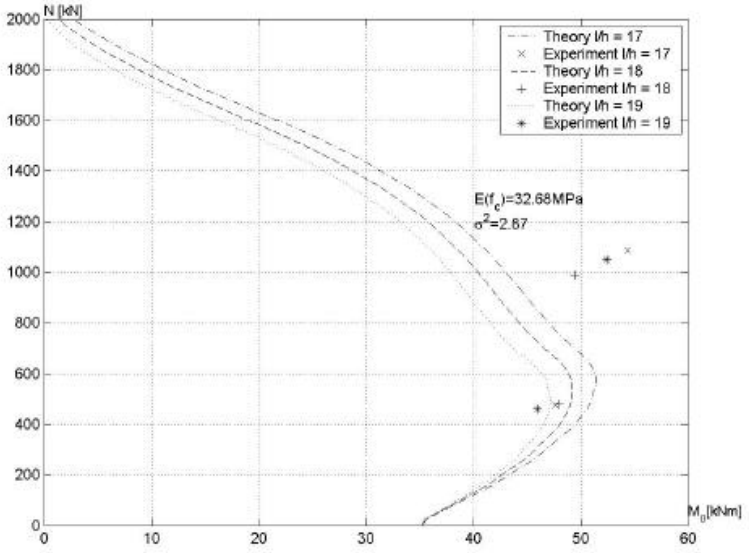

Figure 12.54 The results of calculations plotted in an interaction diagram, ρ = 1.34%

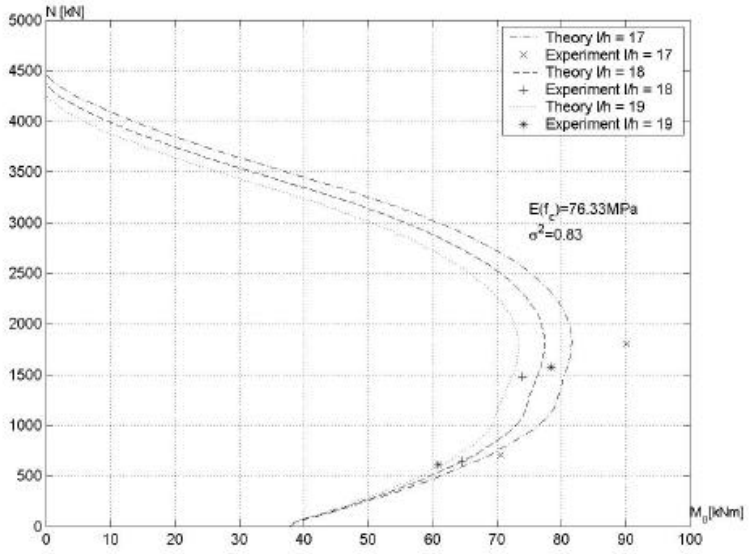

Figure 12.55 The results of calculations plotted in an interaction diagram, ρ = 1.34%

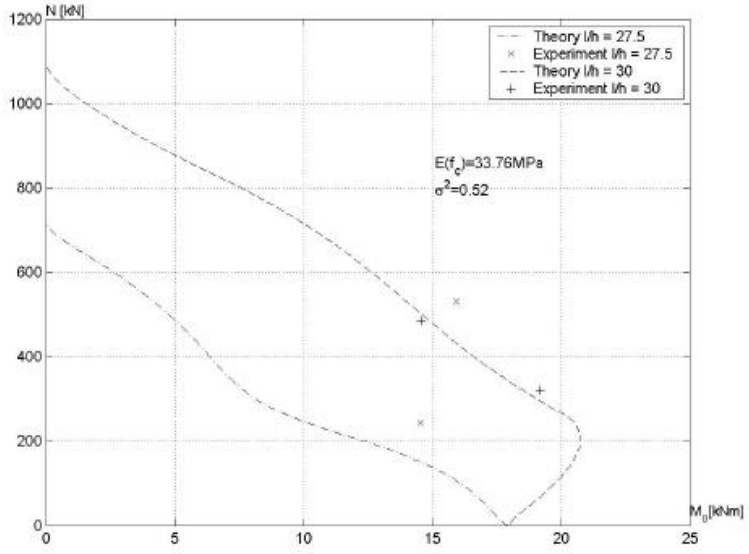

Figure 12.56 The results of calculations plotted in an interaction diagram, ρ = 3.35%

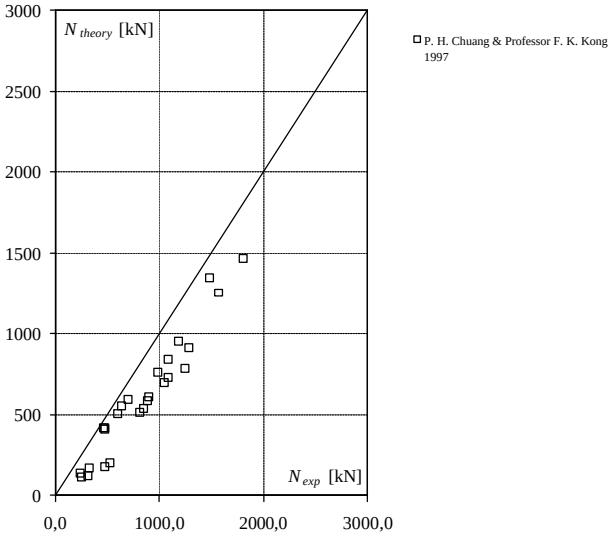

Figure 12.57 The results of calculations by the equilibrium method compared with experiments for eccentrically loaded beam-columns

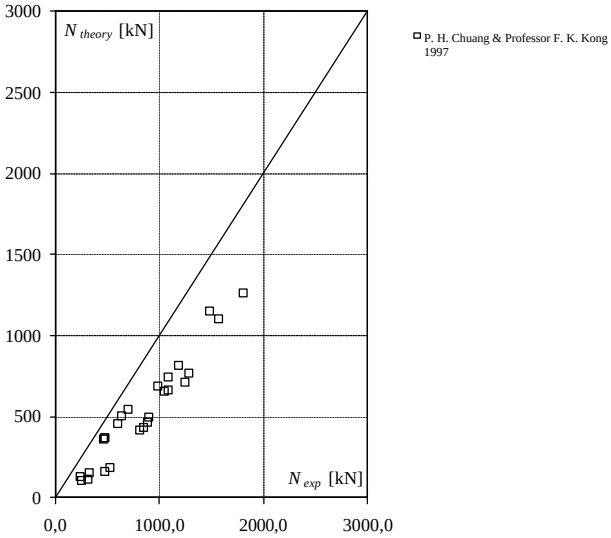

Figure 12.58 The results of calculations by the Danish Code of Practice compared with experiments for eccentrically loaded beam-columns

12.12 Foster, S. J. & Attard, M. M. 1997

Test No.	b	h	d/h	100ρ	f_c	f_y	$e_{i,e}/h$	$e_{i,0}/h$	l/h	N_{exp}	u_m	Type	N_{exp}	N_{exp}
	[mm]	[mm]			[MPa]	[MPa]				[kN]	[mm]		N_{teo}	N_{DS}
2L8-30	150,0	150,0	0,9	2,0	43,0	480,0	0,1	0,1	9,7	960,0	6,5	B	0,98	1,13
2L8-60	150,0	150,0	0,9	2,0	43,0	480,0	0,1	0,1	9,7	857,0	6,0	B	0,88	1,02
2L8-120	150,0	150,0	0,9	2,0	43,0	480,0	0,1	0,1	9,7	912,0	6,0	B	0,95	1,09
2L20-30	150,0	150,0	0,9	2,0	40,0	480,0	0,1	0,1	9,7	750,0	4,8	B	0,99	1,22
2L20-60	150,0	150,0	0,9	2,0	43,0	480,0	0,1	0,1	9,7	700,0	6,2	B	0,88	1,08
2L20-120	150,0	150,0	0,9	2,0	43,0	480,0	0,1	0,1	9,7	782,0	5,2	B	1,00	1,22
2L50-30	150,0	150,0	0,9	2,0	40,0	480,0	0,3	0,3	9,7	440,0	9,0	B	0,94	1,23
2L50-60	150,0	150,0	0,9	2,0	43,0	480,0	0,3	0,3	9,7	472,0	8,5	B	0,95	1,21
2L50-120	150,0	150,0	0,9	2,0	40,0	480,0	0,3	0,3	9,7	440,0	9,0	B	0,96	1,23
4L8-30	150,0	150,0	0,9	3,0	43,0	480,0	0,1	0,1	9,7	1100,0	9,0	B	1,04	1,20
4L8-60	150,0	150,0	0,9	3,0	43,0	480,0	0,1	0,1	9,7	1150,0	6,0	B	1,06	1,24
4L8-120	150,0	150,0	0,9	3,0	43,0	480,0	0,1	0,1	9,7	975,0	5,7	B	0,91	1,06
4L20-30	150,0	150,0	0,9	3,0	40,0	480,0	0,1	0,1	9,7	1020,0	7,0	B	1,23	1,49
4L20-60	150,0	150,0	0,9	3,0	40,0	480,0	0,1	0,1	9,7	968,0	3,5	B	1,18	1,44
4L20-120	150,0	150,0	0,9	3,0	40,0	480,0	0,1	0,1	9,7	900,0	4,0	B	1,08	1,34
4L50-30	150,0	150,0	0,9	3,0	40,0	480,0	0,3	0,3	9,7	517,0	18,5	B	1,01	1,32
4L50-60	150,0	150,0	0,9	3,0	40,0	480,0	0,3	0,3	9,7	550,0	8,0	B	1,00	1,28
4L50-120	150,0	150,0	0,9	3,0	40,0	480,0	0,3	0,3	9,7	525,0	8,0	B	0,97	1,26
2M8-30	150,0	150,0	0,9	2,0	75,0	480,0	0,1	0,1	9,7	1348,0	5,0	B	0,87	1,00
2M8-60	150,0	150,0	0,9	2,0	75,0	480,0	0,1	0,1	9,7	1432,0	5,0	B	0,93	1,06
2M8-120	150,0	150,0	0,9	2,0	75,0	480,0	0,1	0,1	9,7	1239,0	4,0	B	0,80	0,93
2M20-30	150,0	150,0	0,9	2,0	74,0	480,0	0,1	0,1	9,7	1160,0	6,0	B	0,93	1,14
2M20-60	150,0	150,0	0,9	2,0	74,0	480,0	0,1	0,1	9,7	1231,0	6,0	B	0,99	1,21
2M20-120	150,0	150,0	0,9	2,0	74,0	480,0	0,1	0,1	9,7	1067,0	5,0	B	0,87	1,05
2M50-30	150,0	150,0	0,9	2,0	74,0	480,0	0,3	0,3	9,7	630,0	9,5	B	0,88	1,12
2M50-60	150,0	150,0	0,9	2,0	74,0	480,0	0,3	0,3	9,7	747,0	11,5	B	1,07	1,37
2M50-120	150,0	150,0	0,9	2,0	74,0	480,0	0,3	0,3	9,7	652,0	11,5	B	0,89	1,16
4M8-30	150,0	150,0	0,9	3,0	74,0	480,0	0,1	0,1	9,7	1102,0	3,0	B	0,68	0,79
4M8-60	150,0	150,0	0,9	3,0	75,0	480,0	0,1	0,1	9,7	1404,0	4,0	B	0,87	1,00
4M8-120	150,0	150,0	0,9	3,0	74,0	480,0	0,1	0,1	9,7	1404,0	3,5	B	0,86	0,99
4M20-30	150,0	150,0	0,9	3,0	75,0	480,0	0,1	0,1	9,7	1052,0	4,0	B	0,79	0,97
4M20-60	150,0	150,0	0,9	3,0	75,0	480,0	0,1	0,1	9,7	1004,0	5,0	B	0,77	0,94
4M20-120	150,0	150,0	0,9	3,0	75,0	480,0	0,1	0,1	9,7	1226,0	5,0	B	0,92	1,13
4M50-30	150,0	150,0	0,9	3,0	74,0	480,0	0,3	0,3	9,7	656,0	9,5	B	0,87	1,10
4M50-60	150,0	150,0	0,9	3,0	75,0	480,0	0,3	0,3	9,7	686,0	9,5	B	0,90	1,14
4M50-120	150,0	150,0	0,9	3,0	74,0	480,0	0,3	0,3	9,7	677,0	9,5	B	0,85	1,10
2H8-30	150,0	150,0	0,9	2,0	93,0	480,0	0,1	0,1	9,7	1576,0	3,5	B	0,85	0,98
2H8-60	150,0	150,0	0,9	2,0	93,0	480,0	0,1	0,1	9,7	1647,0	4,5	B	0,88	1,02
2H8-120	150,0	150,0	0,9	2,0	93,0	480,0	0,1	0,1	9,7	1806,0	3,6	B	0,98	1,12
2H20-30	150,0	150,0	0,9	2,0	92,0	480,0	0,1	0,1	9,7	1207,0	6,5	B	0,81	1,00
2H20-60	150,0	150,0	0,9	2,0	92,0	480,0	0,1	0,1	9,7	1247,0	5,3	B	0,85	1,03

2H20-120	150,0	150,0	0,9	2,0	92,0	480,0	0,1	0,1	9,7	1473,0	5,6	B	1,01	1,22
2H50-30	150,0	150,0	0,9	2,0	92,0	480,0	0,3	0,3	9,7	749,0	9,7	B	0,94	1,17
2H50-60	150,0	150,0	0,9	2,0	92,0	480,0	0,3	0,3	9,7	685,0	10,0	B	0,86	1,07
2H50-120	150,0	150,0	0,9	2,0	92,0	480,0	0,3	0,3	9,7	851,0	8,3	B	1,06	1,33
4H8-30	150,0	150,0	0,9	3,0	91,0	480,0	0,1	0,1	9,7	1601,0	4,8	B	0,82	0,95
4H8-60	150,0	150,0	0,9	3,0	92,0	480,0	0,1	0,1	9,7	1702,0	5,5	B	0,88	1,02
4H8-120	150,0	150,0	0,9	3,0	92,0	480,0	0,1	0,1	9,7	1654,0	4,2	B	0,85	0,99
4H20-30	150,0	150,0	0,9	3,0	88,0	480,0	0,1	0,1	9,7	1352,0	7,0	B	0,89	1,09
4H20-60	150,0	150,0	0,9	3,0	88,0	480,0	0,1	0,1	9,7	1358,0	7,5	B	0,88	1,09
4H20-120	150,0	150,0	0,9	3,0	92,0	480,0	0,1	0,1	9,7	1374,0	7,0	B	0,87	1,06
4H50-30	150,0	150,0	0,9	3,0	88,0	480,0	0,3	0,3	9,7	781,0	10,5	B	0,87	1,09
4H50-60	150,0	150,0	0,9	3,0	88,0	480,0	0,3	0,3	9,7	791,0	9,5	B	0,88	1,11
4H50-120	150,0	150,0	0,9	3,0	92,0	480,0	0,3	0,3	9,7	818,0	9,5	B	0,88	1,10
2L8-120R	150,0	150,0	0,9	2,0	56,0	480,0	0,1	0,1	9,7	1092,0	4,5	B	0,91	1,06
2L20-120R	150,0	150,0	0,9	2,0	56,0	480,0	0,1	0,1	9,7	897,0	5,0	B	0,92	1,13
4L8-120R	150,0	150,0	0,9	3,0	56,0	480,0	0,1	0,1	9,7	1247,0	4,0	B	0,95	1,11
4L20-120R	150,0	150,0	0,9	3,0	53,0	480,0	0,1	0,1	9,7	945,0	6,0	B	0,93	1,13
4L50-30R	150,0	150,0	0,9	3,0	40,0	480,0	0,3	0,3	9,7	546,0	10,0	B	1,04	1,35
2M8-30R	150,0	150,0	0,9	2,0	68,0	480,0	0,1	0,1	9,7	1326,0	1,0	B	0,94	1,08
2M20-60R	150,0	150,0	0,9	2,0	73,0	480,0	0,1	0,1	9,7	1303,0	7,0	B	1,06	1,30
2M20-120R	150,0	150,0	0,9	2,0	73,0	480,0	0,1	0,1	9,7	1180,0	7,0	B	0,98	1,18
2M50-60R	150,0	150,0	0,9	2,0	67,0	480,0	0,3	0,3	9,7	670,0	8,4	B	1,02	1,30
2M50-120R	150,0	150,0	0,9	2,0	73,0	480,0	0,3	0,3	9,7	672,0	13,2	B	0,95	1,21
4M20-60R	150,0	150,0	0,9	3,0	68,0	480,0	0,1	0,1	9,7	1198,0	4,4	B	0,98	1,20
4M20-120R	150,0	150,0	0,9	3,0	73,0	480,0	0,1	0,1	9,7	1105,0	7,2	B	0,84	1,02
4M50-60R	150,0	150,0	0,9	3,0	73,0	480,0	0,3	0,3	9,7	800,0	8,5	B	1,02	1,31
4M50-120R	150,0	150,0	0,9	3,0	70,0	480,0	0,3	0,3	9,7	633,0	9,5	B	0,83	1,08

Table 12.12 Data used for calculations, taken from [30]

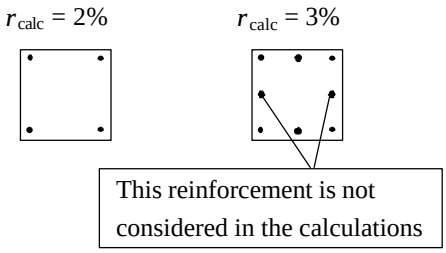

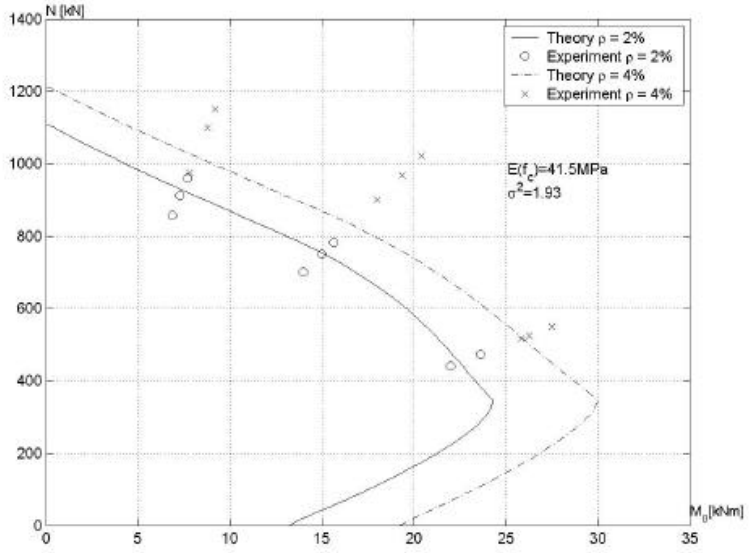

Figure 12.59 The results of calculations plotted in an interaction diagram

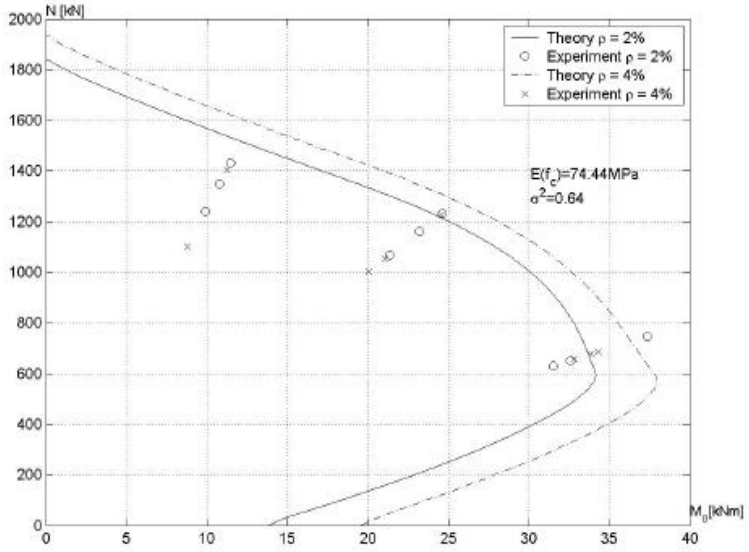

Figure 12.60 The results of calculations plotted in an interaction diagram

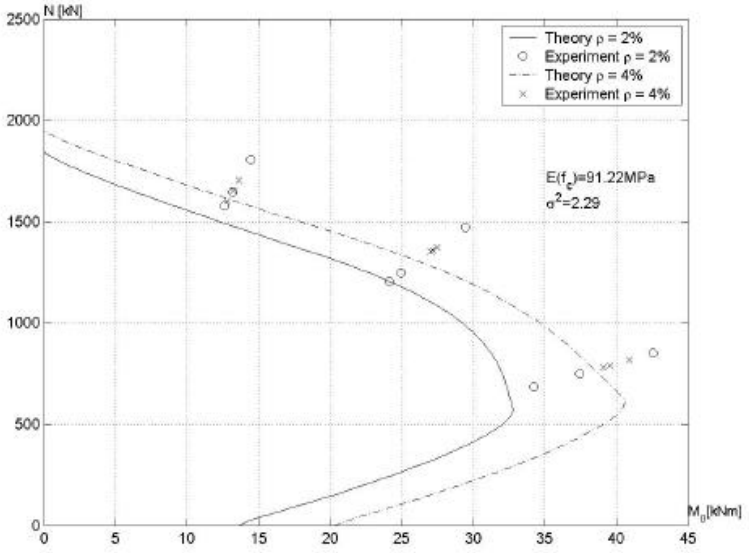

Figure 12.61 The results of calculations plotted in an interaction diagram

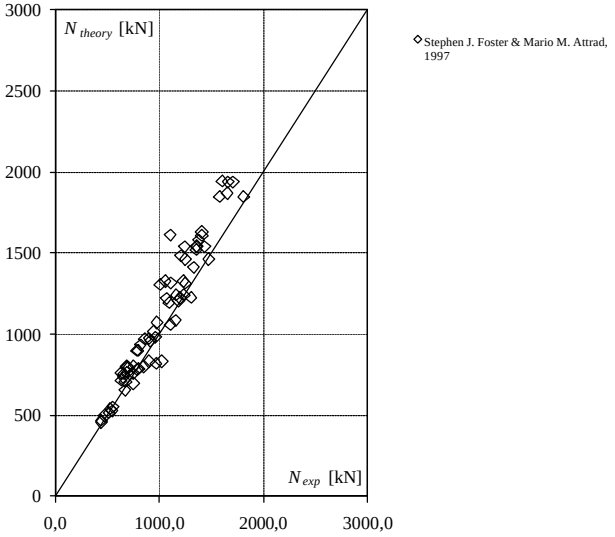

Figure 12.62 The results of calculations by the equilibrium method compared with experiments for eccentrically loaded beam-columns

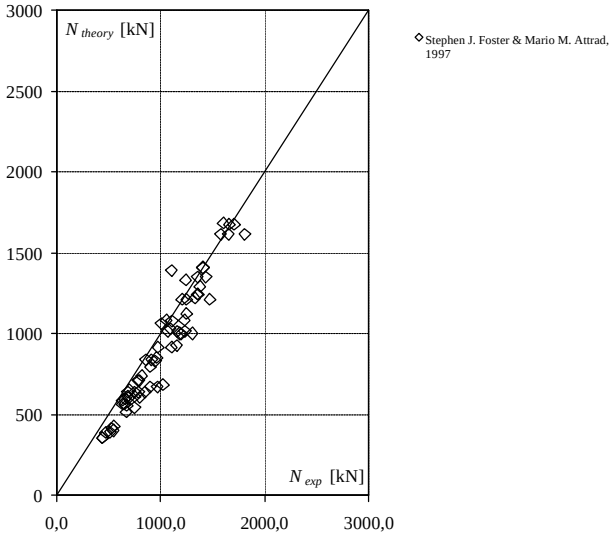

Figure 12.63 The results of calculations by the Danish Code of Practice compared with experiments for eccentrically loaded beam-columns

12.13 Cleason, C. 1997

Test No.	b	h	d/h	100ρ	f_c	f_y	$e_{i,t}/h$	$e_{i,b}/h$	l/h	N_{exp}	u_m	Type	N_{exp}	N_{exp}
	[mm]	[mm]			[MPa]	[MPa]				[kN]	[mm]		N_{teo}	N_{DS}
1A	120,0	120,0	0,9	3,0	43,0	684,0	0,2	0,2	20,0	320,0	26,0	B	0,85	0,95
2A	120,0	120,0	0,9	3,0	43,0	684,0	0,2	0,2	20,0	280,0	46,0	B	0,75	0,83
3A	120,0	120,0	0,9	3,0	86,0	684,0	0,2	0,2	20,0	370,0	36,0	B	0,60	0,69
4A	120,0	120,0	0,9	3,0	86,0	684,0	0,2	0,2	20,0	330,0	47,0	B	0,54	0,61
5B	200,0	200,0	0,9	2,0	33,0	636,0	0,1	0,1	15,0	990,0	22,0	B	0,86	1,02
6B	200,0	200,0	0,9	2,0	33,0	636,0	0,1	0,1	15,0	990,0	21,0	B	0,86	1,02
7B	200,0	200,0	0,9	2,0	91,0	636,0	0,1	0,1	15,0	2310,0	23,0	B	0,88	1,05
8B	200,0	200,0	0,9	2,0	92,0	636,0	0,1	0,1	15,0	2350,0	20,0	B	0,89	1,06
9C	200,0	200,0	0,9	2,0	37,0	636,0	0,1	0,1	20,0	900,0	40,0	B	0,82	0,92
10C	200,0	200,0	0,9	2,0	37,0	636,0	0,1	0,1	20,0	920,0	36,0	B	0,84	0,94
11C	200,0	200,0	0,9	2,0	93,0	636,0	0,1	0,1	20,0	1530,0	39,0	B	0,67	0,77
12C	200,0	200,0	0,9	2,0	93,0	636,0	0,1	0,1	20,0	1560,0	41,0	B	0,68	0,78

Table 12.13 Data used for calculations, taken from [31]

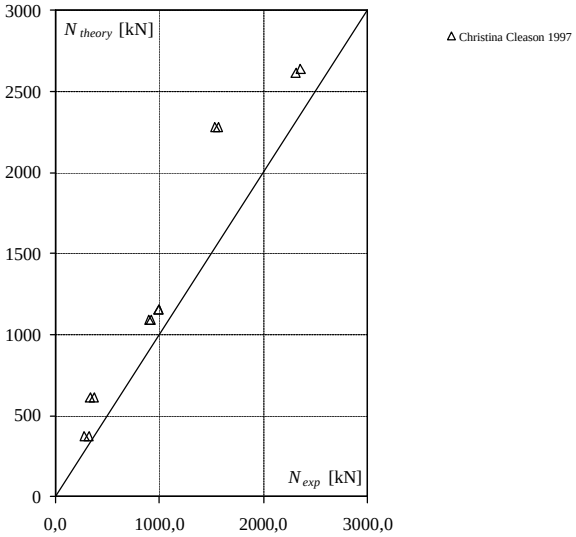

Figure 12.64 The results of calculations by equilibrium method compared with experiments for eccentrically loaded beam-columns

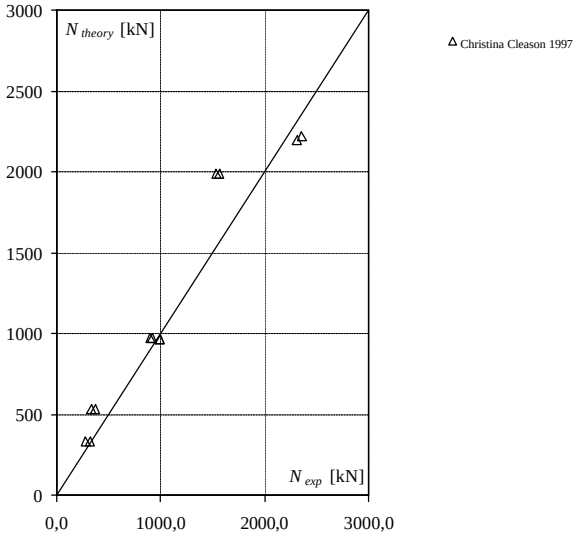

Figure 12.65 The results of calculations by the Danish Code of Practice compared with experiments for eccentrically loaded beam-columns

Report
BYG – DTU R-042
2002
ISSN 1601-2917
ISBN 87-7877-101-3